SUBDUCTION ZONES

Robert J. Stern
Geosciences Department
University of Texas at Dallas
Richardson, Texas, USA

Received 24 January 2001; revised 24 June 2002; accepted 11 November 2002; published 31 December 2002.

[1] Subduction zones are where sediments, oceanic crust, and mantle lithosphere return to and reequilibrate with Earth's mantle. Subduction zones are interior expressions of Earth's 55,000 km of convergent plate margins and are the geodynamic system that builds island arcs. Excess density of the mantle lithosphere in subduction zones provides most of the power needed to move the plates while inducing convection in the overriding mantle wedge. Asthenospheric mantle sucked toward the trench by the sinking slab interacts with water and incompatible elements rising from the sinking plate, and this interaction causes the mantle to melt. These melts rise vertically through downwelling mantle to erupt at arc volcanoes. Subduction zones are thus interior Earth systems of unparalleled scale and complexity. Subduction zone igneous activity formed most ore deposits and continental crust, and earthquakes caused by the downgoing plate present a growing hazard to society. This overview summarizes our present understanding of subduction zones, using perspectives of the incoming plate, downgoing plate, mantle wedge, and arc-trench complex. Understanding the operation of subduction zones stands as one of the great challenges facing the Earth sciences in the 21st century and will require the efforts of global interdisciplinary teams. *INDEX TERMS:* 1010 Geochemistry: Chemical evolution; 1030 Geochemistry: Geochemical cycles (0330); 7299 Seismology: General or miscellaneous; 8120 Tectonophysics: Dynamics of lithosphere and mantle—general; 8155 Tectonophysics: Plate motions—general; *KEYWORDS:* island arc, Wadati-Benioff Zone, subduction, tectonics
Citation: Stern, R. J., Subduction zones, *Rev. Geophys.*, *40*(4), 1012, doi:10.1029/2001RG000108, 2002.

1. INTRODUCTION

[2] Subduction zones are descending limbs of mantle convection cells and are the dominant physical and chemical system of Earth's interior. The sinking of lithosphere in subduction zones provides most of the force needed to drive the plates and cause mid-ocean ridges to spread, with the result that plate tectonics and subduction zones are surficial and interior expressions of Earth's dominant tectonic mode. Subduction zones are also our planet's largest recycling system. They deliver raw materials to the subduction factory, where oceanic lithosphere, sediments, and seawater reequilibrate with ambient mantle, triggering melting and incidentally creating continental crust. What is not recycled in the upper few hundred kilometers of a subduction zone sinks to the core-mantle boundary, where this residue may be reheated for a billion years or so until it is resurrected as a mantle plume [*Hofmann*, 1997]. There is a continuum from subduction, involving normal oceanic lithosphere, to collision, involving continental lithosphere or oceanic lithosphere with thickened crust. When continental crust is caught in the maw of a subduction zone, the smooth operation of the subduction zone is spectacularly disrupted, and a mountain range such as the Himalayas may result [*O'Brien*, 2001]. Nevertheless, continental crust has been carried down to depths of 100 km or more before resurfacing [*Ernst*, 1999].

[3] Among the terrestrial planets, only Earth appears to have subduction zones and plate tectonics. Mercury and Earth's moon are tectonically and magmatically dead, while Venus is dominated by thick lithosphere and mantle plumes [*Phillips and Hansen*, 1998]. Linear magnetic anomalies [*Connerney et al.*, 1999] and the presence of rocks similar to andesites [*Rieder et al.*, 1997] in the ancient southern highlands of Mars suggest that plate tectonics and subduction zones may have existed on that planet in the ancient past but no more. Mars has become a "single-plate" planet dominated by the immense volcanoes of the Tharsis region, the solar system's largest "hot spot" volcanoes.

[4] In addition to playing the central role in Earth tectonics, melt generation, and crustal evolution, subduction zones profoundly impact society to our benefit and detriment. Earthquakes and violent eruptions associated with subduction zones cause widespread and unpredictable death and destruction, while most of this planet's ore deposits formed as "specialty" distillates of subduction zones. One can speculate that if subduction zones did not exist to produce continental crust, the large exposed surfaces of rock known as continents would not exist, the Earth's solid surface would be

8755-1209/02/2001RG000108*$15.00*

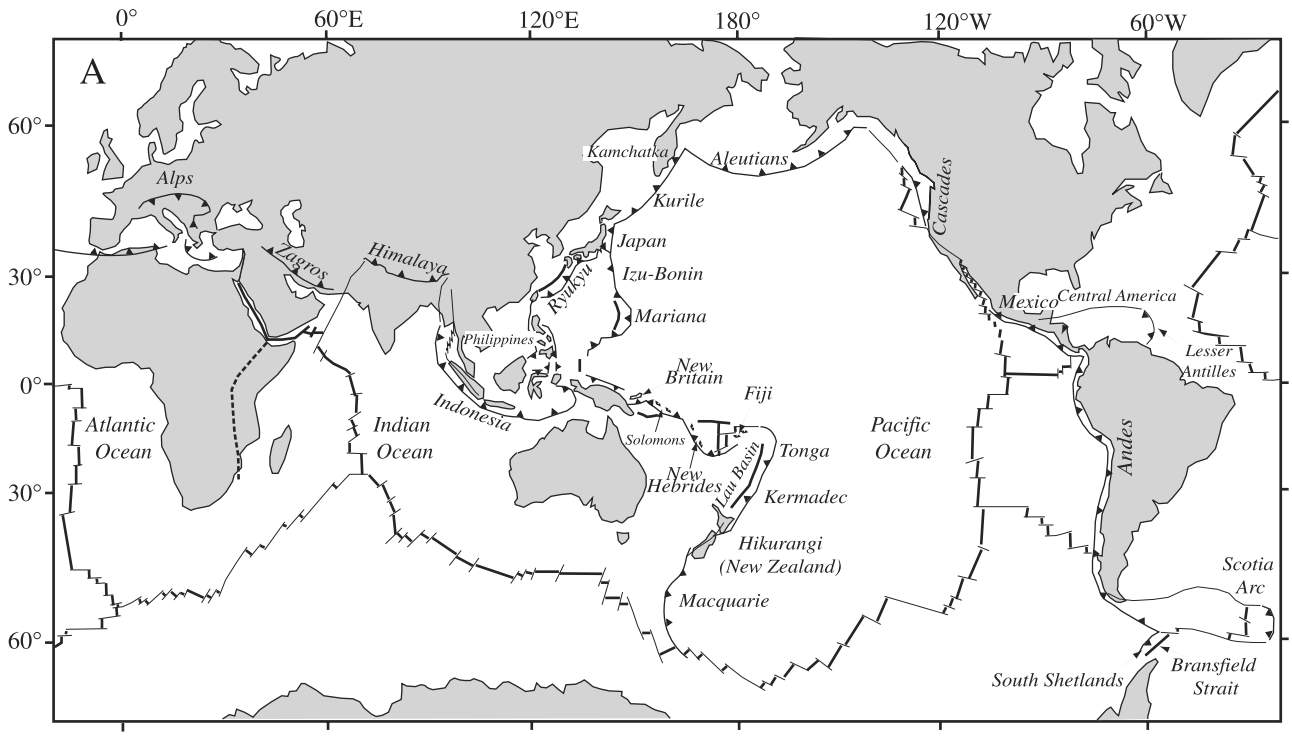

Figure 1. Subduction zones and convergent plate margins. (a) Location of convergent plate margins on Earth (modified after *Lallemand* [1999]). Active back arc basins are also shown. (b) Schematic section through the upper 140 km of a subduction zone, showing the principal crustal and upper mantle components and their interactions. Note that the location of the "mantle wedge" (unlabeled) is that part of the mantle beneath the overriding plate and between the trench and the most distal part of the arc where subduction-related igneous or fluid activity is found. MF stands for magmatic front. (c) Schematic section through the center of the Earth, which shows better the scale of subduction zones. Subducted lithosphere is shown both penetrating the 660 km discontinuity (right) and stagnating above the discontinuity (left). A mantle plume is shown ascending from the site of an ancient subducted slab. Dashed box shows the approximate dimensions of the shallow subduction zone of Figure 1b.

flooded, and terrestrial life, including humans, would not have evolved.

[5] Subduction zones burrow deeply but are imperfectly camoflaged, and we can use geophysics and geochemistry to watch them. Not surprisingly, the shallowest portions are known best. Subduction zones are strongly asymmetric for the first several hundred kilometers. Their dimensions are defined by deep trenches, lines of volcanoes parallel to the trenches, and inclined planar arrays of deep earthquakes that dip away from the trench beneath the volcanoes and extend down to the 660 km discontinuity. Earthquakes in subduction zones occur at enormously greater depths than elsewhere on Earth, where seismicity is limited to the uppermost 20 km. This requires either that brittle conditions extend to much greater depths or that there are unusual causes of seismicity in subduction zones. Seismic tomography provides additional details. This technique uses seismic velocity information from many ray paths, crisscrossing Earth between various points near Earth's surface and reaching different depths in its interior, to produce a three-dimensional (3-D) model of relative velocity. Regions of anomalously fast mantle corresponding to the earthquake plane define the downgoing lithospheric slab, and regions of anomalously slow mantle lie above this. Subducted lithosphere sometimes can be traced this way past the 660 km discontinuity into the lower mantle.

[6] The term subduction zone is sometimes used interchangeably with convergent (destructive) plate margin or island arc, and while all three terms are intimately related, they are not synonomous. Subduction zones are the three-dimensional manifestation of convective downwelling, convergent plate margins are the surficial manifestations of downwelling, and arcs (better referred to as arc-trench complexes) are surficial and crustal manifestations of a subduction zone that is operating beneath it. A useful historical review of the subduction zone concept is given by *White et al.* [1970].

[7] Subduction zones are formally distinct from convergent plate margins because the latter are required by plate tectonics, that is, the motions of rigid spherical shells around the Euler pole of rotation, whereas none of the geometric rules of plate tectonics applies to the behavior of the lithosphere once it descends below the surface. Subduction zones are defined by the inclined

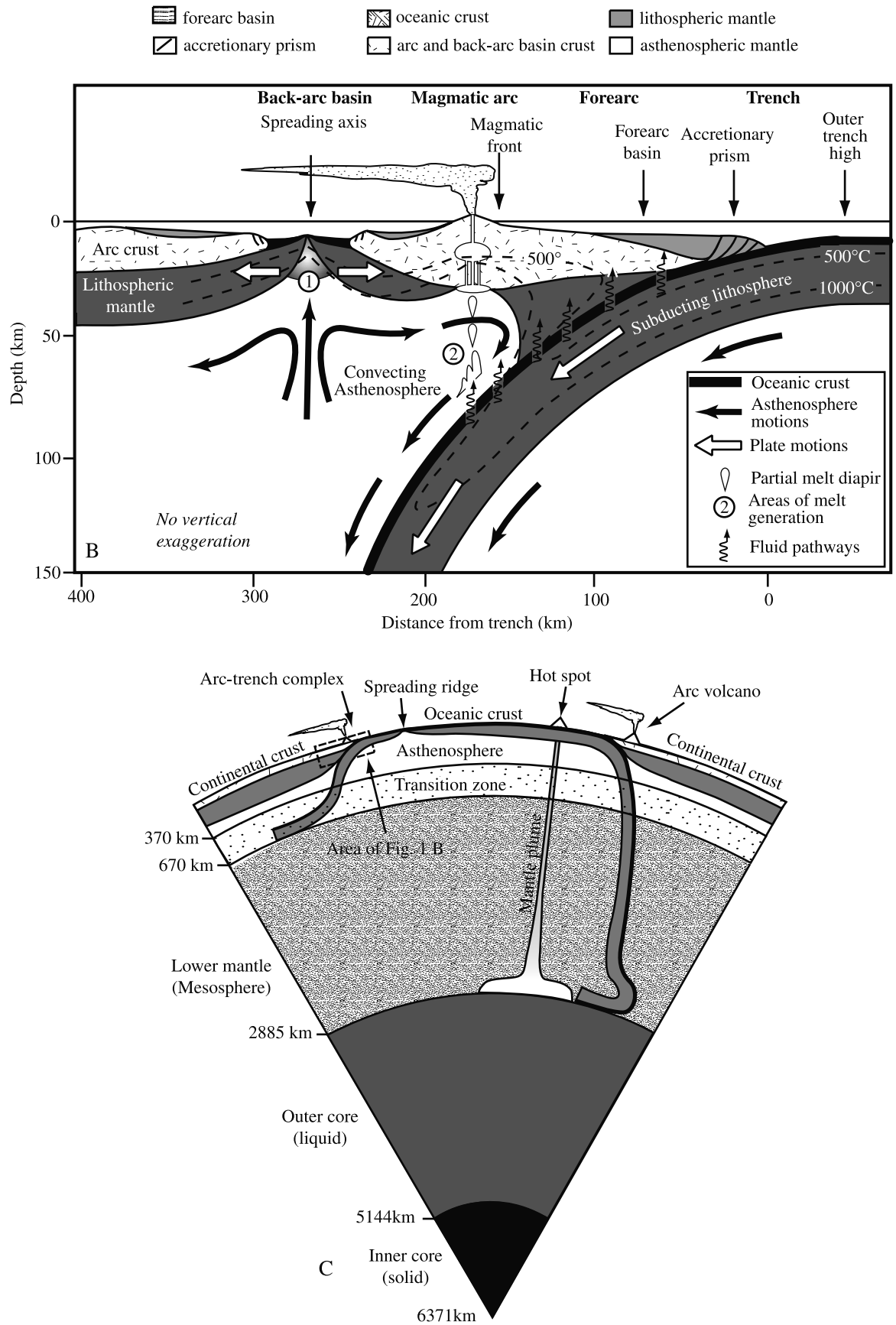

Figure 1. (continued)

Table 1. Subduction Zone Websites

	Website
MARGINS subduction factory	http://www.ldeo.columbia.edu/margins/SubFac.html
MARGINS seismogenic zone	http://www.ldeo.columbia.edu/margins/SeismZone.html
Geochemical Earth Reference Models	http://www.earthref.org/GERM/main.htm
Geochemistry of rocks of the oceans and continents	http://georoc.mpch-mainz.gwdg.de/
Volcano world	http://volcano.und.nodak.edu/vw.html
Global Volcanism Program	http://www.nmnh.si.edu/gvp/
Three-dimensional representation of subduction zones	http://piru.alexandria.ucsb.edu/collections/kirkby_morin/gdyn/main.html
U.S. Geological Survey "Dynamic Earth"	http://pubs.usgs.gov/publications/text/dynamic.html

array of earthquakes known as the "Wadati-Benioff Zone" after the two scientists who first identified it. Subduction zones are also distinct from arc-trench complexes. Arcs are consequences of subduction zone processes preserved in the overlying crust, geological evidence of deformation and chemical recycling caused by subduction. Not all arcs are truly island arcs, but the description fits because it captures the sense of a curved array of discrete volcanoes engendered by subduction. Although they are relatively minor components of subduction zones in terms of mass, arcs are important because they provide accessible samples of the products of interacting mantle and subducted materials and testify to the operation of ancient subduction zones. Arcs are also nurseries for continental crust, where thickened welts of low-density crust are generated and processed further to await accretion to other tracts of buoyant crust.

[8] The relationship between subduction zones and convergent plate margins is better appreciated when their typical representations are considered together. Convergent plate margins appear in map view (Figure 1a), whereas subduction zones are typically shown as cross sections (Figures 1b and 1c). Combining these two perspectives more realistically presents the globe-encircling and mantle-permeating nature of the subduction zone system. Representations of subduction zones in three dimensions have been shown by *Chiu et al.* [1991] and on a website listed in Table 1.

[9] The cumulative length of convergent plate margins is >55,000 km [*Lallemand*, 1999], almost equal to that of mid-ocean ridges (60,000 km [*Kearey and Vine*, 1990]). Lithosphere consumed at subduction zones may pond at the base of the transition zone, 660 km beneath the surface, or may plunge to the core-mantle boundary, 2900 km beneath the surface (Figure 2). The subduction zone system is clearly the most extensive and pervasive feature of our planet. Most geodynamicists agree that the plates move because of the sinking of lithosphere in subduction zones [*Forsyth and Uyeda*, 1975; *Davies and Richards*, 1992]. The scale and role of subduction zones indicate that they are the most important tectonic feature of our planet.

[10] In the following sections the components of subduction zones are described, and their interactions are discussed. This overview is intended to present the most important aspects of subduction zones to a broad spectrum of Earth scientists and students. It is primarily intended for two groups of geoscientists: (1) the advanced undergraduate or beginning graduate student who is beginning to think broadly about what to study and (2) the professional who does not specialize in studying subduction zone processes but is interested or needs to know more about them. The fact that we have just celebrated the fiftieth anniversary of the introduction of the term "subduction" by *Amstutz* [1951] makes this overview all the more appropriate.

2. SUBDUCTION ZONE COMPONENTS

[11] Because some subduction zones extend from the Earth's surface down to the 660 km transition zone and thence to the core-mantle boundary, it is very difficult to show these features at true scale on a single diagram. This is clear from comparing Figures 1a and 1c, where the most familiar features are the shallowest (<200 km deep) and the deeper portions are much more poorly understood. A partial remedy is offered in Figure 3 where the spatial distribution of important features is shown on a semilog scale.

[12] In the following discussion, subduction zones are described in the following order: inputs, processes, and products. A fourfold subdivision is used: incoming plate, downgoing plate, mantle wedge, and arc-trench complex. Much of the material that enters the trench is never recycled and sinks as residue to the core-mantle boundary. Although an important topic, this aspect is not discussed here.

3. INCOMING PLATE

[13] The plate of "plate tectonics" is otherwise known as lithosphere, the relatively strong part of the outer Earth that cools dominantly by conduction. Lithosphere is composed of crust and the uppermost mantle. Mantle lithosphere, crust, and sediments of the incoming plate

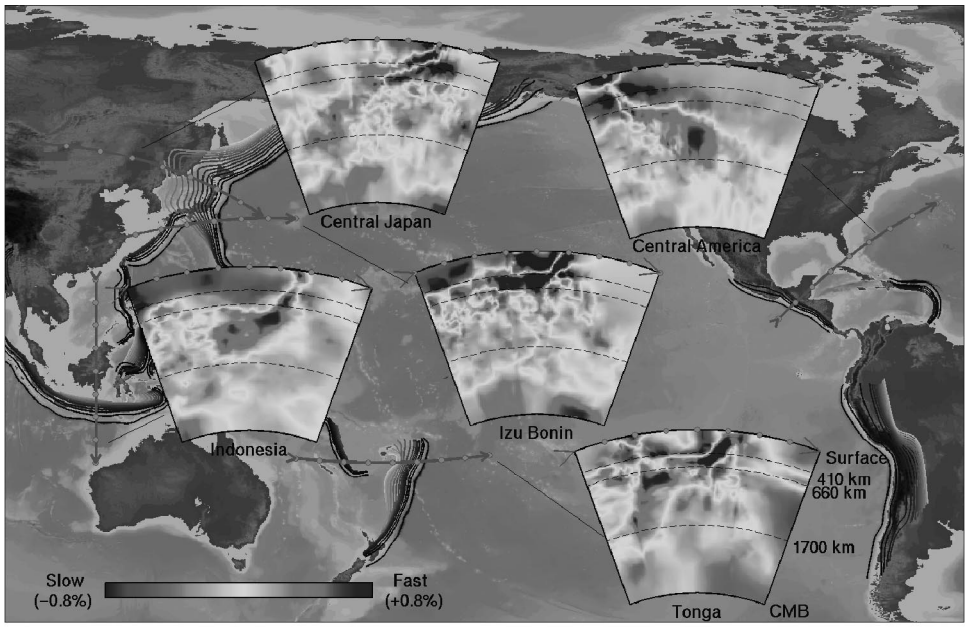

Figure 2. Structure of subducted slabs as inferred from mantle tomography (from *Kárason and van der Hilst* [2000]). Red lines show the surface projection of each section. The base of each section is the core-mantle boundary (CMB); dashed lines show the location of mantle discontinuities at 410, 660, and 1700 km. Red and blue colors in each section denote regions where the *P* wave velocities are relatively slow and fast, respectively, compared to average mantle at the same depth. Fast regions are most easily interpreted as relatively cool areas corresponding to the subducted slab and its viscous mantle blanket. This allows the cool, subducted slab to be traced well below the deepest earthquake. Note that some slabs penetrate the 660 km discontinuity and descend into the lower mantle (e.g., Central America, central Japan, and Indonesia), while other slabs seem to stagnate in the upper mantle (such as Izu-Bonin). The subducted slab beneath Tonga seems to stagnate at the 660 km discontinuity for a while, then cascade into the lower mantle. See color version of this figure at back of this issue.

exert fundamental controls on the behavior of subduction zones but in quite different ways. A justifiable oversimplification is that mantle lithosphere controls the physics of subduction, sediments control the chemistry of subduction, and the crust plays an important role in both chemistry and physics. Note that subducted sediments, crust, and mantle lithosphere may be described separately or in combination and may be called "subducted slab" or just "slab." These controls are discussed in turn in sections 3.1–3.3.

3.1. Mantle Lithosphere

[14] Mantle lithosphere is widely accepted to be slightly more dense than underlying asthenosphere, by ~1–2%, and it is this excess density that powers subduction zones and moves the plates [*Davies*, 1999]. Density excess increases as the lithosphere ages and thickens, and the observed asymmetry in lithosphere age in the eastern versus the western Pacific basin leads to fundamentally different subduction zones on each flank of the Pacific "Ring of Fire." Seafloor about to descend at convergent margins ranges in age from ~170 Ma (east of the Mariana trench) to 0 (spreading ridges being subducted off North and South America). Whereas thickness of the oceanic crust is relatively constant at 6–7 km, lithosphere thickness and the depth of the seafloor varies as a simple function of age [*Stein and Stein*, 1996]. Age of the lithosphere also exerts the first-order control on trench depth [*Grellet and Dubois*, 1982]. Globally, the mean age of the seafloor when it arrives at a trench is ~100 Ma [*Parsons*, 1982], corresponding to a thermal lithosphere thickness of ~100 km. Mantle lithosphere should have an upper portion of harzburgite, residual after mid-ocean ridge basalt (MORB) formation, and a lower layer of less depleted lherzolite [*Irifune*, 1993]. Due to age-dependant thickening, lithosphere becomes negatively buoyant with respect to underlying asthenosphere when it is 10–30 million years old [*Davies*, 1992; *Cloos*, 1993]. It follows that most oceanic lithosphere upon reaching the appropriate trench sinks readily, and it is this large amount of gravitational potential energy that moves the lithosphere and drives plate tectonics. Nevertheless, a significant proportion of convergent margins subduct seafloor that is <10–30 Ma; such buoyant lithosphere will resist subduction.

[15] *Hamilton* [1988, p. 1507] emphasizes that the widely accepted idea that "... a subducting plate rolls over a hinge and slides down a slot that is fixed in the mantle ..." is generally wrong. The subducted plate commonly sinks at a steeper angle than the dip of the

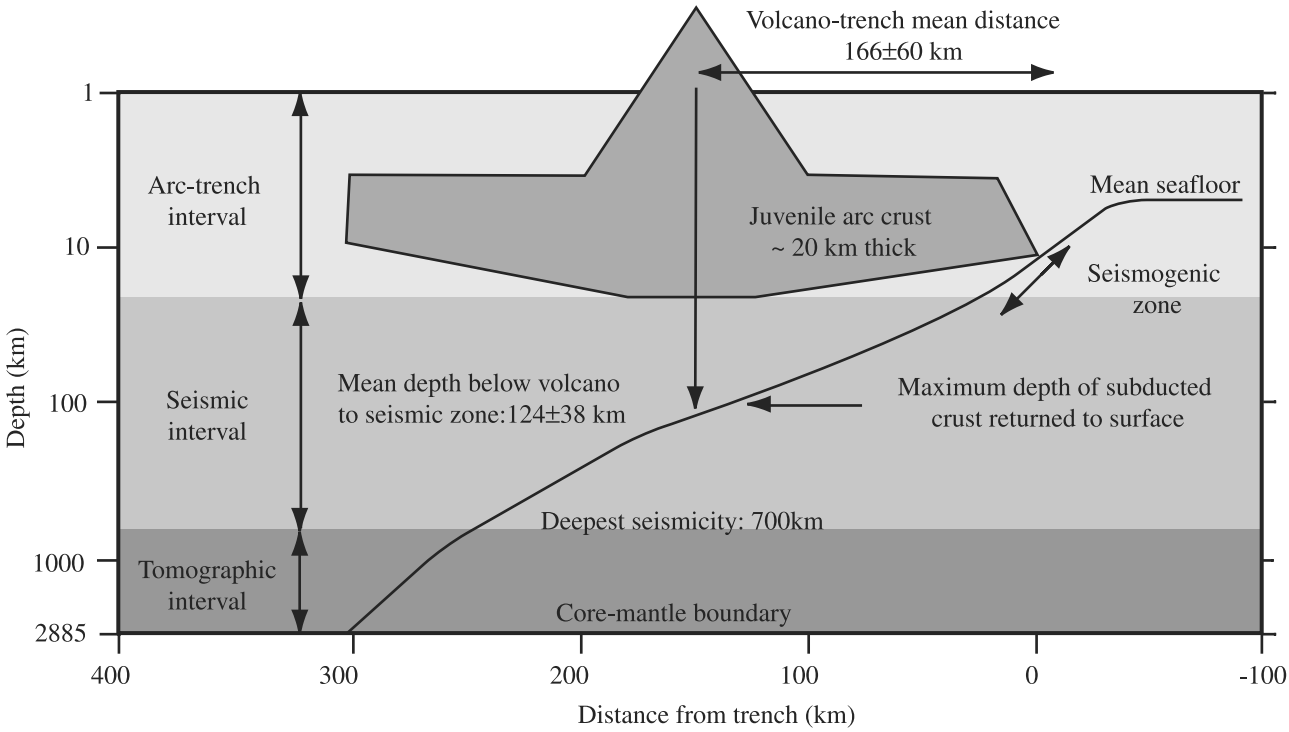

Figure 3. Semilog scale plotting the depth dimension for subduction zones from 1 km below the surface to the core-mantle boundary. Mean depth of ocean (3880 m) is from *Kennett* [1982]. Typical crustal thickness (~20 km) for juvenile arc crust is from *Suyehiro et al.* [1996]; crust associated with Andean-type convergent margins may be up to 70 km thick. Mean distance of arc volcanoes to trench (166 ± 60 km) and of depth beneath arc volcano to seismic zone (124 ± 38 km) are from *Gill* [1981]. Greatest depth of subducted material returned to surface (~100 km) is from *Ernst* [1999]. Note vertical axis encompasses >3 orders of magnitude.

seismic zone [*Garfunkel et al.*, 1986], causing the trench to migrate toward the ocean or "roll back." Old, dense lithosphere readily sinks, while young, buoyant lithosphere resists subduction. Subduction of old lithosphere results in relatively steep subduction zones, whereas subduction of young lithosphere is characterized by shallower dips [*Jarrard*, 1986]. Subduction of young, buoyant lithosphere results in strong coupling between the plates, and these subduction zones tend to have higher magnitude earthquakes compared to those subducting old lithosphere. Subduction zone dip also affects flow of asthenosphere in the mantle wedge, with shallow dips restricting this flow [*Kincaid and Sacks*, 1997].

[16] The very different behavior of subduction zones involving young and old lithosphere is also shown in the strain regime manifested behind the magmatic arc: Some subduction zones spawn back arc basins with rifting or even seafloor spreading, whereas others induce folding and thrusting behind the arc. *Jarrard* [1986] subdivided subduction zones into seven strain classes, with class 1 being strongly extensional and class 7 being strongly compressional. He found that the strain regime in the overlying plate is highly correlated with the age of the subducted lithosphere and the absolute motion of the overriding plate.

[17] A first-order differentiation of subduction zones distinguishes those subducting old lithosphere (Mariana type) from those subducting young lithosphere (Chilean type) (Figure 4). Mariana-type subduction zones are strongly extensional (strain class 1) with weak coupling between the two plates, whereas Chilean-type subduction zones are strongly compressional (strain class 7) with strong coupling between the two plates.

3.2. Crust

[18] Subducted crust affects subduction zones in several ways. First, its density and thickness largely determine whether the subduction zone operates normally or fails. Normal oceanic crust is invariably subductable, but subduction of continental crust leads to subduction zone failure. Failure of a subduction zone happens when sufficient buoyant material is introduced into it to disrupt downwelling. This is called collision or terrane accretion. Contrasts in lithospheric bulk density (crust plus mantle) of <0.1 gm cm^{-3} determine whether normal subduction or collision occurs [*Cloos*, 1993]. Buoyancy analysis indicates that only bodies of continental and intraoceanic arc crust greater than ~15 km thick cause subduction zone failure and that oceanic plateaus must have crust greater than ~30 km thick to have a similar effect [*Cloos*, 1993]. The third dimension is critical for evaluating the total effect of buoyant crust on a subduction zone. For example, end-on subduction of a linear tract of arc crust may locally disrupt a subduction

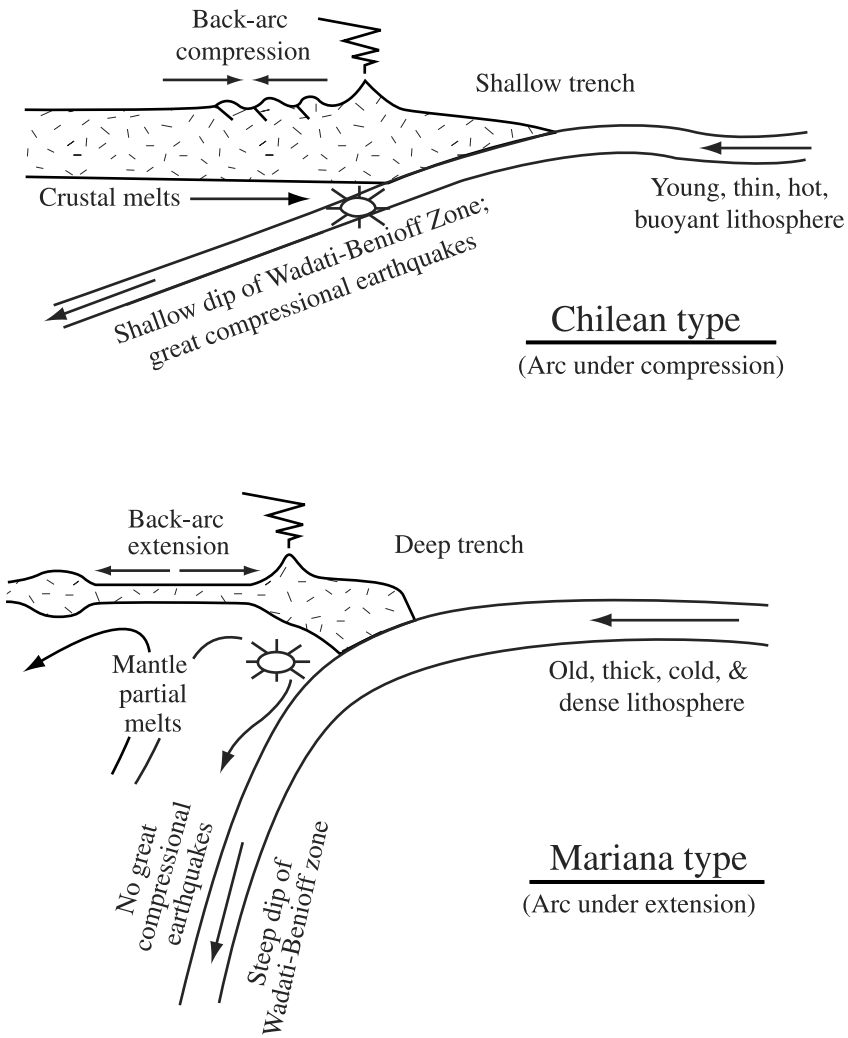

Figure 4. End-member types of subduction zones, based on the age of lithosphere being subducted (modified after *Uyeda and Kanamori* [1979]).

zone but not cause it to fail, as is the case for the Izu Collision Zone, Japan [*Mazzotti et al.*, 1999]. Delivery of similarly buoyant crust parallel to the trench is more likely to lead to subduction zone failure, as in the case of the attempted subduction of the broad Ontong Java Plateau by the Vitiaz Trench during Miocene time [*Cooper and Taylor*, 1985].

[19] Second, oceanic crust transports a significant fraction of the chemicals processed in subduction zones. Oceanic crust is ~6 km thick and is composed of MORB and diabase underlain by gabbroic equivalents. Fresh MORB is depleted in incompatible trace elements and contains almost no water. Abundances of water, CO_2, and incompatible trace elements (especially K and U) increase significantly because of hydrothermal alteration, which also leads to formation of amphibolites at greater depth in the crust, and seafloor weathering. Oceanic crust also contains a large proportion of the water carried into subduction zones [see *Wallmann*, 2001, Figure 1]. Alteration most profoundly affects the uppermost 500 m of basalts, for which *Staudigel et al.* [1996] infer 2.7% H_2O, 3.0% CO_2, and a twofold to threefold increase in K. Formation of amphibolites in the lower crust sequesters significant amounts of water but little else [*Carlson*, 2001]. The presence of even small amounts of serpentinite in the oceanic crust is important for water cycling through subduction zones, because equal volumes of serpentinite carries an order of magnitude more water than hydrated mafic crust and because serpentinite is stable to much greater pressures (13% H_2O versus 1–2% in hydrated mafic crust and 7 GPa or more versus ~3 GPa [*Pawley and Holloway*, 1993; *Ulmer and Trommsdorf*, 1995]).

[20] Crust produced at slow and fast spreading ridges stores water bound in minerals differently. Whereas fast spreading ridges are robust magmatic systems that produce crust composed almost entirely of basalt, diabase, and gabbro, slow spreading ridges have intermittent igneous activity, or it may be absent altogether, so that this crust may be largely composed of serpentinized peridotite. Because serpentine contains more water than altered basalt or gabbro and because crust produced at

slow spreading ridges contains more serpentinite than crust formed at fast spreading ridges [*Karson*, 1998], slow spreading crust may carry proportionally more water into subduction zones than fast spreading crust.

[21] Oceanic crust produced by fast spreading is probably pervasively hydrated, but associated peridotites are not, except at transform faults and fracture zones. Oceanic crust produced at slow spreading ridges is probably much more heterogeneous, with masses of unaltered crust (as wide as a few tens of kilometers) separated by major fault zones that penetrate the full thickness of the crust and result in substantial serpentinization of mantle rocks. The issue of how much serpentinized peridotite makes up the oceanic crust produced at slow spreading ridges is an important and unresolved controversy. Recently, *Carlson* [2001] concluded from seismic velocity data for the slow spreading North Atlantic that no more than 13% of this oceanic crust could be composed of serpentinized ultramafics.

[22] We need to understand better how much of the subducted lithosphere is serpentinized, both in order to understand the subduction zone water budget and to understand how much work is required to bend plates. Very deep (up to 50 km) earthquakes related to normal faulting on the outer trench rise may allow seawater to infiltrate and serpentinize mantle at much greater depths in the lithosphere than would be expected to otherwise occur [*Peacock*, 2001]. If so, this would increase the proportion of serpentinite in the lithosphere, with the effect of significantly increasing the amount of mineralogically bound water carried into subduction zones. Because serpentine is very weak, this would also weaken the lithosphere and greatly reduce the amount of work needed to bend the plate.

[23] It has been relatively difficult to identify components derived from subducted oceanic crust in arc lavas. O isotopic compositions are shifted to much heavier values for the upper, altered crust, but this is balanced by lighter compositions in deep crustal amphibolites. O isotopic compositions of fresh arc lavas are generally very similar to that expected for basalts extracted from normal mantle [*Eiler et al.*, 2000]. At present, B isotopes seem to have the greatest promise for identifying subducted crustal components in arc lavas [*Ishikawa and Nakamura*, 1994; *Smith et al.*, 1995].

3.3. Sediments

[24] Sediments carried on the subducting plate do little to aid or impede the subducting lithosphere but are crucial for element recycling. The nature of subducted sediments may also influence the nature of great shallow earthquakes. Estimates of the mass of sediments subducted annually range from about 1×10^{15} g yr^{-1} [*Veizer and Jansen*, 1985; *Hay et al.*, 1988] to 3–4 $\times 10^{15}$ g yr^{-1} [*von Huene and Scholl*, 1991].

[25] Sediments may be the ultimate source of many of the unusual enrichments and other chemical signatures found in arc lavas. The presence in some arc lavas of ^{10}Be, which is produced only in the upper atmosphere and which has a half-life of 1.6 million years, testifies to the recycling of sediments through the subduction zone [*Morris et al.*, 1990]. The covariation of other, fluid-mobile trace elements (such as K, Sr, Ba, and Th) has also been interpreted to indicate the importance of sediment recycling [*Plank and Langmuir*, 1993]. In contrast to the limited range in compositions present in the mantle lithosphere and oceanic crust, the compositional variety of sedimentary columns being subducted provides potentially distinctive inputs into subduction zones. For example, sediments entering a few subduction zones are dominated or strongly influenced by carbonate sediments (e.g., Peru-Chile, Central America, and the Aegean), and some subduction zones are dominated or strongly influenced by terrigeneous sediments (e.g., the Aleutians, Cascades, and Nankai) or siliceous sediments (e.g., Kamchatka [*Rea and Ruff*, 1996]). The most unusual sedimentary sequence on any subducted plate has to be the Messinian (~7 Ma) evaporites on Mediterranean crust, the subduction of which may be responsible for unusual compositions of Mediterranean arc volcanoes.

[26] A mean composition for subducted sediments, global subducting sediment (GLOSS), is a useful approximation of the average composition of subducted sediment [*Plank and Langmuir*, 1998]. GLOSS is similar in composition to upper continental crust (Table 2). GLOSS is dominated by terrigeneous material (76%) but contains significant proportions of biogenic calcium carbonate (7%) and silica (10%), along with 7% mineral-bound water. According to a similar calculation, *Rea and Ruff* [1996] concluded that there is about twice as much carbonate as silica in the nonterrigeneous component. Sediments carry 1–2 km^3 yr^{-1} of interstitial water into subduction zones [*von Huene and Scholl*, 1991; *Moore and Vrolijk*, 1992]. Most of this pore water is squeezed out at very shallow depths, and it is estimated that a few cubic meters of water are squeezed out annually for each meter along the trenches [*Rea and Ruff*, 1996]. This "shallow water" recycling of ~1 km^3 yr^{-1} requires ~1.5 billion years to completely recycle the ocean.

4. DOWNGOING PLATE

[27] Most of the action associated with subduction zones happens deep below the surface. Our understanding of these processes is largely inferential, based on geophysics and geochemistry of active systems and on studies of exhumed subduction zones. Sections 4.1–4.4 outline some of the most important considerations.

4.1. Subduction Zones Are Mostly Cool

[28] Seismicity is the diagnostic expression of subduction zones, and this is controlled differently at different depths. Shallow earthquakes (<50 km depth) manifest

Table 2. Chemical Composition of Typical Subduction Zone Inputs and Outputs[a]

	GLOSS	*N-MORB*	*Boninite*	*Arc Tholeiite*	*Back Arc Basin Basalt*	*Andean Dacite*	*Continental Crust*
SiO_2, %	58.55	50.45	58.62	49.87	51.3	64.91	57
TiO_2	0.62	1.62	0.14	0.87	0.69	0.86	0.9
Al_2O_3	11.91	15.26	11.76	15.86	17.12	16.32	15.9
FeO*	5.21	10.43	9.28	10.53	7.08	4.03	9.1
MnO	0.32		0.15	0.2	0.14	0.06	
MgO	2.48	7.58	10.04	7.31	7.55	1.86	5.3
CaO	5.95	11.3	6.89	12.15	13.33	4.08	7.4
Na_2O	2.43	2.68	2.44	2.35	2.14	4.37	3.1
K_2O	2.04	0.11	0.67	0.69	0.5	3.23	1.3
P_2O_5	0.19		0.01	0.17	0.15	0.28	
CO_2	3.01						
H_2O	7.29						
Total	100	99.43	100	100	100	100	100
Mg#[b]	45.9	56.4	65.9	55.3	65.5	45.1	50.9
Sc, ppm	13.1	41	30	34	37	5.06	30
V	110		176	324	214	92	230
Cr	78.9		481	144	218	16	185
Co	21.9	47	35	46	34	23	29
Ni	70.5	150	103	43	82	12	128
Cu	75	74	89	145	102	31	75
Zn	86.4		66	75	50	69	80
Rb	57.2	1.26	13	5.6	9.3	85	37
Cs	3.48	0.014		0.19	0.13	4.69	1.5
Sr	327	113	86	423	365	752	260
Ba	776	13.9	35	126	150	1231	250
Y	29.8	35.8	4	17.5	15.7	8	20
Zr	130	104	27	43.8	51	173	100
Hf	4.06	2.97	0.75	1.21	1.26	8	3
Nb	8.94	3.51	0.66	0.76	3.05	3.25	8
Ta	0.63	0.19	0.06	0.04	0.16	0.44	0.8
La	28.8	3.9	0.86	4.24	9.76	40.28	16
Ce	57.3	12	1.8	9.73	19.03	86.73	33
Nd	27	11.18	1.24	7.65	10.61	33.59	16
Sm	5.78	3.75	0.47	2.11	2.59	5.43	3.5
Eu	1.31	1.335	0.14	0.82	0.895	1.77	1.1
Gd	5.26	5.08	0.46	2.54	2.73	4.68	3.3
Dy	4.99	6.3	0.62	2.84	2.57	2.19	3.7
Er	2.92	4.14	0.48	1.66	1.44	0.76	2.2
Yb	2.76	3.9	0.68	1.49	1.38	0.55	2.2
Lu	0.413	0.59	0.12	0.29	0.21	0.10	0.3
Pb	19.9	0.49	1.99	4.11	1.64	17.22	8
Th	6.91	0.187	0.23	0.55	1.5	16.50	4.2
U	1.68	0.071	0.21	0.28	0.41	4.70	1.1

[a]Compositions of subduction zone inputs are global subducting sediment (GLOSS) and mid-ocean ridge basalt (MORB) and of outputs are boninite, arc tholeiite, Andean dacite, and continental crust. Sources of data are as follows: GLOSS [*Plank and Langmuir*, 1998]; fresh normal MORB [*Hofmann*, 1988]; boninite (X-108, Marubewan, Chichijima, and Bonin Islands [*Pearce et al.*, 1992]; arc tholeiite (AYC42 and Vanuatu [*Peate et al.*, 1997]; back arc basin basalt (T7-48:1 (J. A. Pearce et al., unpublished data, 2001); Andean dacite (TAP-001, Taapaca, and Chilean Andes [*Wörner et al.*, 1992]; and continental crust [*Taylor and Mclennan*, 1985; *McLennan and Taylor*, 1996].

[b]Mg# is magnesium number (100Mg/Mg + Fe).

coupling between subducted and overriding plate. Fast subduction of young, buoyant lithosphere leads to stronger coupling and larger maximum earthquakes, while slow subduction of old lithosphere leads to weak coupling and smaller maximum earthquakes in this depth range. Weak coupling is also a characteristic of convergent margins with active back arc basins (Figures 4 and 5b). The fact that the biggest maximum earthquakes tend to occur beneath Andean-type arcs (arcs built on continental crust) may also be partly due to the greater strength of continental crust compared to oceanic crust under cold, wet forearc conditions [*McCaffrey*, 1994].

[29] In contrast, earthquakes deeper than ~50 km are controlled by the thermal state of the subducted lithosphere. Deep earthquakes mark where the subducted slab is relatively cool, and the maximum depth reflects how long it takes to reheat the subducted slab so that it no longer ruptures [*Molnar et al.*, 1979; *Jarrard*, 1986].

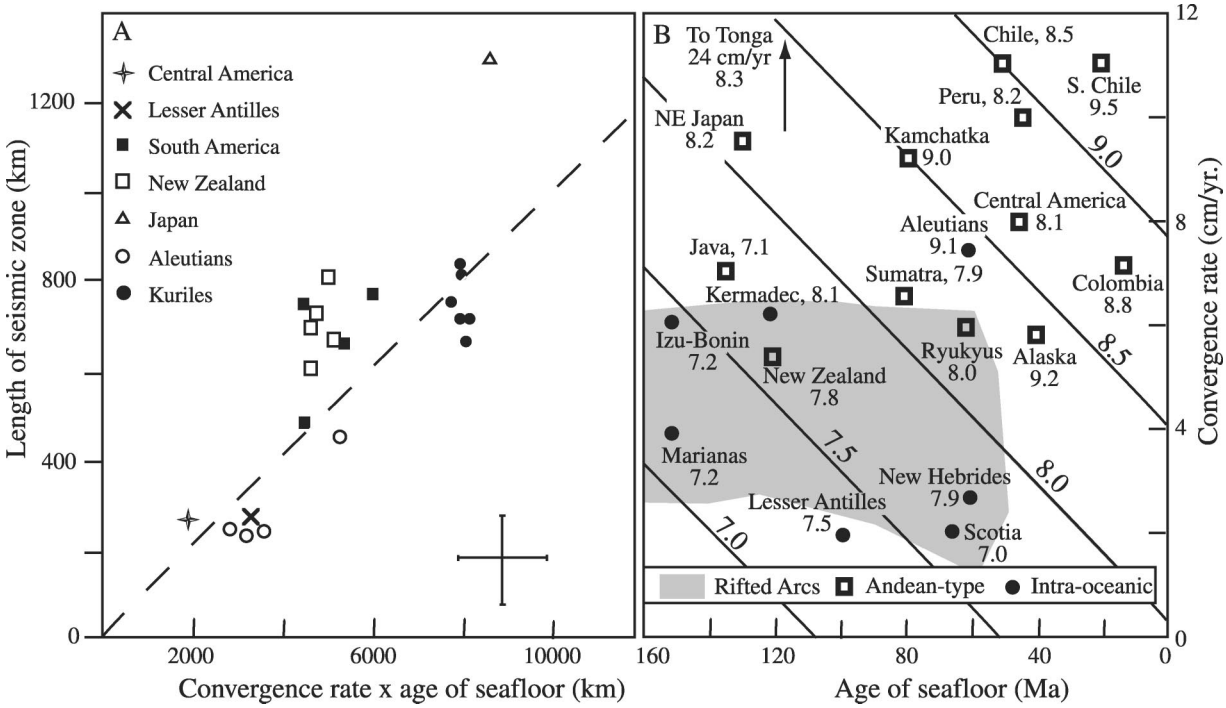

Figure 5. Importance of convergence rate and age of subducted lithosphere. (a) Plot of length of seismic zone as a function of the product of convergence rate and age of subducted lithosphere. Approximate uncertainties are given by error bars. Dashed line corresponds to length of seismic zone equal to convergence rate multiplied by age divided by 10 (modified after *Molnar et al.* [1979]). (b) Plot of convergence rate versus lithosphere age, showing the strong influence this relationship has on seismicity (modified after *Ruff and Kanamori* [1980], using GPS-defined convergence rates for Pacific-Tonga [*Bevis et al.*, 1995]. The number at each subduction zone is the associated maximum M_w (seismic moment magnitude), and the contours of constant M_w are defined by regression analysis. Shaded area outlines subduction zones associated with back arc spreading or interarc rifting. Note that most of the biggest earthquakes occur at Andean-type margins.

Because the subducted slab is mostly heated by conduction, we predict that old (cold) lithosphere that is subducted quickly should depress geotherms the most, take the longest time to heat up, and have the deepest earthquakes. This prediction has been empirically confirmed. A plot of seismic zone length versus the product of the convergence rate (V) and the age of the subducted slab at the trench (A) approximate the simple relationship: seismic zone length $= V \times A/10$ (Figure 5a) [*Molnar et al.*, 1979]. The magnitude of the largest earthquake in a given subduction zone also seems to depend on the age of the subducted lithosphere and how fast it is subducting. Old, slow lithosphere sinks quietly; young, fast lithosphere yields more large earthquakes (Figure 5b).

[30] The relationship between the age, convergence rate, and thermal state of the subducted lithosphere is outlined by *Kirby et al.* [1991]. Depression of mantle isotherms in the subduction zone is proportional to the thermal parameter $\phi = A(V_n \sin \delta)$, where V_n is the convergence rate perpendicular to the trench and δ = dip of the subduction zone. This relationship is strikingly similar to the simple relationship between seismicity and the product of age and convergence rate just discussed. In detail, the thermal structure of a subduction zone

Figure 6. (opposite) Geophysical images of subduction zones. (a) *P* wave tomographic image of NE Japan (modified after *Zhao et al.* [1994]). There is no vertical exaggeration. (b) *P* wave tomographic image of Tonga subduction zone (modified after *Zhao et al.* [1997]). There is no vertical exaggeration. For both Figures 6a and 6b, red and blue colors denote regions where the *P* wave velocities are relatively slow and fast, respectively, compared to average mantle at the same depth. (c) *P* wave velocity structure across the Cascadia Subduction Zone (modified after *Parsons et al.* [1998]). Yellow dots show earthquakes during 1970–1996 between 45° and 47° latitude, $>M1$ at depths >25 km and $>M4$ at shallower depths. Note vertical exaggeration is 2x. Note that the subduction zones in Figure 6a and 6b subduct old, cold lithosphere, which is relatively easy to identify tomographically, whereas the subduction zone in Figure 6c subducts young lithosphere, which differs less in velocity relative to the surrounding mantle and is more difficult to image tomographically. See color version of this figure at back of this issue.

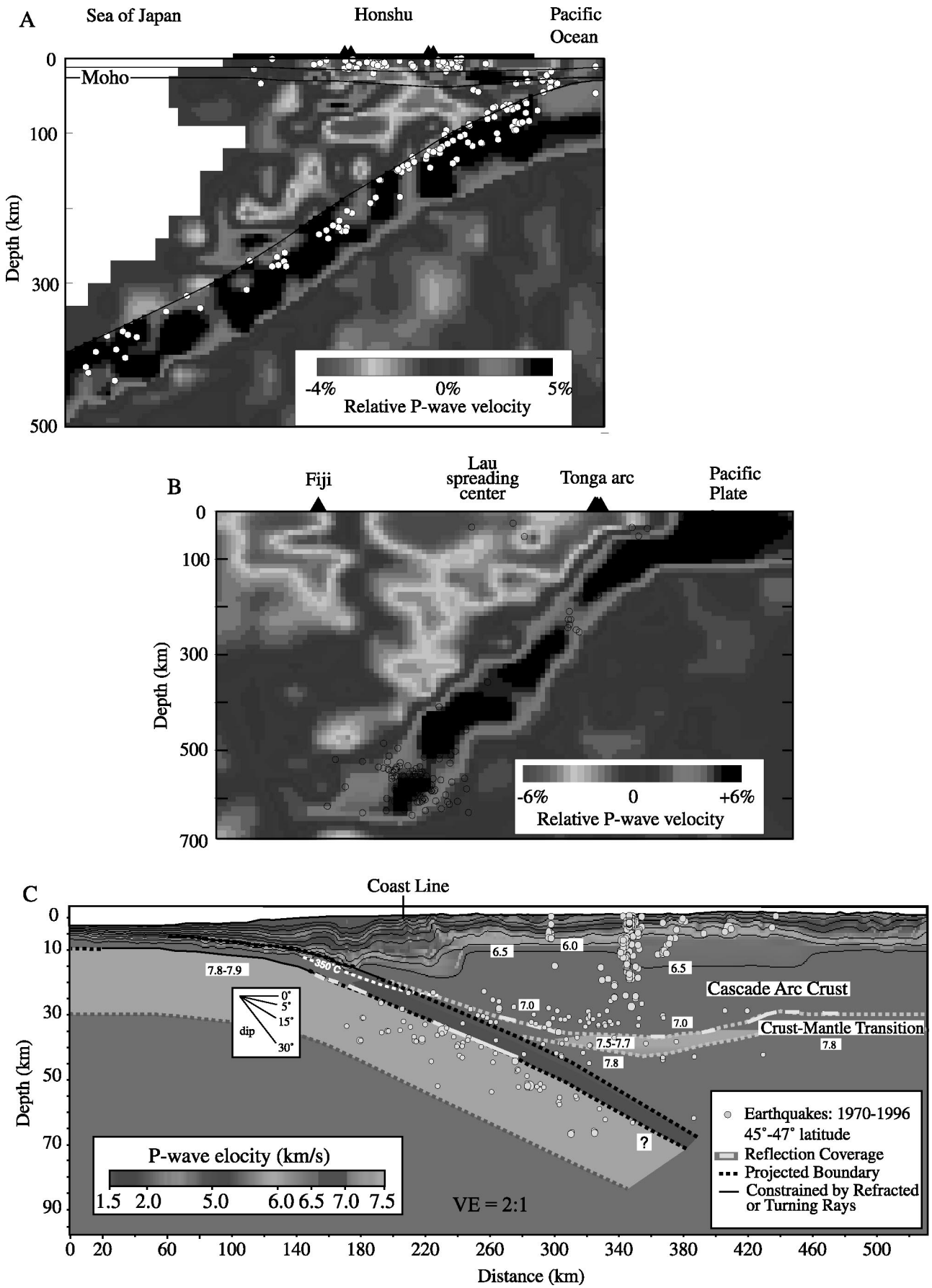
A
Sea of Japan
Honshu
Pacific Ocean
Moho
Depth (km)
0
100
300
500
-4%
0%
5%
Relative P-wave velocity
B
Fiji
Lau spreading center
Tonga arc
Pacific Plate
Depth (km)
0
100
300
500
700
-6%
0
+6%
Relative P-wave velocity
C
Coast Line
Depth (km)
0
10
30
50
70
90
7.8-7.9
350°C
6.5
6.0
6.5
7.0
7.0
7.5-7.7
7.8
7.8
Cascade Arc Crust
Crust-Mantle Transition
dip
0°
5°
15°
30°
?
P-wave elocity (km/s)
1.5 2.0 5.0 6.0 6.5 7.0 7.5
VE = 2:1
Earthquakes: 1970-1996
45°-47° latitude
Reflection Coverage
Projected Boundary
Constrained by Refracted or Turning Rays
0 20 60 100 140 180 220 260 300 340 380 420 460 500
Distance (km)

depends, in order of importance, on the age and speed of the incoming lithosphere, shear stresses across the subduction interface, induced convection in the overlying mantle wedge, geometry of subduction, enthalpies of metamorphic reactions, fluids migrating through the subduction zone, and radioactive heating. Low heat flow in forearcs (typically 25–50 mW m^{-2} [*Peacock*, 1996]), seismic coupling to depths of ~50 km [*Tichelaar and Ruff*, 1993], tomographic results showing that subduction zones are seismically fast (Figures 6a and 6b) [*Zhao*, 2001], and high-pressure, low-temperature metamorphic rocks exhumed from modern and ancient subduction complexes [*Fryer et al.*, 1999; *Cloos and Shreve*, 1988a] all indicate that subduction zones are cooler than the surrounding mantle.

[31] *Peacock* [1996] provides an excellent overview of thermal modeling of subduction zones. Models for the thermal evolution of two near-end-member subduction zones in NE Japan and SW Japan are shown in Figures 7a and 7b, respectively. A subduction zone that rapidly digests old, cold lithosphere (Figure 7a) is much colder at a given depth than one that slowly subducts young lithosphere (Figure 7b). This difference is shown in Figure 7c, where the temperature of subducted SW Japan oceanic crust is typically 300°–500°C hotter than that of equivalent portions subducted beneath NE Japan. There are of course many uncertainties in these models, foremost among which is estimating shear stresses between the subducted and overriding plate. Thermal models indicate that faster convergence leads to cooler subduction zone temperatures for shear stresses <20 MPa and warmer temperatures for shear stresses >20 MPa. Estimates of shear stresses based on surface heat flow measurements vary from 0 to ~100 MPa. On this basis, *Peacock* [1996] concluded that subduction zone shear stresses in the range of 10–30 MPa are most reasonable.

[32] These models of subduction zone thermal structure are supported by seismic imaging. Two important factors for tomographic imaging of subduction zones are the presence of significant differences in material properties, manifested as seismic velocities, and the seismic "illumination" of the subduction zone by deep earthquakes. Both vary with the thermal parameter, so it is not surprising that our best tomographic images are of western Pacific subduction zones (Figures 6a and 6b). Producing corresponding images of eastern Pacific and other subduction zones involving young lithosphere remain as significantly greater challenges (Figure 6c).

[33] The coolness of subduction zones allows the slab to be tomographically traced to great depth. Some slabs, such as that beneath Izu-Bonin (Figure 2), may stagnate at the 660 km discontinuity, but most slabs appear to penetrate into the lower mantle. There does not seem to be a relationship between the age of the subducting plate at the trench and whether or not the slab is able to penetrate into the lower mantle. The stagnating Izu-Bonin slab is ~100 Myr old at the trench, whereas the Central America slab is ~20 Myr old. This may partly reflect the fact that the age of the lithosphere subducted beneath Central America becomes much older down the slab and that this excess density is controlling the geometry of deep subduction. It takes tens of millions of years for the fastest-sinking slab to reach the core-mantle boundary. A slab sinking vertically at 10 cm yr^{-1} (a relatively fast rate) will reach the core-mantle boundary in 29 million years.

4.2. Metamorphism of and Fluid Loss From the Subducting Slab

[34] As a subducted plate descends, it is progressively heated and squeezed, changing the mineralogy and volatile content of sediments, crust, and mantle lithosphere. There is an impressive body of experimental and thermodynamic data that bear on these changes, but understanding this progressive metamorphism promises to challenge us for a long time. Uncertainties regarding the thermal structure of subduction zones and the complex mineralogical changes expected for the wide range of subducted components might appear to be the largest obstacles impeding detailed mineralogic profiles of the downgoing plate. Unfortunately, it is not clear how valid equilibrium models will be, because phase transformations are likely to be kinetically retarded, particularly for cold material being slowly heated and squeezed.

[35] The behavior of Mg_2SiO_4 polymorphs most clearly demonstrates the importance of kinetic effects in subduction zones. Olivine and its high-pressure and hydrated polymorphs make up most of the upper mantle and the subducted lithosphere. At equilibrium away from subduction zones, olivine should change into β-spinel structure (wadsleyite) at ~410 km depth. Wadsleyite should change into γ-spinel structure (ringwoodite) at ~520 km, which then should yield perovskite ($MgSiO_3$) plus magnesiowustite (MgO) at 660 km depth [*Helffrich and Wood*, 2001] (Figures 1c and 8). The olivine-wadsleyite transition is thought to define the boundary between the upper mantle and the transition zone, whereas the ringwoodite-perovskite + magnesiowustite reaction is thought to define the transition zone–lower mantle boundary. The wadsleyite-ringwoodite transition involves little change in density, but the olivine-wadsleyite and ringwoodite-perovskite transitions significantly increase the density of the subducted lithosphere (6% and 8% increase, respectively).

[36] At equilibrium in subducted lithosphere the conversion of olivine to wadsleyite should occur considerably shallower than 410 km, whereas the conversion of ringwoodite to perovskite + magnesiowustite should occur deeper than 660 km (Figure 8) [*Irifune*, 1993]. This is because the Clapeyron slope (dP/dT) for the olivine-wadsleyite reaction is positive, whereas that for the ringwoodite to perovskite + magnesiowustite transition is negative. The shallower nature of the first conversion increases the relative density of the subducting lithosphere, favoring continued sinking, whereas the deeper

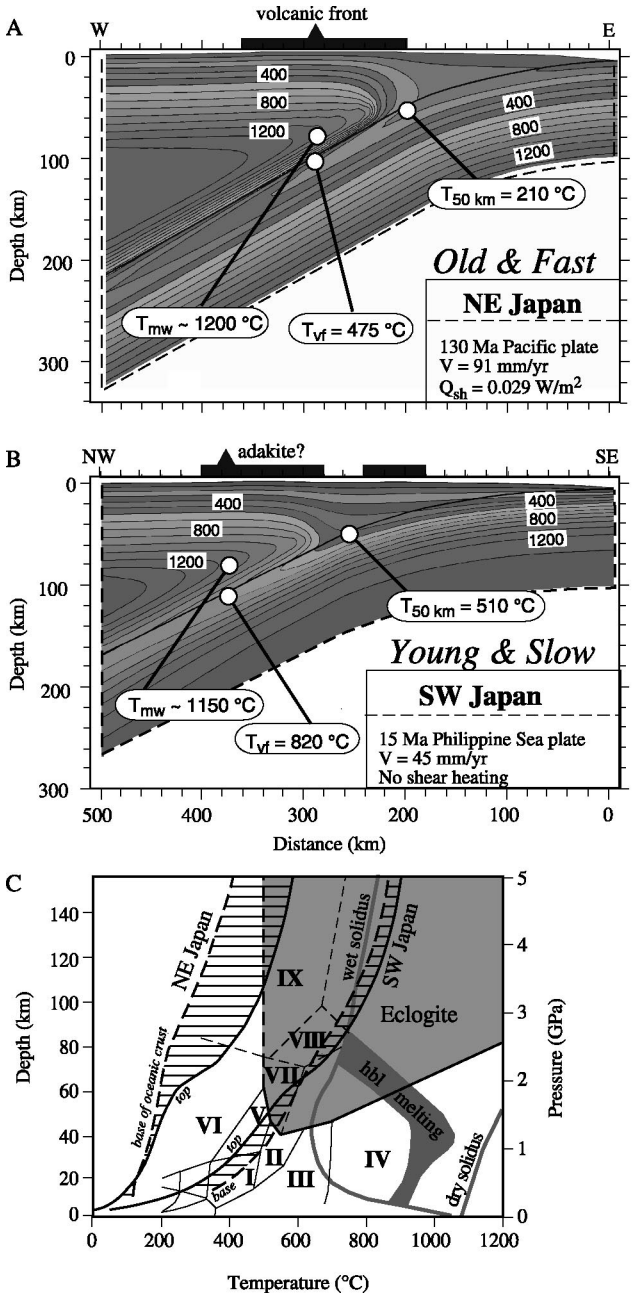

Figure 7. Thermal models of end-member (young and hot versus old and cold) subduction zones. (a) NE Japan arc, a good example of a cold subduction zone. (b) SW Japan arc, a good example of a hot subduction zone. Note the great difference in the temperature of the slab interface at 50 km depth ($T_{50\mathrm{km}}$) and beneath the volcanic front (T_{vf}) but the small difference in the maximum temperature of the mantle wedge beneath the volcanic front (T_{mw}). (c) Pressure-temperature diagram showing metamorphic facies and melting relations for basaltic oceanic crust, along with trajectories for crust subducted beneath NE and SW Japan Roman numerals identify fields for metamorphic facies: I, greenschist; II, epidote amphibolite; III, amphibolite; IV, granulite; V, epidote blueschist; VI, lawsonite blueschist (green field shows location of the eclogite field, with the dark dashed line separating this from blueschist); VII, chloritoid-amphibolite-zoisite eclogite; VIII, zoisite-chloritoid eclogite; and IX, lawsonite-chloritoid eclogite. Note that oceanic crust subducted beneath SW Japan enters the eclogite field at ~40 km depth and, if hydrous, begins to melt at ~90 km, whereas oceanic crust subducted beneath NE Japan barely enters the eclogite field at 120 km depth. Figures 6a–6c are modified after *Peacock and Wang* [1999] and *Peacock* [2002]. See color version of this figure at backof this issue.

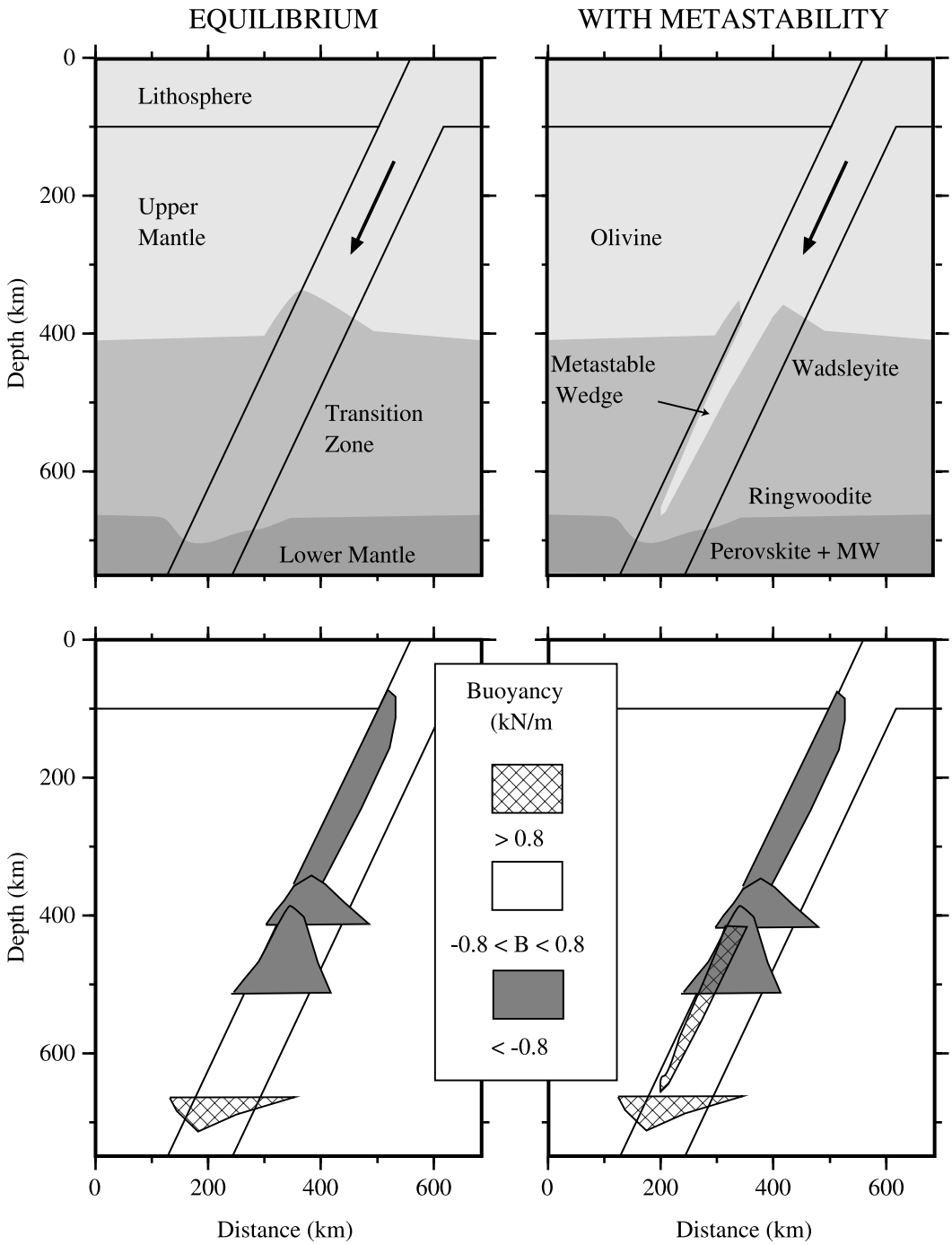

Figure 8. Model of subducted slabs (modified after *Stein and Rubie* [1999]). (top) Predicted mineral phase boundaries and (bottom) resulting buoyancy forces in a downgoing slab with (left) equilibrium mineralogy and (right) for a nonequilibrium metastable olivine wedge. Assuming equilibrium mineralogy, the slab has significant negative thermal buoyancy (dark shading in bottom graphs), due to both its colder temperature and the elevated 410 km discontinuity, and significant positive compositional buoyancy (cross hatching) associated with the depressed 660 km discontinuity. If a metastable wedge is present, it adds positive buoyancy and hence decreases the net negative buoyancy force driving subduction. Units are in 10^3 N m^{-3}.

nature of the second conversion decreases relative slab density. These predictions are consistent with the observation that deep earthquakes first appear at ~325 km depth, about where the olivine-wadsleyite phase change is first expected, and cease at ~700 km depth, where the ringwoodite-perovskite + magnesiowustite change should be complete. Although the presence of less dense metastable olivine in the subducted lithosphere may act to modulate subduction rates at depth, numerical models of mantle convection suggest that the 660 km discontinuity generally should not act as a barrier to continued slab sinking [*Davies*, 1995]. This conclusion is supported

by mantle tomography, which suggests that some slabs can be traced down well beyond 660 km (Figure 2).

[37] An exciting area of research concerns the hypothesis that deep (>325 km) subduction zone earthquakes are caused by transformational faulting, when broad regions of metastable olivine in the interior of the subducted lithosphere rapidly convert to wadsleyite or ringwoodite (Figure 8) [*Kirby et al.*, 1996]. This hypothesis is consistent with the fact that deep earthquakes are most common in the coldest subduction zones, where kinetic retardation should be maximized. This hypothesis has been criticized by *Wiens* [2001], who prefers to interpret deep earthquakes as resulting from temperature-activated phenomenon, such as thermal shear instabilities or fault zone melting, and by *Collier et al.* [2001], who mapped elevations of 60–70 km on the 410 km discontinuity in the coldest part of the Izu-Bonin slab and saw no indication of olivine metastability.

[38] Another important reaction in subducted lithospheric mantle is the breakdown of serpentinite to olivine, orthopyroxene, and water, which results in a very large density increase as it releases a lot (13 wt %) of water. Depending on temperatures, antigorite (a variety of serpentine) is stable up to pressures of 8 GPa, ~250 km deep in a subduction zone [*Ulmer and Trommsdorf*, 1995], providing an effective way to transport water to great depths. Double seismic zones, with the upper zone corresponding to the top of the subducted slab and the lower zone lying 20–40 km deeper, are found in several subduction zones (mostly in the western Pacific). The lower zone may be due to conversion of serpentinite to olivine + orthopyroxene + water [*Peacock*, 2001]. Water may also be transported in serpentinites that form above the subducted crust, beneath the forearc, that are then dragged down with the descending plate.

[39] Subducted sediments transport most of the incompatible elements carried into subduction zones. Uncertainties about the changes that accompany subduction of mafic and ultramafic rocks are compounded in the case of sediments for several reasons: (1) In contrast to relatively homogenous mafic and ultramafic units the bulk composition of subducted sediments varies widely from one arc to another. Different sedimentary sections also have different scales of heterogeneity within them. Understanding how one sedimentary package behaves as it is squeezed and heated may not provide much insight into the changes occurring in a different sedimentary succession being subducted elsewhere. (2) Because sediments lie closest to the subduction interface, they are readily scraped off. We do not know how much of the sedimentary column that arrives at the trench travels all the way down the subduction zone. Also, because sediments lie closest to the subduction interface, uncertainties about shear heating translate into large uncertainties about their thermal structure.

[40] In spite of these uncertainties a number of general observations may be made. First, the progressive heating and squeezing of sediments causes progressive transformations that increase density and decrease water content. Second, the solubility of cations in hydrous fluids increases rapidly with temperature and pressure; for example, SiO_2 in aqueous fluid increases 1000 to 100,000 times as pressure increases from 0 to 2 GPa [*Manning*, 1996], corresponding to a depth of 70 km. Third, fluid-mobile elements and light isotopes fractionate as subduction and dewatering proceeds, so that light element isotope ratios of sediments before these enter the trench should not characterize sediments beneath arc volcanoes. Fourth, clay-rich sediments melt at temperatures similar to mafic crust at comparable pressures corresponding to depths greater than ~50 km (700°–800°C at 120 km [*Nichols et al.*, 1996; *Johnson and Plank*, 1999]). Trace element systematics of some arc lavas associated with cold subduction zones have led some authors to conclude that sediment melting generally occurs [*Elliott et al.*, 1997]. Fifth, kinetic retardation may only be a problem in the lithosphere because abundant water in subducted crust and sediments may catalyze reactions.

[41] Most of the water carried to depth in subduction zones is sequestered in hydrous minerals in altered and metamorphosed crust and serpentinite. Hydrous basalt and gabbro should convert to blueschist at relatively low pressures (~30 km depth), depending on the thermal regime (Figure 7c) and kinetics. As hydrous basalt (with up to 5% H_2O) is metamorphosed to blueschist (~3% H_2O) and then amphibolite (~1–2% H_2O), it progressively releases water. Amphibolites in subducted lower crust may persist to ~100 km depth. Blueschist- and amphibolite-facies crust are likely to convert to eclogite only where relatively young and hot lithosphere is subducted (Figure 7c). Seismological studies suggest that eclogite is generally not an important part of subducted crust down to depths of 100–250 km [*Abers*, 2000].

[42] How fluid escapes from the subducted slab is critical for understanding how the overlying mantle melts. Some workers argue that pressure-sensitive dehydration reactions release water from the subducted slab at specific depths, forming "hydrous curtains" where this water rises into the overlying mantle wedge [*Tatsumi and Eggins*, 1995]. The line of arc volcanoes in this case might correspond to the surface projection of the controlling dehydration reaction. In contrast, *Schmidt and Poli* [1998] concluded that water is released continuously from subducted materials down to a maximum depth of 70 km (for hot slabs) to >300 km (for cold slabs). They infer that ~10^6 kg H_2O m^{-2} of oceanic lithosphere is carried to greater than ~20 km depth, corresponding to the base of the overlying crust. They also infer that 30–70% of the subducted water will be released below the forearc, where it will likely serpentinize the overlying mantle, and that another 18–37% of the subducted water will persist to depths where it might help generate arc magmas (Figure 9).

[43] Understanding carbonate recycling at subduction zones is a particularly important challenge given the

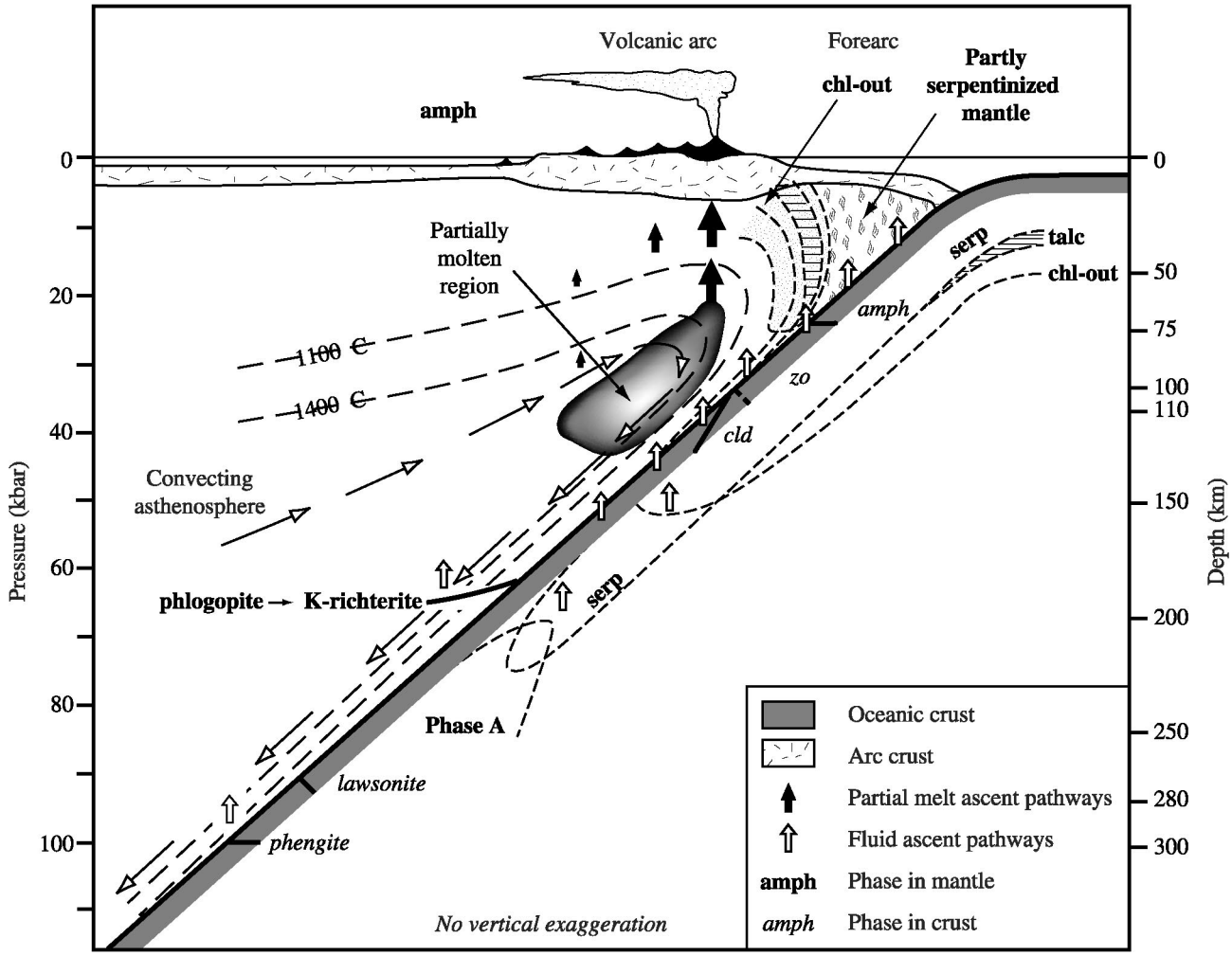

Figure 9. Model for dehydration of subducted materials (modified after *Schmidt and Poli* [1998]). Dehydration of subducted peridotite and oceanic crust occurs continuously to ~150–200 km; thus water is continuously supplied to the overlying mantle. The shaded region in the mantle wedge labeled "partially molten region" is expected to melt to a significant degree. The volcanic front forms where the amount of melt can separate and rise to the surface. Open arrows indicate rise of fluid, solid arrows indicate rise of melts. Long arrows indicate flow of asthenosphere in the mantle wedge. Stippled area marks stability field of amphibole beneath the forearc. Dashed lines outline stability fields of hydrous phases in peridotite. The horizontally ruled region shows where talc is stable. For some thermal structures a portion of the peridotitic lithosphere will be <600°C at 62 kbar; serpentine will react to "phase A," and thus H_2O will be subducted to large depth. In the oceanic crust, temperatures can be low enough to preserve lawsonite and phengite to their maximum pressure stability; however, at somewhat warmer conditions (slower subduction, shallower angle, and younger crust), zoisite (zo) will be the last potassium-free phase to decompose, and the top of the oceanic crust (phengite-rich sedimentary layer) might melt. Single-phase transitions, which cause a potassium-rich fluid pulse, could result from the breakdown of phengite in oceanic crust and from the phlogopite to K-richterite reaction in K-metasomatized mantle. Chl stands for chlorite; Cld stands for chloritoid.

need to understand the atmospheric carbon cycle. Subducted carbonate takes three principal forms: "ophicarbonates" associated with serpentinized mantle, carbonate in metabasalts, and carbonate sediments [*Kerrick and Connolly*, 2001a]. In contrast to the situation for water, where dehydration is complete at ~600°–650°C, decarbonation requires higher temperatures. Experimental and theoretical investigations suggest that subducted ophicarbonates may persist to depths greater than that sampled by arc volcanoes [*Kerrick and Connolly*, 1998]. Decarbonation of metabasalts also appears to be unusual and may only occur beneath forearcs or in hot subduction zones [*Molina and Poli*, 2000; *Kerrick and Connolly*, 2001b]. Thermodynamic modeling indicates that pure or siliceous limestones lose little CO_2 in subduction zones, although clay-rich marls break down completely. Infiltration of hydrous fluids seems essential to decarbonate most marine sediments [*Kerrick and Connolly*, 2001a]. These inferences are consistent with the observation that fluid inclusions in eclogite-facies

rocks are mostly hydrous brines (often exceedingly rich in silica) that contain minor dissolved CO_2 [*Scambelluri and Philippot*, 2001].

[44] In spite of strong arguments that decarbonation of the subducted slab is generally limited, observations of CO_2 flux and inferences based on $CO_2/^3He$ in volcanic gases lead to the conclusion that about half of the CO_2 flux from volcanoes comes from arc volcanism and that ~80% of this is recycled from subducted materials [*Marty and Tolstikhim*, 1998]. Carbonate-bearing marine sediments are thought to be a major source for CO_2 released by arc volcanoes [*Sano and Williams*, 1996]. This is discussed further in section 6.2 below.

4.3. Do Subducted Crust or Sediments Melt?

[45] When the significance of subduction zones was first recognized in the late 1960s and early 1970s, arc magmas were thought to result from frictional melting of subducted crust and sediments along the subduction interface. Subsequent interpretations of geophysical, geochemical, and isotopic data and thermal models indicate that most subduction zone magmas form by melting mantle peridotite. Recent studies suggest that the slab releases water continuously as sediments, crust, and mantle descend together, and many mineral dehydration reactions occur simultaneously. If subducted crust is very young (<10–20Ma) and slowly subducted, it may be warm enough to melt, possibly aided by greater friction across the subduction interface [*Peacock et al.*, 1994]. Melting of subducted crust produces "adakites," first recognized in the Aleutians [*Kay*, 1978]. Adakites are now recognized as compositionally distinctive dacites and are found in southern Chile, Ecuador, Panama, the Cascades, Kamchatka, SW Japan, the Philippines, and New Guinea [*Martin*, 1999]. The very high Sr/Y (Figure 10) and steep rare earth element (REE) patterns of adakites indicate equilibrium with an eclogitic residue after melting of subducted oceanic crust [*Defant and Drummond*, 1990]. The likelihood that such silicic melts travel through ~100 km of the mantle without significantly reacting with peridotite provides important clues about how melts ascend from subduction zones through the overlying mantle and erupt at the surface. Caution should be used interpreting all adakitic lavas as slab melts, because felsic lavas in equilibrium with garnet may also form by melting or fractionation at the base of thickened arc crust [*Smithies*, 2000].

[46] Melting of subducted sediments has been suggested to explain the high abundances of some elements in arc lavas that are not very soluble in hydrous fluids, such as Th and ^{10}Be [*Elliott et al.*, 1997]. All of the ^{10}Be in arc lavas must be derived from subducted sediments, and *Hawkesworth et al.* [1997] conclude that most of the Th in arc volcanics is derived from subducted sediments. The apparent inadequacy of hydrous fluids for transporting these elements has led to the suggestion that sediments must melt in order to extract Be and Th and deliver this inventory to the source of arc magma. *Johnson and Plank* [1999] argue that the sediments in most subduction zones melt but that subducted crust only melts when it is young and hot. The conclusion that subducted sediments routinely melt conflicts with thermal models for subduction zones, which generally predict temperatures that are well below the melting temperature of sediments at the pertinent pressures [*Peacock*, 1996], although recent models incorporating temperture-dependent viscosities in the mantle wedge obtain significantly higher temperatures along the subduction interface [*van Keken et al.*, 2002].

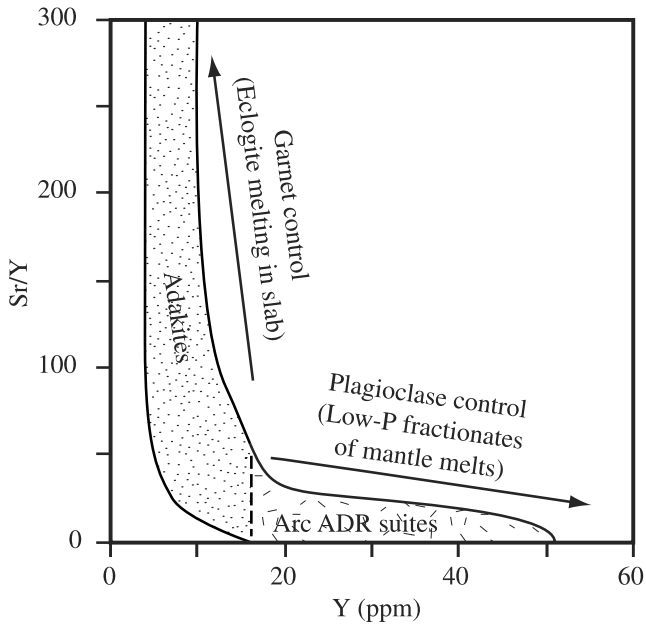

Figure 10. Diagnostic trace element differences between adakites and more common andesite-dacite-rhyolite (ADR) suites (modified after *Defant and Drummond* [1990]). Adakites form by melting at high pressure in equilibrium with garnet (garnet has a high partition coefficient for Y and low partition coefficients for Sr) and so have low-Y contents and high Sr/Y. ADR suites form at lower pressure in equilibrium with plagioclase (plagioclase has a high partition coefficient for Sr and low partition coefficients for Y) and so have high Y contents and low Sr/Y.

4.4. Seismogenic Zone

[47] Large, shallow earthquakes in subduction zones contribute ~90% of the total seismic moment released worldwide [*Pacheco and Sykes*, 1992]. These earthquakes have focal mechanisms indicating thrust faulting along the subduction interface. Only 2–5% of the total down-dip length of the Wadati-Benioff Zone generates this kind of earthquake, and this segment is known as the seismogenic zone (Figure 2). Because they are so powerful and shallow, these earthquakes constitute a special hazard to those who live near convergent margins. For a more comprehensive overview of these kinds of earthquakes than is possible here, see *Yeats et al.* [1997, chap. 11] and the seismogenic zone website (Table 1).

[48] About 42 great underthrust events with moment magnitude (M_w) = 8.0 or greater have occurred in the twentieth century. To a first approximation the maximum magnitude of these earthquakes is proportional to the convergence rate and inversely related to the age of the lithosphere being subducted, and it also appears that more energetic earthquakes occur where the upper plate includes continental crust (Figure 5b). Because M_w is directly related to the area of rupture, this implies that larger areas of rupture are associated with the subduction of younger and faster plates.

[49] Important information about the seismogenic zone is obtained from the area that is ruptured during an earthquake and the cyclicity of rupturing. The largest events rupture the entire downdip extent of the seismogenic zone, with the along-strike rupture determining the final size of the event. The SW Japan seismogenic zone is very instructive in this regard, because of its regular behavior over 1300 years of historical records, with a recurrence interval of 1.5–2.5 centuries [*Yeats et al.*, 1997]. This seismogenic zone can be subdivided along strike into two principal segments, one in the SW (segments Z, A, and B of *Yeats et al.* [1997]) and the other to the NE (segments C, D, and E of *Yeats et al.* [1997]). Adjacent smaller segments always seem to rupture together within an interval of 2–3 years. It is not clear what controls the boundary between the two principal segments.

[50] The shallowest part of a subduction zone is aseismic because the rocks and sediments along this part of the interface are weak. The seismogenic zone typically lies at depths of 35–55 km, although Mexico has a seismogenic zone that lies at 20–30 km depth. The updip limit of earthquake activity on the subduction interface must reflect increasing strength of materials in the subduction channel or the position of subduction channel "control point" (Figure 16a) [*Cloos and Shreve*, 1988b]. Some workers relate the updip limit to the dehydration and replacement of stable sliding smectite clays to stronger illite-chlorite-rich clays at 100°–150°C, which occurs at depths on the order of 5–15 km [*Hyndman et al.*, 1997]. Changing pore pressure is another candidate for controlling the updip limit.

[51] The downdip limit of the seismogenic zone is defined by the reappearance of weak rocks, either because they are hot (greater than ~350°C) or are intrinsically weak, such as serpentinite. This depth lies very close to that expected for the Moho. Subduction of young lithosphere may result in temperatures of 350°C at relatively shallow depths along the subduction interface (e.g., SW Mexico), but where old lithosphere is subducted, this temperature is not reached until well below the forearc Moho [*Ruff and Tichelaar*, 1996]. The downdip limit determines the landward extent of the seismic source zone, which is important for great earthquake hazard at inland localities.

[52] Some may be surprised that the seismogenic zone generally ends at the Moho. At comparable depths away from subduction zones, mantle rocks are generally much stronger than those of continental crust because olivine-dominated rheologies are stronger at elevated temperatures than quartz-dominated rheologies. Indeed, if the mantle adjacent to the subduction interface were dry, the seismogenic zone would likely continue to depths well below the Moho. The fact that seismogenic zones typically end at Moho depths implies that mantle beneath the forearc is unusually weak, most likely because it is pervasively serpentinized by fluids from the subducted slab. Continental forearcs are probably stronger, and more seismogenic, than oceanic forearcs [*McCaffrey*, 1994] because they have thicker crust.

[53] Three convergent margins (Kermadec, the Solomons, and Kamchatka) have double seismogenic zones [*Pacheco et al.*, 1993]. These could manifest an upper seismogenic zone along the plate interface with a downdip limit defined by the appearance of serpentinite beneath the forearc Moho and a lower, intraslab seismogenic zone having an updip limit defined by the disappearance of serpentinite and a lower limit defined by the 350°C isotherm in dry peridotite. Further research in this field promises to yield a better understanding of the degree of serpentinization of forearc mantle.

5. MANTLE WEDGE

[54] The mantle wedge is that part of the mantle that lies above the subduction zone and where subducted inputs are mixed with convecting mantle to generate magmas, fluids, and ultimately continental crust. Convecting asthenosphere is the important part, because this interacts with slab-derived fluids and melts to generate arc magmas. The dynamics of this magmagenetic system are fundamentally different from Earth's two other magma-producing regimes, hot spots (mantle plume) and mid-ocean ridges. Hot spot and ridge melts are due associated with upwelling mantle, but the mantle wedge melts where the mantle descends and is associated with the coldest thermal regime found on our planet, two features otherwise expected to ensure that melting does not occur. It is the fluxing effect of dense aqueous solutions, squeezed from subducted materials and rising to interact with asthenospheric mantle, that is ultimately responsible for convergent margin magmas. It is this interaction between sinking slab, rising fluids, and moving mantle that defines the deep-Earth reprocessing system sometimes referred to as the "subduction factory."

[55] There is much we need to know in order to understand how the subduction factory operates: How does this fluid move from subducted slab across and up through downwelling mantle to the region where melting occurs? What happens to the composition of this fluid as it moves from source to melt zone? How do melts rise from the zone of melt generation to the surface? These issues cannot be addressed in detail here,

but a few of the most important aspects are discussed in sections 5.1–5.4, including motions of the mantle wedge, movement of fluids, melt generation, and melt transport. For more information, see the subduction factory website (Table 1).

5.1. Motions of the Mantle Wedge

[56] It is widely recognized that asthenospheric mantle overlying the subducted slab, the mantle wedge, moves with the sinking plate, resulting in "induced convection" (Figures 9, 11, and 12). Early workers thought that convection was induced by the slab mechanically dragging the asthenosphere, but it is now recognized that this mechanism may not be important at the low viscosities expected in asthenosphere (10^{20}–10^{21} Pa s [*Ida*, 1983]). This conclusion is supported by recent dynamic modeling of the Tonga convergent margin [*Billen and Gurnis*, 2001]. Convection of the mantle wedge must occur in order to ensure a constant supply of asthenosphere that is hot enough to melt, and the controlling mechanism is now thought to be cooling of mantle adjacent to the descending slab. Because viscosity in the mantle varies inversely with temperature and because cooling of the asthenosphere adjacent to the subducting slab proceeds with the square root of time, there should be a "viscous blanket" that thickens with descent of the slab and that is strongly coupled to the slab [*Kincaid and Sacks*, 1997]. Slab-derived fluids should interact with mantle entrained in the viscous blanket, but the implications of this have not been explored.

[57] Mantle wedge asthenosphere lost to the viscous blanket must be replaced; this requires that fresh asthenosphere flows toward the trench. Fresh mantle can be supplied from behind the arc but could just as well come from the sides, as recently documented for Tonga [*Smith et al.*, 2001]. Seismological studies of shear wave splitting indicate that preferred orientations of olivines, interpreted as parallel to flow lines, are oriented parallel to the arc [*Wiens and Smith*, 2001]; this suggests that replenishment of wedge material is much more three-dimensional than commonly appreciated. Shallow asthenosphere should flow subhorizontally toward the trench and then turn to descend steeply adjacent to the slab, resulting in "corner flow" circulation (Figure 11). More realistic models for the mantle wedge that better reflect the asthenosphere-lithosphere boundary beneath the forearc (compare subforearc regions of Figures 11 and 15) and link temperature, viscosity, and mantle flow in the region next to the descending slab are needed.

[58] Continuous infiltration of fluids from the slab may convert the innermost portions of an originally dense viscous blanket into serpentinite [*Iwamori*, 1998]. This may continue to descend in spite of its buoyancy because it is sandwiched between the slab and less serpentinized, outer portions of the viscous blanket.

[59] We do not know the extent to which pervasively serpentinized mantle beneath the forearc descends with the subducting slab. This mantle may be sufficiently serpentinized (as discussed in section 4.4), perhaps to the point of forming a talcose subduction interface [*Peacock and Hyndman*, 1999], that subduction may be almost frictionless, without inducing downwelling beneath the forearc. If serpentinized forearc mantle descends with the slab, this would be an important part of tectonic erosion observed in some nonaccretionary forearcs and could be a very effective mechanism for transporting water deep into subduction zones.

5.2. Movement of Fluids From Subducted Slab to Melt Zone

[60] The release of aqueous and carbonic fluids from subducted sediments, crust, and mantle has been discussed in section 4.2. These dense fluids must travel many kilometers through downwelling mantle in order to reach the "hot corner," where it is sufficiently hot to melt (Figure 11). We have a lot to learn about how fluids move through the mantle at these great pressures, but three general mechanisms can be proposed: (1) porous flow, (2) channelized flow, and (3) diapiric ascent. Porous flow is relatively slow and maximizes interaction of the fluid with mantle; this mechanism is implicit in the fluid transport mechanism shown in Figure 12. Fluids are shown being continuously released from the subduction zone and metasomatizing the overlying mantle. Migration of fluids away from the slab and toward the hot corner may be accomplished by several cycles of mantle metasomatism, descent, and breakdown. Near the surface, fluids move through solids because these are porous, but in the mantle porosity cannot exist unless there is a melt or fluid phase to hold it open. If a fluid is present and the dihedral angle, the angle formed between two mineral/fluid interfaces meeting at a grain boundary, usually designated θ, is $>60°$, then the fluid exists as isolated pores and cannot move. If, however, $\theta < 60°$, the fluid is interconnected along grain edges (triple junctions) and therefore able to move by porous flow. A "wetting" fluid ($\theta < 60°$) can also penetrate fluid-absent rock by dissolving its way along grain edges [*Watson et al.*, 1990; *Nakamura and Watson*, 2001], with precipitation occurring elsewhere in the system to maintain chemical equilibrium. Experiments indicate that the dihedral angle of water in contact with olivine decreases as temperature and pressure increase, so that fluid migration through the mantle may not occur until pressures corresponding to that of the depth of the viscous blanket beneath the magmatic front are reached [*Watson et al.*, 1990; *Mibe et al.*, 1999]. Porous flow rates could be on the order of meters per year and would result in continued reequilibration of fluid with mantle peridotite [*Navon and Stolper*, 1987]. Channelized flow is much more rapid and could result when trapped fluids connect as a result of faulting at intermediate depths, causing a hydrofracture that expels water into the mantle wedge [*Davies*, 1999]. The fluid in this case would arrive at the zone of melt generation with compositions in

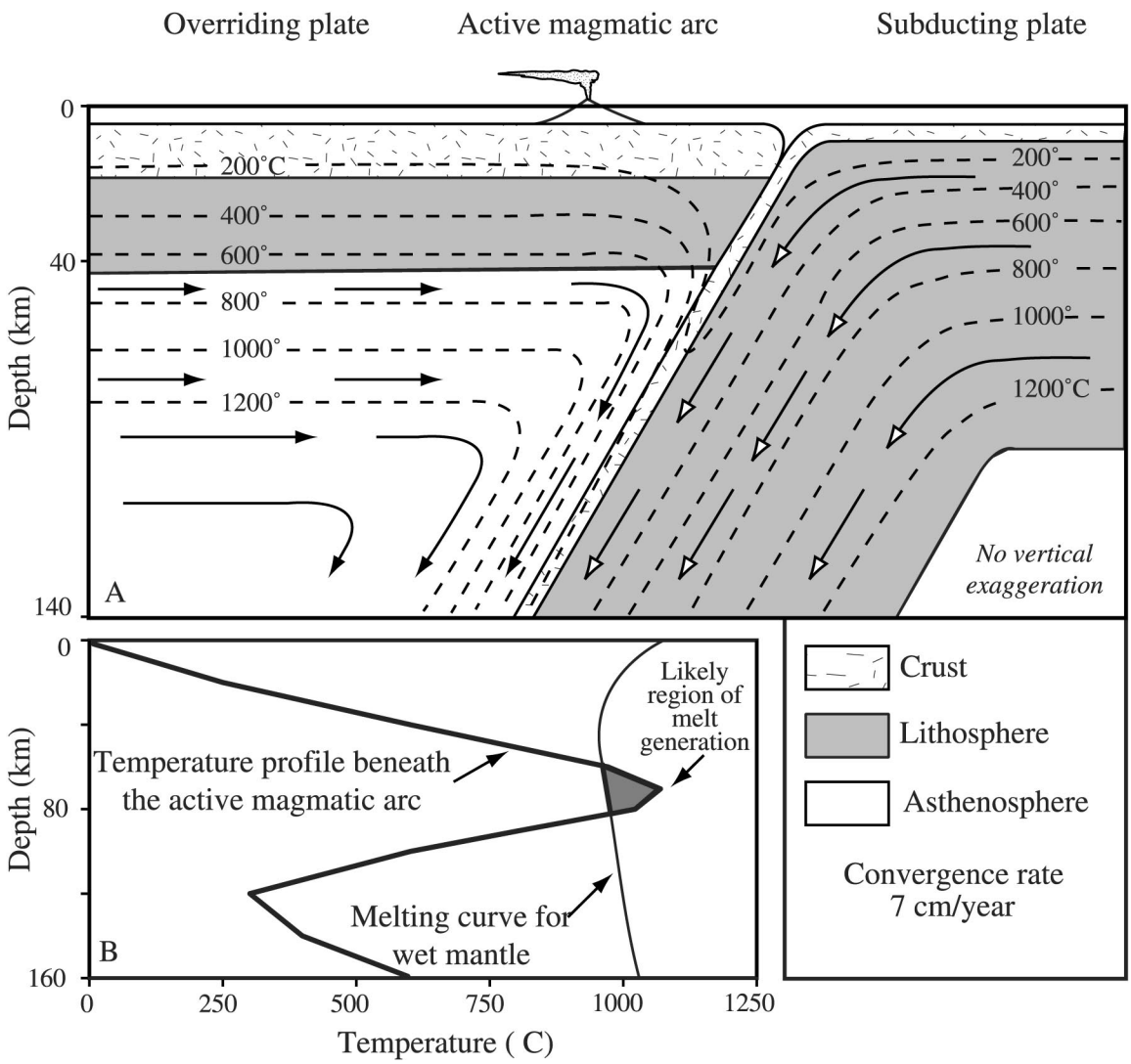

Figure 11. (a) Material movement (arrows) and temperature structure (dashed lines) of a simplified convergent margin (modified after finite element models of *Davies and Stevenson* [1992]). Crust and mantle lithosphere of the subducting plate move at a constant velocity of 7 cm yr^{-1}, dragging the asthenosphere with it beneath the overriding plate. Note also that the isotherms remain approximately parallel with the original seafloor, even deep into the subduction zone. The shaded area in the mantle wedge approximates the location of detail shown in Figure 12. (b) Temperature profile beneath the arc volcanoes (bold line) and melting curve for wet mantle (thin line). Note that the temperature reaches a maximum at ~80 km depth and then decreases as the subducted lithosphere is approached, reaching a minimum at a depth of ~120 km. The temperature is high enough for mantle melting only at a depth of ~80 km, ~40 km above the subducted plate.

equilibrium with the slab. Finally, because serpentinite is stable to great depth in the mantle and is buoyant, this could form diapirs that ascend from the viscous blanket toward the melt zone. The fact that adakites can be extracted from the slab suggests that diapirs can traverse large distances through the mantle wedge. Studies of U-Th disequilibria in fresh arc lavas are uniquely powerful for addressing rates of elemental fractionation and magma transport. This work suggests that fractionation of U from Th occurs 30,000–120,000 years prior to eruption, indicating integrated fluid and melt ascent rates on the order of 1–4 m yr^{-1} [*Hawkesworth et al.*, 1997]. Recent studies of U-Th disequilibrium suggest that ascent rates may be even faster than this, with timescales for the entire magmagenetic sequence that begins with fluid addition from the dehydrating slab and ends with eruption, which may be as short as a few thousand years [*Turner et al.*, 2000].

[61] Fluids also move from the slab through the subforearc mantle to vent sites associated with serpentine mud volcanoes in the Mariana forearc. This unique occurrence offers valuable lessons in both the composition of slab-derived fluids and about the way these fluids move through the mantle and helps constrain the thermal structure of subducted materials [*Fryer et al.*, 1999]. The presence of blueschist fragments in these mud vol-

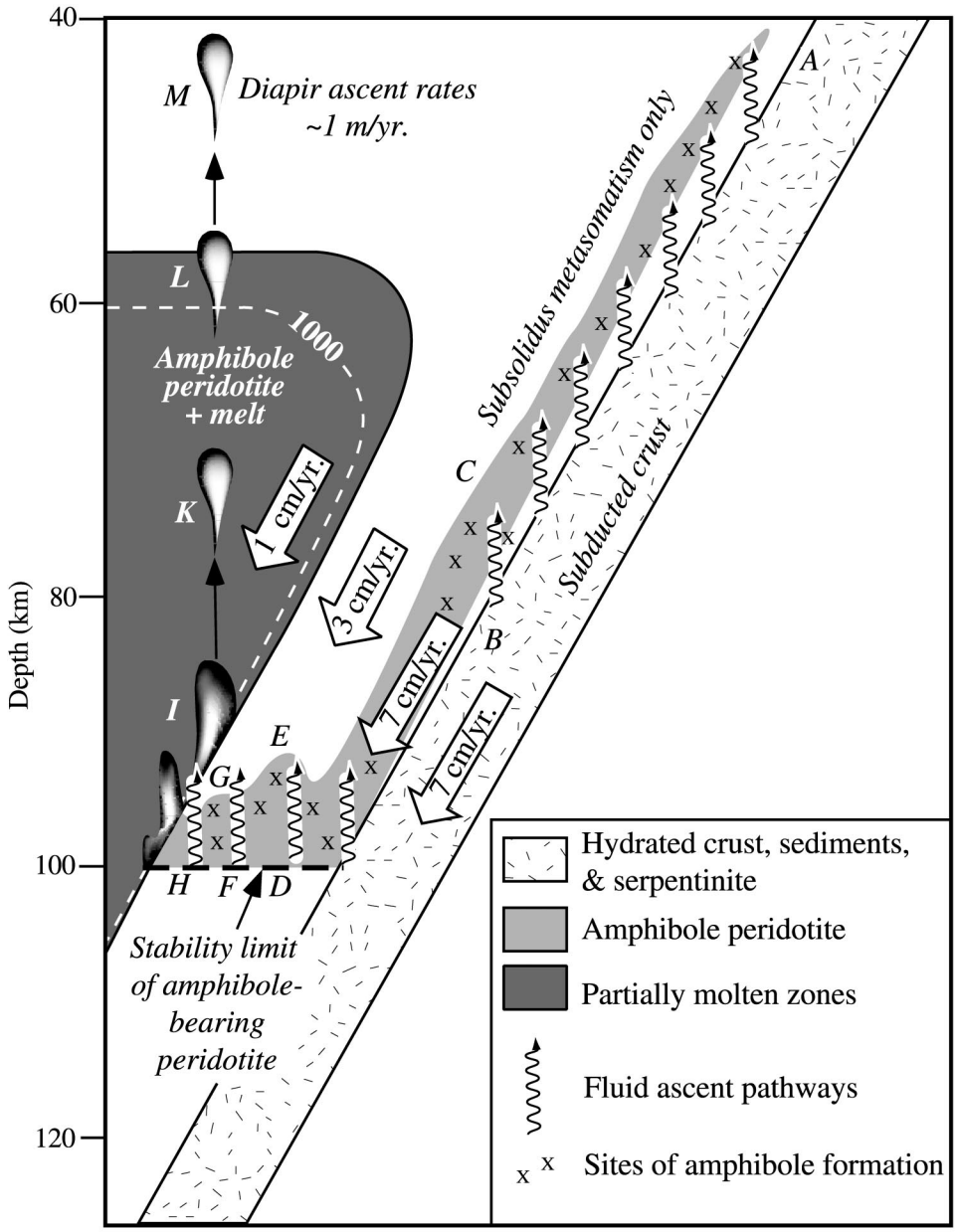

Figure 12. Detailed cartoon of the mantle wedge (region of detail depicted by shading in Figure 11), showing how fluids might move from the subducted slab into a region where melts could be generated (modified after *Davies and Stevenson* [1992] and *Stern* [1998]). Water is carried in the descending slab (A), and dense aqueous fluids are continuously released from subducted sediments, crust, and serpentinites (B). These fluids rise into the overlying mantle to form hydrous phases in mantle peridotite (C). Amphiboles are shown forming here, but it could also be another hydrous mineral. Metasomatized mantle descends with the subducted slab. At the maximum depth of stability for amphibole peridotite, ~100 km, it breaks down to anhydrous peridotite and aqueous fluid (D). The fluid rises vertically, moving away from the subducted slab and toward hotter regions in the mantle. At some point the rising water will react with anhydrous peridotite to form amphibole again (E). This descends until the amphibole breaks down again (F). Amphibole peridotite forms (G), descends, and breaks down again (H). The dark shaded area is mantle that can melt if sufficient water is provided. Above point H the mantle is sufficiently hot that water added to it leads to melting (I). The mantle is still moving downward, so melt will not be able to rise until enough of it accumulates to form a sufficiently large diapir (K) as a result of Rayleigh-Taylor instability. Partially molten diapirs are less dense than the surrounding mantle and can rise through it at a rate of perhaps 1 m yr^{-1} (L). At the base of the overlying mantle lithosphere (M), magma separates from the unmelted part of the diapir to feed an arc volcano.

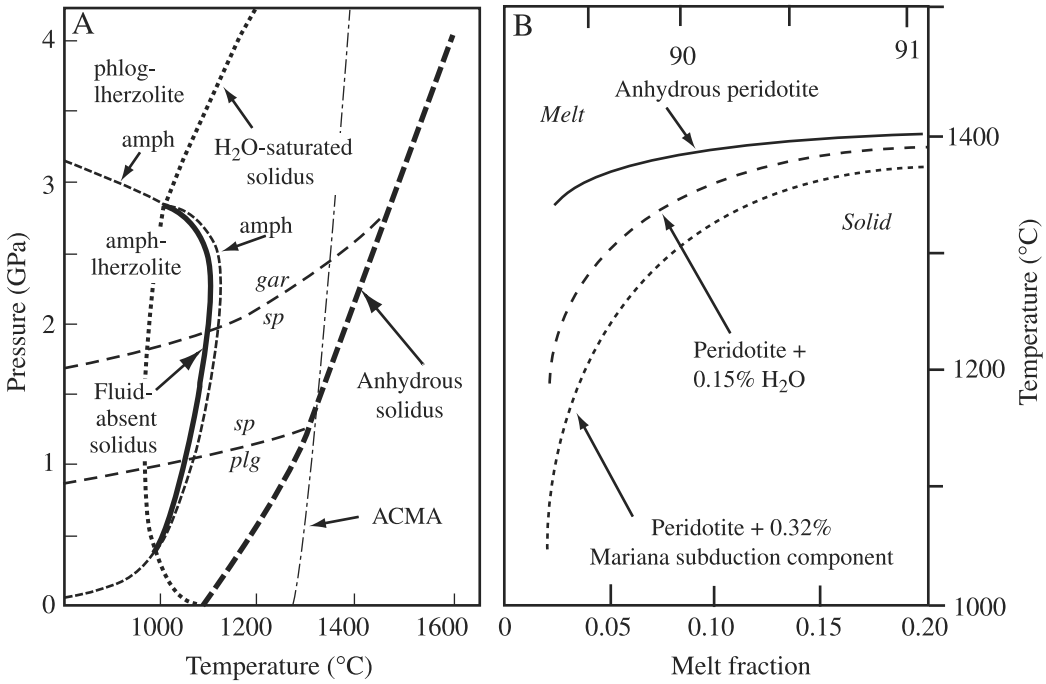

Figure 13. Effect of water on melting of peridotite. (a) Pressure-temperature diagram for H_2O undersaturated (0.2–0.5 wt % H_2O) and anhydrous partial melting of mid-ocean ridge basalt (MORB) and pyrolite mantle composition (modified after *Ulmer* [2001]). Dashed lines indicate the stability limits of garnet peridotite (gar), spinel peridotite (sp), plagioclase peridotite (plg), and amphibole peridotite (amph). The dash-dot line corresponds to the average curent mantle adiabat (ACMA) corresponding to a potential temperature of 1280°C. (b) Plot of melt fraction versus temperatures of anhydrous batch melts of a depleted MORB mantle source at 1.5 GPa with the liquidus temperatures of hydrous batch melts from peridotite containing 0.15% H_2O and 0.32% of simplified Mariana subduction component, which is an aqueous fluid with dissolved solutes [*Stolper and Newman*, 1994]. Upper axis shows forsterite content of equilibrium olivine. Figure 13b is from *Gaetani and Grove* [1998].

canoes [*Maekawa et al.*, 1995] proves that material is being transferred from the slab to the overlying mantle wedge.

5.3. Melt Generation

[62] The addition of aqueous fluids to normal asthenosphere leads to melting at temperatures as much as several hundred degrees lower than dry melting (Figure 13). Melt generation will be even more extensive if unusually hot asthenosphere advects into the melting region [*Tamura et al.*, 2002]. Melting due to fluid fluxing of the mantle wedge is thought to be responsible for 10 ± 5% melting of the mantle, with 10% melting for every 0.2% water added [*Pearce and Peate*, 1995]. Regions likely to melt are shown in Figures 6a and 6b in red (relatively slow) and in Figure 7 have temperatures >1100°C; the location of the temperature maximum is also shown in Figure 11b. The REE signature of arc basalts suggests that this melting occurs at depths shallower than the garnet peridotite stability field, that is, shallower than ~85 km [*Robinson and Wood*, 1998]. Melting due to decompression is also important, as will be discussed in section 5.4.

[63] Arc lavas are compositionally distinctive, and this allows ancient convergent margin sequences to be identified [*Pearce et al.*, 1984]. These differences reflect the differing ability of hydrous fluids to transport ions. Some elements, including the large-ion lithophiles (LILs), K, Rb, Cs, Sr, Ba, Pb, and U, are transported in such fluids, while others are relatively immobile, such as the high field strength elements (HFSE), Y, Zr, Hf, Nb, Ta, and heavy rare earth elements, as well as Ti and the transition elements [*Brenan et al.*, 1995; *Ayers et al.*, 1997]. The distinctive enrichments of LILs relative to HFSE seen on "spidergrams" (Figure 14) reflect the mixing of LILs carried in the aqueous fluid with the mantle inventory of HFSE. The reason that incompatible HFSE such as Nb and Ta are less abundant in arc basalts relative to MORB or hot spot lavas is controversial. Some authors interpret this as being due to the presence of residual Ti-bearing minerals in the mantle source region, which have high partition coefficients for Ta and Nb. Others infer that the mantle source experienced a previous depletion event, perhaps by melting beneath an associated back arc basin [*Woodhead et al.*, 1993]. Some researchers infer from the lower abundance of HFSE in arc lavas that melting is more extensive than for MORB or hot spot lavas.

[64] The enrichment of LIL elements in arc basalts reflects the addition of a "subduction component" that is

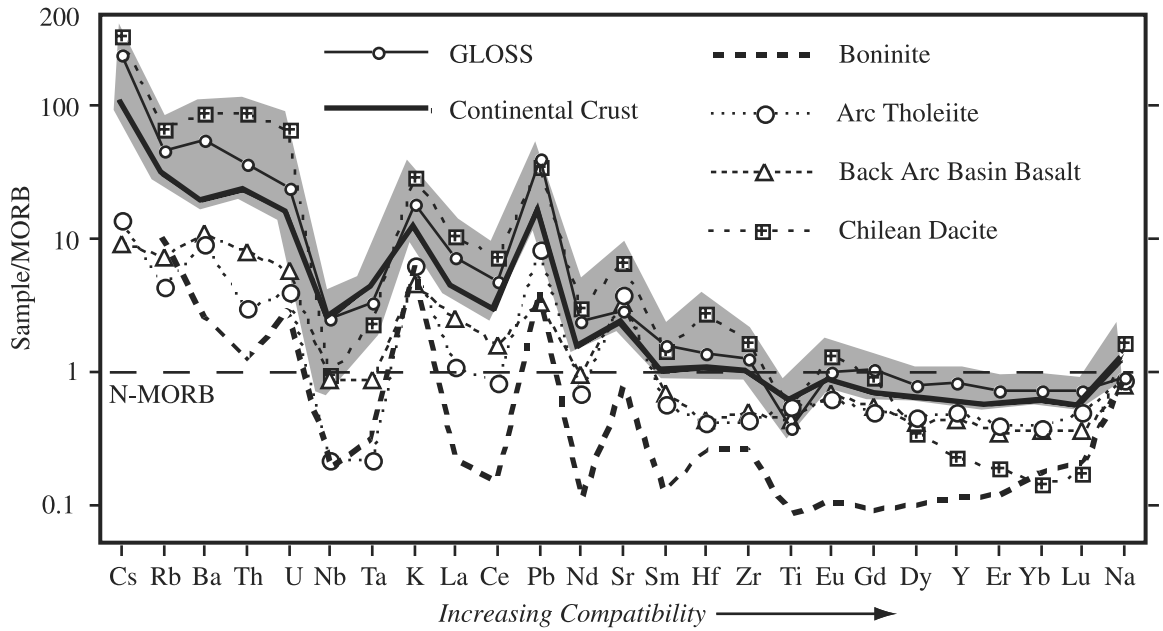

Figure 14. Incompatibility plot (spidergram) for important subduction zone inputs (global subducting sediment (GLOSS) and normal mid-ocean ridge basalt (NMORB)) and typical outputs (boninite, arc tholeiite, back arc basin basalt, dacite, and continental crust) from Table 2. Elements on the horizontal axis are listed in order of their incompatibility in the mantle relative to melt; elements on the left are strongly partitioned into the melt, whereas those on the right are strongly partitioned into peridotite minerals. Composition of NMORB and element order is after *Hofmann* [1988]. Note the characteristic enrichments of GLOSS and subduction zone outputs relative to MORB with respect to fluid-mobile large-ion lithophile elements: Rb, Ba, U, K, Pb, and Sr; note the relative depletion of these in high field strength elements: Nb, Ta, Zr, Ti, Y, and heavy rare earth elements. Note also the greater enrichment and overall similarity of the "continental suite" (GLOSS, continental crust, and Chilean dacite) on the one hand and the "oceanic suite" (boninite, arc tholeiite, back arc basin basalt, and MORB) on the other. Shaded field encompasses the continental suite.

carried by the aqueous fluid and added to the mantle source region, presumably at the time of melting. It is controversial whether the subduction component reflects equilibrium established within the slab or the mantle wedge. Certainly part of the subduction component must be overwhelmingly derived from the subducted slab, particularly water, B, and cosmogenic ^{10}Be [*Morris et al.*, 1990]. There is a strong correlation between subducted sedimentary inputs of LIL elements and volcanic outputs of these elements, suggesting that magmatic budgets are controlled by sedimentary inputs [*Plank and Langmuir*, 1993]. However, other aspects of subduction zone melts, particularly the radiogenic isotopic compositions of Sr, Nd, and to a lesser extent Pb, require only that a percent or less of subducted component be present [*Hawkesworth et al.*, 1993]. The remarkably uniform and nonradiogenic nature of Sr isotopic compositions of intraoceanic arc lavas contrasts remarkably with the heterogeneous and radiogenic nature of Sr isotopic compositions of subducted sediments [*Morris and Hart*, 1983]. Similarly, the isotopic composition of O in intraoceanic arc lavas is also remarkably uniform and mantle-like [*Eiler et al.*, 2000], again indicating that arc melts are overwhelmingly derived from mantle melting.

5.4. Melt Transport

[65] Melts generated in the hot corner must ascend across a region of lateral or even descending mantle flow to feed arc volcanoes. In spite of this, variations in bulk composition of arc basalts can be explained by variations in melting column height controlled by the thickness of the overlying crust [*Plank and Langmuir*, 1988]. This implies near-adiabatic ascent of mantle material. The simplest explanation for how melts traverse flowing mantle is that partially molten diapirs form and ascend (Figure 11). This requires development of buoyant Rayleigh-Taylor instabilities in the melt zone, which rise as diapirs through the mantle wedge along trajectories determined by the balance between buoyancy forces and mantle flow. This mode of transport has been studied experimentally by *Hall and Kincaid* [2001]. These workers concluded that buoyant flow depends on how large the supply of melt is. If relatively little buoyant material is produced, relatively small diapirs will form, and because ascent velocity is a strong function of diapir size, these will ascend slowly. Increasing supply leads to larger, more rapidly ascending diapirs. Large supplies of buoyant material culminate in development of an interconnected conduit, which leads to very rapid ascent of

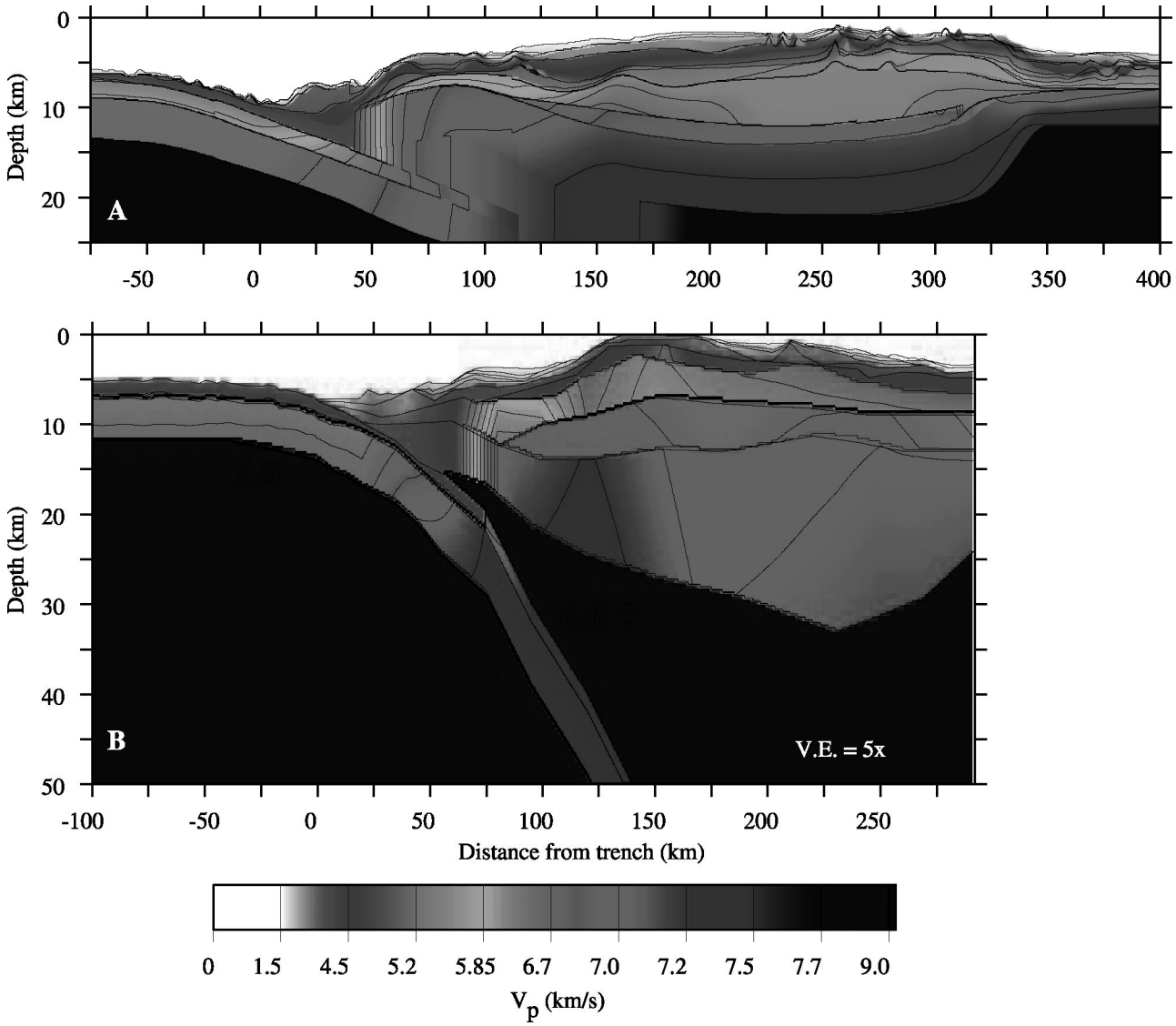

Figure 15. Crustal structure of typical arcs, based on *P* wave velocities. Note vertical exaggeration is ~5x. (a) Izu arc, 33°N (modified after *Suyehiro et al.* [1996]). (b) Eastern Aleutian arc (modified after *Holbrook et al.* [1999]). Note differences in thickness and velocity structure. We do not have comparable tomographic images of Andean-type arc crust. See color version of this figure at back of this issue.

melts. Arc melts may ascend by this manner to the base of the lithosphere or crust.

6. ARC-TRENCH COMPLEX

[66] A mature and stable subduction zone causes magmatic and tectonic phenomena in the overlying lithosphere, which can be recognized as "arc-trench complexes," often shortened to "arcs" or "island arcs." Compared to a scale of hundreds to thousands of kilometers for subduction zones, the few tens-of-kilometers thickness of arc-trench complexes is the tip of the plate tectonic "iceberg," but arcs are more important than these relative dimensions imply. Arcs are the one place where subduction zone products can be studied directly. Ancient arcs also provide a record of plate tectonic processes that persists long after subduction ends, a record that would otherwise be difficult to reconstruct. Arcs are the nurseries where the building blocks of continental crust develop, and trenches define the future sutures where these blocks will be assembled.

[67] Arc-trench complexes differ fundamentally depending on whether they are built on continental lithosphere (Andean-type arcs) or oceanic lithosphere (intraoceanic or primitive arcs). The crust of Andean-type arcs can be up to 80 km thick, about twice that of normal continental crust [*Allmendinger et al.*, 1997; *Yuan et al.*, 2000]. Thickening is mostly due to shortening associated with subduction of young lithosphere, but magmatic underplating also contributes. Intraoceanic arcs are typically 20–35 km thick (Figure 15).

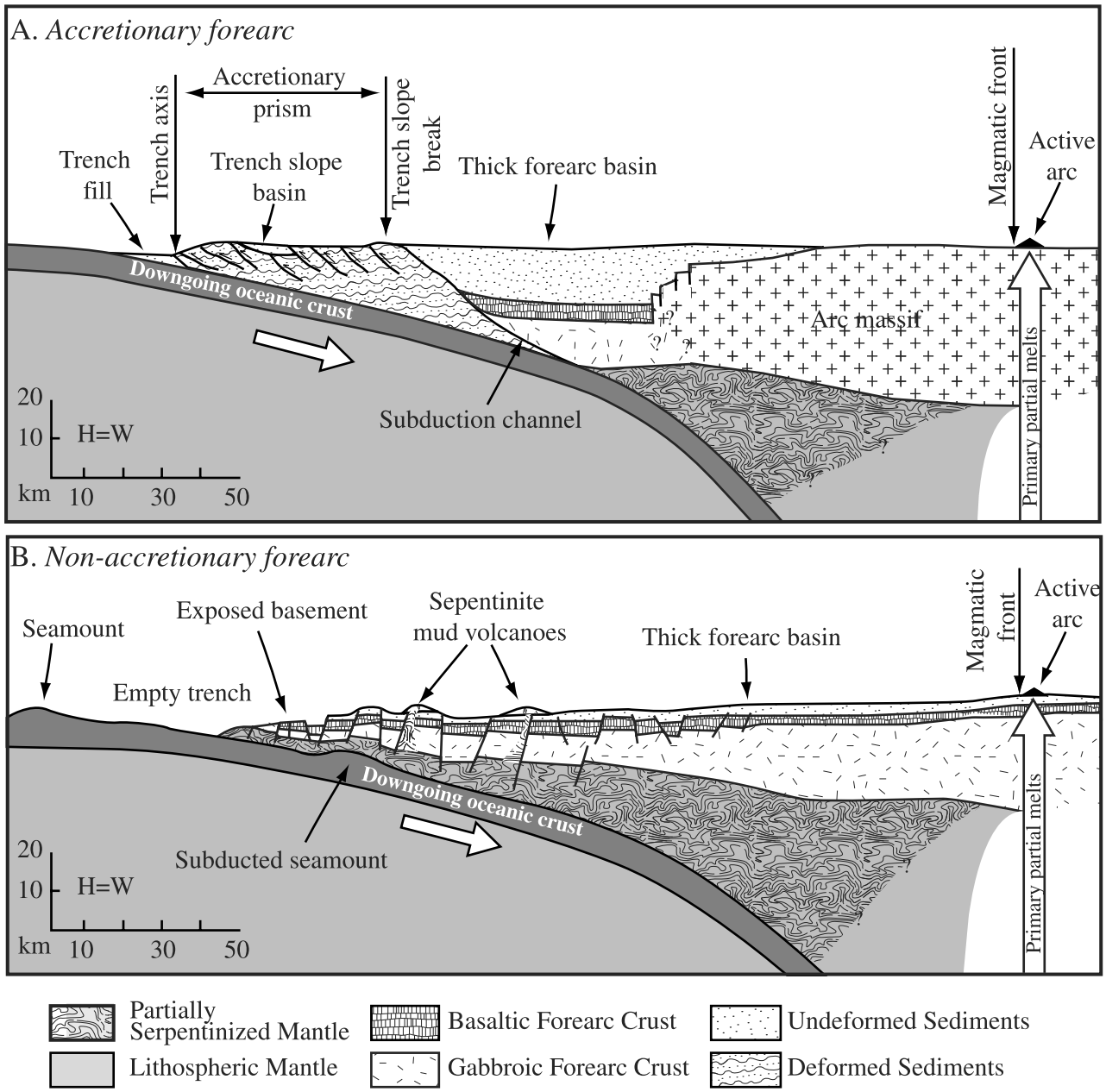

Figure 16. End-member forearc types: (a) accretionary forearc (modified after *Dickinson* [1995]) and (b) nonaccretionary forearc (P. Fryer, personal communication, 2001). Note that the abundance of sediments associated with accretionary forearcs is manifested as an accretionary prism and as a thick forearc basin and that the relative lack of sediments leaves the nonaccretionary forearc exposed.

[68] Arc-trench systems are naturally divided into forearc, magmatic arc, and back arc components. These are further described and discussed in sections 6.1–6.3.

6.1. Forearc

[69] The forearc lies between the trench and the magmatic front and is 166 ± 60 km wide [*Gill*, 1981]. A first-order distinction can be made between forearcs that broaden by addition and imbrication of material along the trench (accretionary margins) and those that do not (Figure 16). This depends on the thickness of sediment being subducted. If greater than 400–1000 m, sediments will be scraped off the downgoing plate and transferred to the overriding plate to form an accretionary prism [*Dahlen*, 1990; *von Huene and Scholl*, 1991; *Le Pichon et al.*, 1993]. The total length of convergent plate margins is about equally divided between accretionary and nonaccretionary types [*von Huene and Scholl*, 1993]. About 80% of sediments that arrive at trenches are not accreted [*von Huene and Scholl*, 1991].

[70] Accretionary forearcs form where sediment supply is high, typically adjacent to or near continents. Accretionary forearcs grow by frontal accretion, as sediment is "bulldozed" off the subducting plate to form an

accretionary wedge or prism. These are highly deformed and composed of arcward dipping, thrust-bound packets with emplacement ages that become younger toward the trench [*Underwood and Moore*, 1995]. The forearc can also be thickened by underplating of subducted sediments in the "subduction channel" (Figure 16a) [*Cloos and Shreve*, 1988a]. The high sedimentation rates associated with accretionary forearcs also make these important depocenters, with robust forearc basins forming between the accretionary prism and the magmatic arc (Figure 16a) [*Dickinson*, 1995].

[71] Nonaccretionary forearcs form where sediment supply is low, typically distant from continents, and thus they also have poorly developed forearc basins. Because the accretionary prism and forearc basin are missing, the igneous infrastructure of the forearc is exposed. Nonaccretionary forearcs provide unique insights into how subduction zones begin and their early history, the significance of ophiolites, and the nature of fluids released from relatively shallow parts of subduction zones.

[72] One of the major uncertainties in nonaccretionary forearcs concerns how much of the forearc is removed by "subduction erosion" or "tectonic erosion," whereby crust and mantle of the upper plate is carried down with the subducting plate. Removal of significant volumes of the forearcs of NE Japan, Central America, South America, the Marianas, and Tonga has been inferred. This is thought to have occurred as material was removed from the base of the upper plate (basal erosion) and by slumping of material into the trench, which then was carried down (frontal erosion). Mechanisms for basal tectonic erosion include "rasping" at the base of the forearc by seafloor which has been roughened by horst-and-graben faulting developed between the forearc bulge and the trench [*Hilde*, 1983]. Frontal erosion is inferred from disrupted topography at the base of the inner trench wall and is most evident in the wake of subducting seamounts [*von Huene and Scholl*, 1991].

[73] Forearc basement is relatively cool and stable and so preserves a record of how and when the associated subduction zone began; this record is accessible in nonaccretionary forearcs. Forearcs of the Izu-Bonin-Mariana and Tonga-Kermadec arc systems contain an especially clear record of the early history of these subduction zones. Earlier ideas that forearcs are largely composed of "trapped" oceanic crust that formed before the pertinent subduction zone [*Dickinson and Seely*, 1979] are not generally supported by recent studies. Forearc crust generally seems to have been formed by seafloor spreading about the same time as its subduction zone was initiated [*Bloomer et al.*, 1995], although a minor amount of trapped oceanic crust has been identified [*DeBari et al.*, 1999]. This indicates that subduction initiation is associated with early extension, not shortening [*Stern and Bloomer*, 1992]. Most ophiolites appear to be samples of forearc basement, formed at the time of subduction initiation and emplaced when subduction zones are terminated by collision [*Bloomer et al.*, 1995; *Shervais*, 2001].

[74] The Mariana forearc has a number of serpentine mud volcanoes, up to 2 km tall and 30 km in diameter, which "erupt" serpentine mud [*Stern and Smoot*, 1998; *Fryer et al.*, 2000]; this is the only convergent margin where active serpentine mud volcanism is known. Flows from these mud volcanoes carry abundant cobbles and boulders of serpentinized peridotite and minor metabasalt and metagabbro. Refractory peridotites (mostly harzburgite and minor dunite) are most common [*Ishii et al.*, 1992]. Harzburgite spinels are generally more Cr-rich than those found in MORB-type abyssal peridotites, indicating that these are residues left after extensive melting. *Parkinson and Pearce* [1998] interpret the trace element signature of some of these harzburgites as residual MORB mantle (15–20% fractional melting) subsequently modified by interaction with boninitic melt. These peridotites are similar to those recovered from the Mariana inner trench wall.

[75] Mafic crustal blocks (both arc and MORB affinities) are ~10% as common as peridotite blocks in the serpentine mud. Low-temperature metamorphism affects most samples, ranging from zeolite to lower greenschist facies. *Maekawa et al.* [1993] documented clasts containing blueschist-facies mineralogy (lawsonite, aragonite, sodic pyroxene, and blue amphibole) and used these to estimate metamorphic conditions of 150°–250°C and 5–6 kbar in the subducted plate. This is the first documented link between an active subduction zone and blueschist-facies metamorphism.

[76] Vent chimneys composed of aragonite, calcite, and hydrated Mg-silicate are found near summits of active serpentine mud volcanoes. Compared to ambient seawater, fluids emanating from vents in the summit area are slightly cooler and have higher pH and alkalinity. The vent waters are enriched in methane, silica, and H_2S [*Fryer et al.*, 1990]. Pore waters from the cores drilled near the summit of Conical Seamount are some of the most unusual ever sampled in oceanic sediments, containing less than half of the chloride and bromide concentrations of seawater, pH up to 12.6, and methane along with ethane and propane [*Mottl*, 1992]. Relative to seawater, these fluids are enriched in alkalinity, sulfate, K, Rb, and B and are depleted in Li, Mg, Ca, and Sr. Mottl [1992] concluded that these fluids originated from the downgoing slab, 30 km beneath the seafloor. Sampling fluids from serpentine mud volcanoes built at different heights above the Mariana subduction zone suggest that systematic variations in fluid chemistry manifest progressive decarbonation reactions in the downgoing slab [*Fryer et al.*, 1999].

[77] Two issues relating to forearc lithosphere await resolution. The first concerns the definition of lithospheric mantle, which, on the basis of observed low heat flow, clearly underlies normal forearcs. Lithospheric mantle is normally thought to be colder, denser, and stronger than asthenosphere [*Anderson*, 1995], but be-

neath forearcs, extensive hydration and serpentinization may make the "lithosphere" colder but weaker and less dense than asthenosphere. In this case, how is forearc lithosphere to be defined, and how can the lithosphere-asthenosphere boundary beneath forearcs be geophysically identified? The second issue concerns the geometry of the boundary between convecting asthenosphere and forearc "lithosphere." All models for convective flow in the mantle above the subduction zone require corner flow, where asthenosphere descends. Isotherms in convecting asthenosphere parallel the mantle flow, to a first approximation, so the lithosphere-asthenosphere boundary may be more vertical than horizontal, as is normally the case [e.g., see *Takahashi et al.*, 1998] (see Figures 1b and 9).

6.2. Magmatic Arc

[78] There are three principal tectonic settings where melted mantle moves to Earth's surface: island arcs, mid-ocean ridges, and hot spots. Each is caused and manifested differently. Mid-ocean ridges are line source loci of volcanism reflecting two-dimensional (2-D) upwelling and decompression melting of shallow mantle. Hot spots are point source volcanic loci manifesting isolated regions in the deep mantle, which melt because of the intrinsic properties of the region itself. To a first approximation, magmatic arcs are linear arrays of point sources, caused by Rayleigh-Taylor instabilities in the mantle wedge above subduction zones [*Marsh*, 1979]. As discussed in section 5.3, this melt zone results when hydrous fluids released from subducted materials drastically lower the melting temperature of the overlying asthenospheric mantle.

[79] Magmatic arcs are actually more like ribbons than lines of volcanoes, averaging 97 km wide [*d'Ars et al.*, 1995]. The magmatic front marks the boundary between low heat flow in the forearc and high heat flow beneath the magmatic arc and the back arc region (Figure 1b). Igneous activity is concentrated nearest the magmatic front and diminishes with greater distance from the trench. The magmatic front lies 124 ± 38 km above the inclined seismic zone [*Gill*, 1981], and this relationship does not vary systematically with any subduction variable, such as convergence rate or age of lithosphere being subducted. This relationship is probably controlled by the depth at which the slab must lie in order to allow sufficiently hot asthenosphere to be present in the hot corner such that addition of water from the subducted slab leads to melting (Figure 11). There does not seem to be a characteristic spacing between arc volcanoes [*d'Ars et al.*, 1995]. Volcano spacing may be controlled by the thickness of the upper plate lithosphere [*Vogt*, 1974], gravitational instability in the melt source [*Marsh*, 1979], or distance between asthenospheric "hot fingers" advected into the mantle wedge [*Tamura et al.*, 2002].

[80] Arc magmas are generally fractionated, porphyritic, and wet [*Perfit et al.*, 1980; *Ewart*, 1982; *Tatsumi and Eggins*, 1995], especially when compared to mid-ocean ridge or hot spot magmas. These three observations are related. Arcs are the only one of the three great magmatic regimes where the region in the mantle that is melting and the overlying crust and lithosphere stay relatively fixed. Consequently, crustal thickening is characteristic of arcs. The thickening rate of intraoceanic arc crust is ~350 m Myr^{-1} for the Izu arc. Thicker crust is more difficult for mafic magmas to rise through, especially if it is low-density continental crust; consequently, arc magmas tend to stagnate in the crust, where they fractionate and assimilate. The tendency of arc magmas to fractionate is reinforced by loss of magmatic water at crystal pressures, which results in crystallization even without cooling.

[81] Olivine, pyroxene, hornblende, and especially plagioclase are the typical phenocrysts of arc lavas. Arc lavas are generally not in equilibrium with mantle peridotite but have experienced significant low-pressure fractionation, usually within the crust. The porphyritic nature of arc lavas indicates that these are mostly mixtures of melt and crystals, so that analyzing bulk lava samples may give misleading information about how these melts evolve. Fortunately, trapped melts in the form of glass inclusions are common in arc phenocrysts, and the composition of these glasses gives more reliable information about melt evolution [*Lee and Stern*, 1998; *Kent and Elliott*, 2002].

[82] Arc lavas are dominantly silica-oversaturated and subalkaline and are further subdivided into volumetrically predominant calc-alkaline and tholeiitic suites and less common boninitic and shoshonitic suites. A useful distinction is that arc tholeiites plot in the low-K portion of Figure 17, calc-alkaline lavas lie within the medium and high-K fields, and shoshonitic lavas are yet more enriched in potassium and other incompatible trace elements. Boninites are a type of high-magnesium andesite requiring unusual conditions of hot mantle and abundant water. These conditions are likely to occur only during the early stages in the evolution of an arc, as large amounts of water are injected into normal asthenosphere. Arc magmas may evolve from boninitic to tholeiitic to calc-alkaline to shoshonitic over the 40–100 million year lifetime of a typical arc [*Hawkins et al.*, 1984; *Jolly et al.*, 2001].

[83] Arc magmas contain up to 6 wt % H_2O, compared to generally <0.4% H_2O for MORB and <1.0% H_2O for hot spot tholeiites such as Kilauea [*Johnson et al.*, 1994]. Back arc basin basalts (discussed in section 7) are also wetter than MORB and oceanic island basalts but generally contain less water than arc lavas (Figure 18). The main effects of H_2O on crystallization of mafic melts are to decrease melt liquidus temperature and to suppress plagioclase crystallization relative to olivine and clinopyroxene [*Danyushevsky*, 2001]. The water- and silica-rich nature of arc magmas results in violent eruptions and debris flows. This eruption style, coupled with the location of many arc volcanoes near population

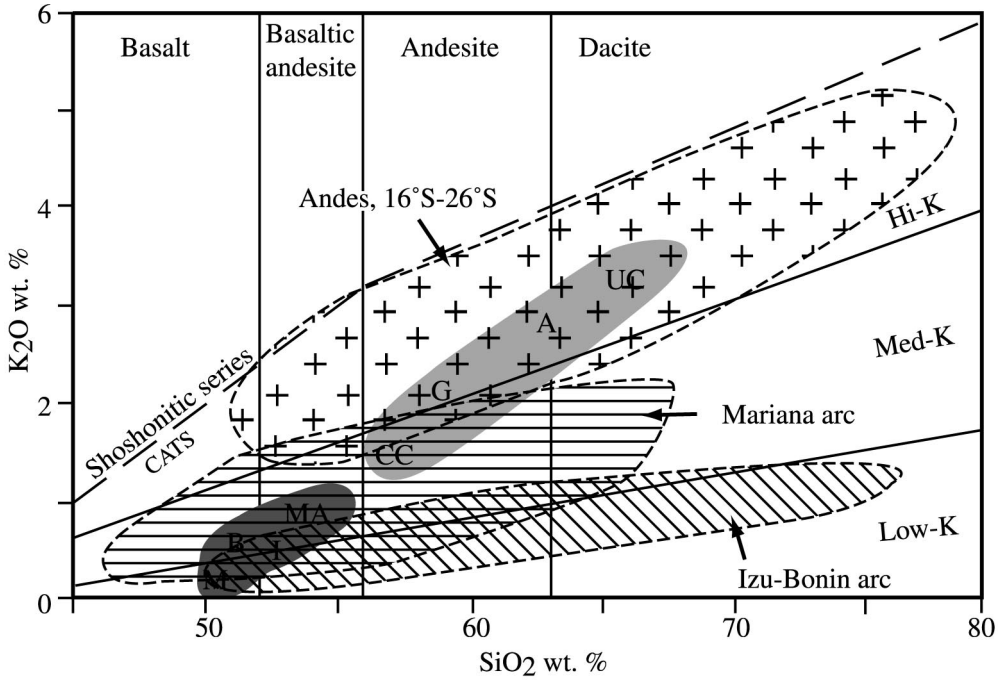

Figure 17. Potassium-silica diagram for representative arcs. Dashed line defines boundary between shoshonitic and calc-alkaline and tholeiitic suites (CATS). Izu-Bonin and Mariana arcs are exemplary of intraoceanic arcs (fields from *Stern et al.* [2002], note that volumetrically subordinate Mariana shoshonites [*Sun and Stern*, 2001] are omitted). Field for Andes, 16°S–26°S encompasses most of 606 Plio-Pleistocene and younger samples from the Central Volcanic Zone (CVZ) (G. Wörner, personal communication, 2002). Abbreviations are as follows: M, typical MORB from Table 2; B, back arc basin basalt from Table 2; I, mean composition of Izu-Bonin arc samples; MA, mean composition of Mariana arc samples; CC, bulk continental crust from Table 2; G, GLOSS from Table 2; A, mean composition of Andes CVZ lavas; and UC, composition of upper continental crust [from *McLennan*, 2001]. Dark shading encompasses mean and typical compositions of the "oceanic suite" (MORB, back arc basin basalt, and mean Mariana and Izu-Bonin lavas), and light shading encompasses mean and typical compositions of the "continental suite" (bulk continental crust, GLOSS, upper continental crust, and mean Andean dacite).

centers and air traffic routes, leads to these eruptions being by far the most dangerous on the planet [*Tilling*, 1996]. Additional water is lost by slow degassing of magma at moderate pressures in the crust, so that arc lavas are quite dry. Fortunately, microanalytical techniques permit analysis of glass inclusions trapped in arc lava phenocrysts, yielding better estimates of how much water was contained in the magma prior to degassing [*Sisson and Layne*, 1993; *Newman et al.*, 2000].

[84] The CO_2 budget for magmatic arcs is problematic. *Sano and Williams* [1996] and *Marty and Tolstikhim* [1998] conclude that arc volcanoes release an order of magnitude more CO_2 than MORB or hot spot lavas, but glass inclusions in phenocrysts from arc lavas contain vanishingly little CO_2. Part of this discrepancy may be due to the very low solubility of CO_2 in CO_2-H_2O mixtures, even at pressures corresponding to the middle to lower crust [*Newman et al.*, 2000]. Lower crustal degassing of CO_2 could be proved by documenting exposed sections of arc lower crust that have been extensively modified by pervasive CO_2 streaming, but such examples are unknown to the author. Extensive degassing of CO_2 from arc magmatic systems is also difficult to reconcile with the results of thermodynamic modeling, which predicts little carbonate breakdown in subduction zones (section 4.2). The issue of how much CO_2 is released from magmatic arcs, and at what depth, is worthy of further investigation.

[85] Arc lavas are characteristically more fractionated than those erupted from hot spots or mid-ocean ridges, but those from Andean-type arcs are more fractionated than those from intraoceanic arcs (Figure 17). Lavas from the Andes are rich in silica and potassium, mostly plotting in the field of high-K andesites and dacites, whereas lavas from the intraoceanic Mariana and Izu-Bonin arcs are mostly medium-K or low-K basaltic andesites. Mean compositions for the intraoceanic arc lavas are more similar to that of typical oceanic crust (MORB), whereas the Andean lava is very close to the composition of upper continental crust. This allows for arc lavas to be subdivided into "continental" and "oceanic" suites (Figure 17). These two great suites of arc lavas can also be distinguished on spidergrams (Figure 14) because the continental suite is more enriched in incompatible elements. These enrichments reflect the thicker, more felsic nature of continental crust underly-

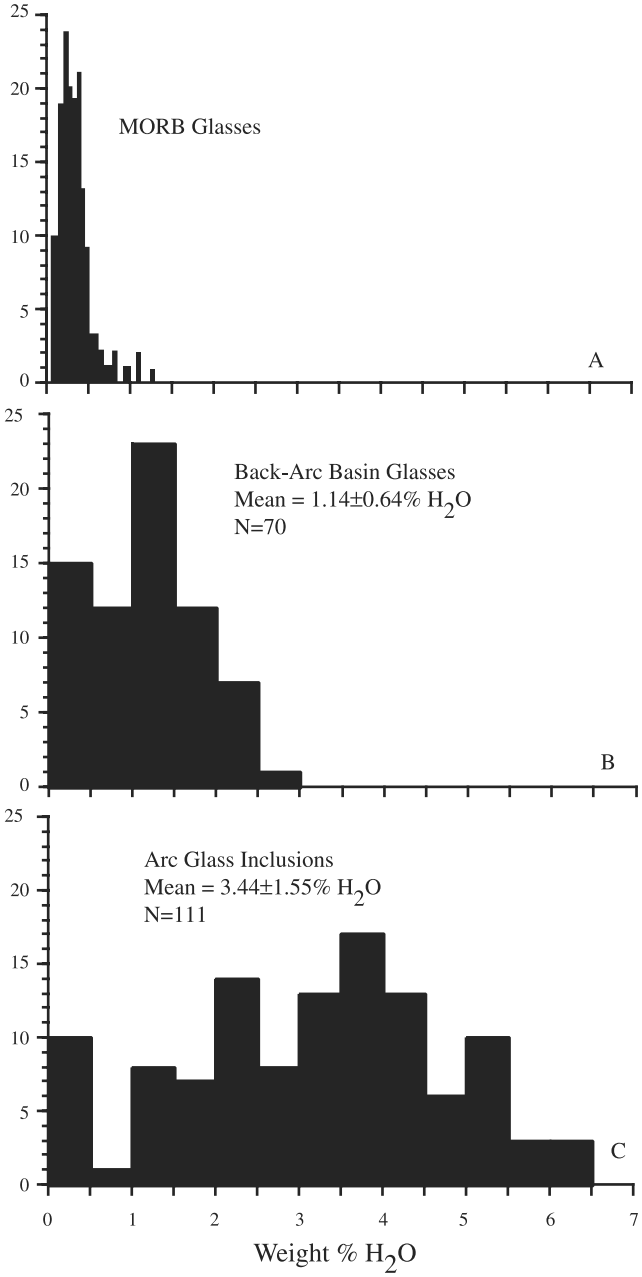

Figure 18. Water contents in (a) MORB glasses (modified after Figure 7a of *Newman et al.* [2000], binned at 0.1% H_2O), (b) back arc basin basalt glasses (data from *Danyushevsky et al.* [1993] and *Newman et al.* [2001]), and (c) arc glass inclusions (phenocrysts analyzed with FTIR or ion probe only (data from *Bacon et al.* [1992], *Sisson and Layne* [1993], *Roggensack et al.* [1996], *Sobolev and Chaussidon* [1996], *Roggensack et al.* [1997], *Sisson and Bronto* [1998], and *Newman et al.* [2000]. Uncertainty is reported as 1 standard deviation.

ing Andean-type arcs. The relatively low density of continental crust causes mantle-derived basaltic melts to stagnate within it or at its base [*Herzberg et al.*, 1983], encouraging fractionation and assimilation. Continental crust melts at a relatively low temperature, encouraging melting of crust by mantle-derived melt [*Hildreth and Moorbath*, 1988]. Felsic melts, including the great calc-alkaline batholiths such as those of the Mesozoic circum-Pacific, may result from melting the crust or from combined assimilation and fractional crystallization in crustal magma reservoirs [*DePaolo*, 1981]. In contrast, the thinner, mafic crust of juvenile arcs is denser and melts at higher temperatures, discouraging stagnation, fractionation, and crustal melting [*Pearcy et al.*, 1990; *Miller and Christensen*, 1994], but even juvenile arcs like Izu-Bonin may have a midcrustal tonalite layer which formed as a result of anatexis of mafic arc crust (Figure 19) [*Kawate and Arima*, 1998].

[86] Thick, compositionally zoned and layered batholiths and eruptions of zoned magma bodies provide further evidence that fractionation in the crust is an important part of arc melt evolution. The common association of craters and calderas at the summits of arc volcanoes suggests that the substrate is weak, as would be expected for shallow magma chambers. In spite of these indications, there is no seismic tomographic evidence for an extensive magma chamber beneath any active arc volcano. It is instructive to recall that mid-ocean ridges were first thought, on the basis of petrologic arguments and the ophiolite model, to be associated with cavernous magma chambers. Magma reservoirs beneath spreading ridges are now known to be more like thin ribbons of magma, even for the most magmatically robust ridges [*Solomon and Toomey*, 1992]. On the basis of this experience and the lack of geophysical evidence to date, models calling for the common association of large magma chambers beneath arc volcanoes should be regarded with suspicion.

[87] Although there is general agreement that juvenile continental crust is mostly formed at magmatic arcs [*Reymer and Schubert*, 1984], we have much to learn about how this happens. Crustal thickening beneath the magmatic arc can readily be accomplished by overplating of lavas and underplating and "interplating" of plutons and cumulates. Underplating is largely accomplished by formation of thick sequences of mafic and ultramafic cumulates, which must exist to complement abundant fractionated arc lavas [*DeBari*, 1997]. For the Aleutian arc, *Kay and Kay* [1985] estimated that 2/3–3/4 as much upper crust is added as lower crust, mostly as cumulates. Intrusions in the lower crust or near the Moho can also thicken the crust. At the same time that arcs thicken by piling lavas on top and plastering cumulates and sill complexes below, existing crust is continuously being reprocessed. A high-quality profile through Izu arc crust reveals a thick layer characterized by $V_p \sim$ 6.0 km s^{-1}, which has been interpreted as tonalitic middle crust (Figure 15a) [*Suyehiro et al.*, 1996]. Similar tonalites are exposed in the Tanzawa Mountains of Japan [*Kawate and Arima*, 1998]. These are interpreted as melts of amphibolites in the middle crust [*Nakajima and Arima*, 1998] that have been exposed by uplift due to collision between the Izu arc and Honshu. Intriguingly, a similar "tonalitic" layer was not found for Aleutian arc crust (Figure 15b) [*Holbrook et al.*, 1999], although to-

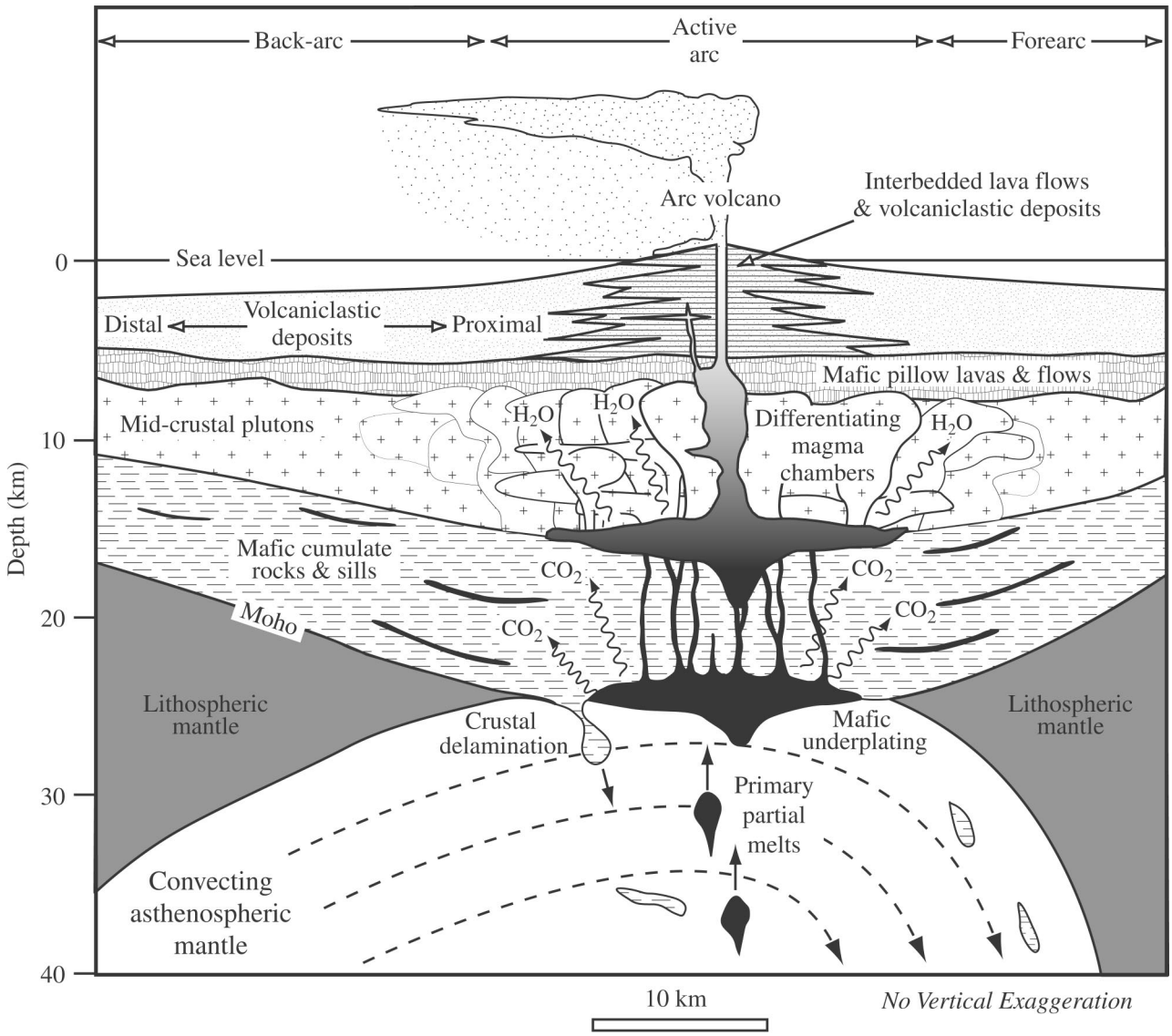

Figure 19. Magmatic arc complexities. Only an idealized section through an intraoceanic arc is shown; similar processes are expected beneath Andean-type arcs. Note that the asthenosphere is shown extending up to the base of the crust; delamination or negative diapirism is shown, with blocks of the lower crust sinking into and being abraded by convecting mantle. Regions where degassing of CO_2 and H_2O is expected are also shown.

nalitic and granodiorite plutonic rocks outcrop along the Aleutians [*Kay and Kay*, 1994]. Midcrustal low-velocity zones are known from beneath the Andean arc [*Yuan et al.*, 2000; *Haberland and Rietbock*, 2001]; these are likely zones where mantle-derived mafic melts fractionate and assimilate older continental crust [*Hildreth and Moorbath*, 1988]. Midcrustal anatexis should also provide dense, mafic lower crustal material as residues.

[88] The discrepancy between the basaltic composition of arc melts derived from the mantle compared to the andesitic bulk composition of the continental crust remains as an outstanding problem [*Kelemen*, 1995; *Rudnick and Fountain*, 1995]. This can be seen by comparing the mean compositions of intraoceanic arc lavas with the bulk composition of continental crust (Table 2 and Figure 17). An attractive possibility for thick arcs is that mafic cumulates, which belong to the crust in a petrologic sense, contain a significant proportion of dense dunites, pyroxenites, and garnet-bearing eclogitic rocks, which have seismic velocities similar to mantle peridotite. Similar cumulate ultramafics and garnet-bearing "eclogites" at the base of the Mesozoic magmatic arc are documented for the Sierra Nevada batholith of California [*Ducea and Saleeby*, 1998]. If these dense cumulates are considered to be part of the mantle, as is likely if crustal thickness is inferred from seismic velocities, then the composition of bulk arc crust would be calculated to be more felsic than the bulk composition of the melts rising from the mantle to the crust.

[89] Delamination or "drip" of dense mafic and ultra-

mafic cumulates beneath magmatic arcs may also help make arc bulk compositions more felsic [*Kay and Kay*, 1993; *Jull and Kelemen*, 2001]. The asthenosphere-lithosphere boundary beneath magmatic arcs probably lies close to the Moho, as suggested by the presence of low-velocity regions in the uppermost mantle (Figure 6a). Low-viscosity asthenospheric mantle circulating beneath the subarc Moho would provide an extremely favorable setting for dense mafic and ultramafic cumulates to sink (Figure 19). Sinking of mafic cumulates into convecting asthenosphere would also lead to a more felsic bulk composition for juvenile arcs than expected from consideration of primitive arc basaltic compositions. *Ducea* [2002] estimates that this mechanism becomes important when the crust is thicker than 20–25 km; if so, this would mark an important transition in the evolution of any arc-trench complex.

6.3. Back Arc Region

[90] The back arc region lies behind the magmatic arc, and it can show a wide range of magmatic and tectonic styles, depending on strain class [*Jarrard*, 1986]. Low-strain arcs (strain classes 1 or 2) are associated with back arc extension, whereas arcs with high strain (strain classes 6 or 7) may be associated with back arc folding and thrusting. Intermediate strain classes may be associated with a back arc region showing little or no tectonic or magmatic activity.

[91] Active extension, rifting and seafloor spreading, characterize the back arc regions above several subduction zones: the Mariana Trough behind the Mariana arc, the Lau-Havre Trough behind the Tonga-Kermadec arc, the North Fiji Basin behind the Vanuatu (New Hebrides) arc, the Manus Basin NE of New Guinea, and the East Scotia Sea behind the South Sandwich arc are excellent examples of back arc basins with active seafloor spreading. Spreading rates approximate the range observed for mid-ocean ridges: from fast (16 cm yr^{-1} in the northern Lau Basin [*Bevis et al.*, 1995]) to slow (4 cm yr^{-1} in the Mariana Trough [*Bibee et al.*, 1980]). Back arc spreading systems are remarkably similar to mid-ocean ridges. Fast spreading back arc basins have inflated ridge morphologies frequently underlain by geophysically imageable axial magma chambers [*Turner et al.*, 1999], while slow spreading back arc basins have axial rift morphology and occasionally expose mantle and lower crustal sections [*Hawkins et al.*, 1990; *Stern et al.*, 1996; *Ohara et al.*, 2002]. Hydrothermal vent fields are common along back arc basin spreading ridges, although the composition of fluids, deposits, and biota is distinctive.

[92] Extensional back arcs may rift as well as spread. Rifting is observed where the extensional regime propagates along the strike of the arc system, such as the northern Mariana Trough [*Martinez et al.*, 1995] and the Havre Trough [*Fujiwara et al.*, 2001], as well as for back arc basins that are in the initial stages of development (Okinawa Trough SW of Japan [*Fabbri and Fournier*, 1999] and the Sumisu Rift in the Izu arc [*Taylor et al.*, 1991]). How much of a back arc basin is underlain by "spread" crust as opposed to rifted crust is usually controversial, particularly for crust on the margins of the basin. Similar to the situation for rifting continents, rifted back arc basins can be amagmatic or volcanic. Back arc basins that form by seafloor spreading have crustal thicknesses that are indistinguishable from that of normal oceanic crust [*Bibee et al.*, 1980]; rifted back arcs have crust that is intermediate in thickness between spread crust and the thickness of the associated, unrifted arc.

[93] Lavas erupted at back arc basins are commonly referred to as back arc basin basalts (BABB), but this term masks differences between melts associated with different evolutionary stages. BABB erupted from spreading ridges are dominated by pillowed basalts that are compositionally similar to MORB [*Hawkins and Melchior*, 1985] but contain more water (Figure 18) and a significant "subduction component" (Figure 14) [*Gribble et al.*, 1998; *Newman et al.*, 2000]. BABB from back arc rifts, however, may be compositionally similar to those erupted from the affected arc. Rift volcanism commonly yields a bimodal assemblage of basalts and felsic lavas. Mafic end-members may be similar to arc lavas (as is found in the northern Mariana Trough and eastern Manus Basin), or they can be indistinguishable from basalts produced by back arc spreading (as is found in the Sumisu Rift [*Gribble et al.*, 1998; *Hochstaedter et al.*, 1990]). These variations in melt chemistry provide important clues to mantle flow beneath a maturing back arc basin. Mantle may be sequentially melted, first, beneath the spreading ridge and, second, beneath the arc, and this may be responsible for much of the depletion observed in arc lavas [*Woodhead et al.*, 1993]. Proximity of the arc to the back arc spreading axis can also enhance melting and magma supply [*Martinez and Taylor*, 2002].

[94] Crustal shortening and compression characterizes the back arc regions of high-strain convergent margins, leading to the development of a system of retroarc foreland basins behind the magmatic arc (Figure 20d). The best Cenozoic examples are found behind the present Andean arc and in western North America [*Jordan*, 1995]. These are fold-and-thrust belts, both of which formed in response to subduction of young, buoyant lithosphere. The Andean system is still active, whereas the North American system, which produced the Sevier-Laramide structures of Cretaceous-Paleogene age, was extinguished when the East Pacific Rise subducted beneath California in mid-Tertiary time.

7. REMAINING QUESTIONS

[95] Subduction zones are central for understanding what drives plate motions and how continental crust is formed. Recycling at subduction zones is key to understanding chemical fluxes between Earth's surface and interior, with profound implications for understanding

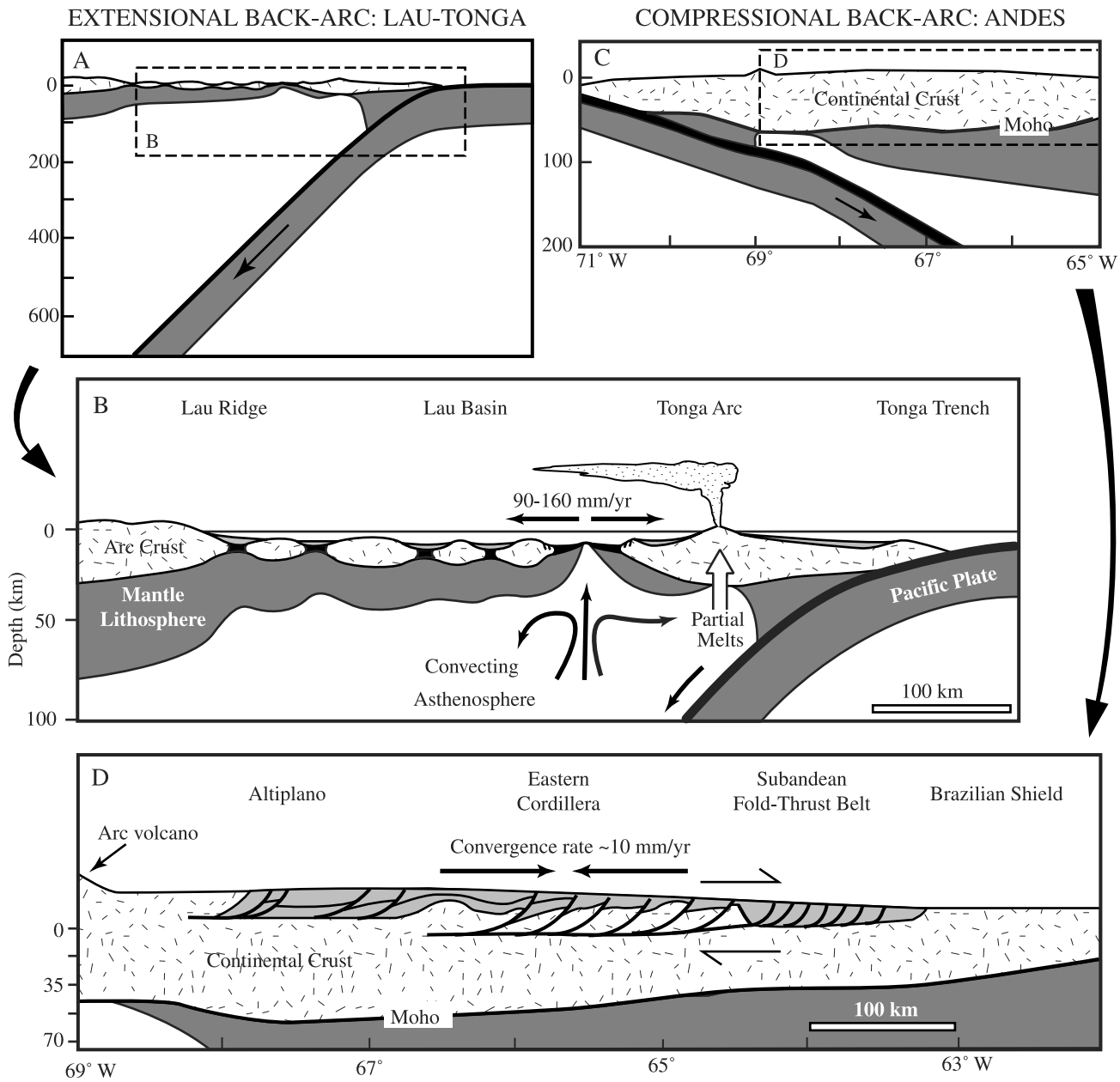

Figure 20. Tectonic variability found behind magmatic arcs, using the Bolivian Andes and the Lau Basin as examples. Dark shading denotes lithosphere; underlying white is asthenosphere. (a) Tectonic setting of Lau Basin (modified after *Zhao et al.* [1997]), emphasizing lithospheric structures. Dashed box shows region of detail shown in Figure 20b. (b) Tectonic setting of Andes between 20°S and 24°S (modified after *Yuan et al.* [2000]) emphasizing crustal structure. Area of detail shown in Figure 20d lies partly within the open-ended dashed rectangle. (c) Cross section across the Lau Basin, emphasizing lithospheric structure, at the latitude investigated by Ocean Drilling Progdram Leg (~20°S) (modified after *Hawkins* [1994]). Extension rate is from GPS measurements of *Bevis et al.* [1995] for velocities of Tonga from Australia; note that the highest rate is at the northern end of Lau Basin (~17°S), and the rate decreases to the south. (d) Cross section across Andean back arc region, emphasizing crustal structure, about 20°S (modified after *Gubbels et al.* [1993]). Shortening rate is from GPS measurements of *Bevis et al.* [2001]. Figures 20c and 20d have the same horizontal scale. There is no vertical exaggeration on any of the sections

long-term climate change. Society is more immediately impacted by volcanic eruptions and earthquake and tsunami hazards that accompany subduction and by the fact that most ore deposits result from subduction and are preserved in island arcs.

[96] Subduction zones are interior Earth systems of unparalleled complexity. Refinements and discoveries of fundamental processes can be expected to result from dynamic models of how subduction zones function, models that should be both quantitative and realistic. Build-

ing these models requires above all that all-important subduction zone processes are understood well enough that they can be quantified.

[97] With the immense complexity of subduction zones, there is an inexhaustible set of problems where our understanding can progress. Such progress should be accompanied by efforts to communicate the significance of results to the broader scientific community. There is also a subset of central problems or questions on which we need to focus research, and the following is an unprioritized "top ten list" of these:

1. How does subduction begin?

2. How much water is carried into subduction zones by serpentinized mantle in the downgoing lithosphere, and does faulting of the outer trench high result in significant serpentinization of lithospheric mantle?

3. What is the thermal structure of subduction zones? Answering this question requires a better understanding of shear stresses across the subduction interface, including how these stresses change with convergence rate and age of subducted lithosphere.

4. How do subducted sediments, crust, and mantle in equilibrium with evolving fluids and melts change as they sink together into the mantle?

5. What happens to subducted carbonates? What fraction of this returns to the surface as carbon dioxide?

6. How do dense, hydrous fluids, bled from the subducting slab, move into and through the overlying mantle wedge? How do these fluids and mantle change as they interact?

7. How does mantle above subduction zones move? If the mantle wedge is composed of unusually low viscosity mantle, what are the implications of this for mantle flow?

8. Does "lithospheric" mantle beneath the forearc interact with convecting asthenosphere of the mantle wedge, especially where convecting asthenosphere "turns the corner" to descend with the downgoing slab?

9. How and where are melts generated? How do they ascend through the mantle, and how do they degas at depth?

10. What happens to melts when they arrive at the base of the crust and as they pass through it? How can we test the idea that arc lower crust delaminates?

[98] Every other scientist who has studied subduction zones is likely to have a different list of top problems, but each would likely reflect the incredible range of physical and chemical processes that need to be understood. The challenges are daunting, and while individual investigators can continue progress alone, more progress can be realized by scientific teams working together. In order to better understand how subduction zones operate, it will be necessary to build such teams from interdisciplinary groups of geologists, geophysicists, geochemists, geodynamic modelers, "mantle hydrologists," etc.

[99] **ACKNOWLEDGMENTS.** Many scientists contributed generously to this overview, including R. A. Berner (Yale), M. Billin and M. Gurnis (CalTech), K. Burke (U. Houston), J. Dixon (U. Miami), P. Fryer (U. Hawaii), S. Holbrook (U. Wyoming), J. Karson (Duke U.), R. W. and S. M. Kay (Cornell), R. Kind (GFZ-Potsdam), E. Lidiak (U. Pittsburgh), P. Lonsdale (Scripps Institution of Oceanography), S. McLennan (SUNY Stonybrook), T. Parsons (USGS), S. Peacock (Arizona State U.), J. Pearce (Cardiff U.), L. Ruff (U. Michigan), M. Schmidt (ETH Zurich), C. Sengor (Turkey), T. Sisson (USGS), S. Stein (Northwestern U.), K. Suyehiro (JAMSTEC), N. Takahashi (Ministry Education, Culture, Sports, and Tech., Japan), P. Ulmer (ETH Zurich), M. Underwood (U. Missouri), R. van der Hilst (MIT), K. Wallmann (GEOMAR), B. Watson (Rensselaer Polytech), D. Wiens (Washington U.), and G. Wörner (U. Göttingen), although errors of omission or commission are solely mine. The manuscript was greatly improved by thoughtful reviews by J. W. Hawkins and two anonymous referees. Special thanks go to Trey Hargrove for improving many of the figures. Figures 15a and 15b were prepared by W.S. Holbrook. My research on subduction zones of the western Pacific has been generously supported by the National Science Foundation. This is UTD Geosciences contribution 981.

[100] Thomas Torgersen was the Editor responsible for this paper. He thanks one cross-disciplinary reviewer and two technical reviewers.

REFERENCES

Abers, G. A., Hydrated subducted crust at 100–250 km depth, *Earth Planet. Sci. Lett., 176*, 323–330, 2000.

Allmendinger, R. W., T. E. Jordan, S. M. Kay, and B. L. Isacks, The evolution of the Altiplano-Puna Plateau of the central Andes, *Annu. Rev. Earth Planet. Sci., 25*, 139–174, 1997.

Amstutz, A., Sur l'évolution des structures alpines, *Arch. Sci., 4*, 323–329, 1951.

Anderson, D. L., Lithosphere, asthenosphere, and perisphere, *Rev. Geophys., 33*, 125–149, 1995.

Ayers, J. C., S. K. Dittmer, and G. D. Layne, Partitioning of elements between peridotite and H_2O at 2.0–3.0 GPa and 900–1100°C, and application to models of subduction zone processes, *Earth Planet. Sci. Lett., 150*, 381–398, 1997.

Bacon, C. R., S. Newman, and E. Stolper, Water, CO_2, Cl, and F in melt inclusions in phenocrysts from three Holocene explosive eruptions, Crater Lake, Oregon, *Am. Mineral., 77*, 1021–1030, 1992.

Bevis, M., et al., Geodetic observations of very rapid convergence and back-arc extension at the Tonga arc, *Nature, 374*, 249–251, 1995.

Bevis, M., E. Kendrick, R. Smalley Jr., B. Brooks, R. Allmendinger and B. Isacks, On the strength of interplate coupling and the rate of back arc convergence in the central Andes: An analysis of the interseismic velocity field, *Geochem. Geophys. Geosyst., 2*, 2001GC000198, 2001.

Bibee, L. D., J. G. G. Shor, and R. S. Lu, Inter-arc spreading in the Mariana Trough, *Mar. Geol., 35*, 183–197, 1980.

Billen, M. I., and M. Gurnis, A low viscosity wedge in subduction zones, *Earth Planet. Sci. Lett., 193*, 227–236, 2001.

Bloomer, S. H., B. Taylor, C. J. MacLeod and et al. Early Arc volcanism and the Ophiolite problem: A perspective from drilling in the western Pacific, in *Active Margins and Marginal Basins of the Western Pacific, Geophys. Monogr. Ser.*, vol. 88, edited by B. Taylor and J. Natland, pp. 67–96, AGU, Washington D. C., 1995.

Brenan, J. M., H. F. Shaw, F. J. Ryerson, and D. L. Phinney, Mineral-aqueous fluid partitioning of trace elements at 900°C and 2.0 GPa: Constraints on the trace element chemistry of mantle and deep crustal fluids, *Geochim. Cosmochim. Acta, 59*, 3331–3350, 1995.

Carlson, R. L., The abundance of ultramafic rocks in Atlantic Ocean crust, *Geophys. J. Int., 144*, 37–48, 2001.

Chiu, J.-M., B. L. Isaaks, and R. K. Cardwell, 3-D configuration of subducted lithosphere in the western Pacific, *Geophys. J. Int., 106*, 99–111, 1991.

Cloos, M., Lithospheric buoyancy and collisional orogenesis: Subduction of oceanic plateaus, continental margins, island arcs, spreading ridges, and seamounts, *Geol. Soc. Am. Bull., 105*, 715–737, 1993.

Cloos, M., and R. L. Shreve, Subduction-channel model of prism accretion, melange formation, sediment subduction, and subduction erosion at convergent plate margins, 1, Background and description, *Pure Appl. Geophys., 128*, 455–500, 1988a.

Cloos, M., and R. L. Shreve, Subduction-channel model of prism accretion, melange formation, sediment subduction, and subduction erosion at convergent plate margins, 2, Implications and discussion, *Pure Appl. Geophys., 128*, 501–545, 1988b.

Collier, J. D., G. R. Helffrich, and B. J. Wood, Seismic discontinuities and subduction zones, *Phys. Earth Planet. Inter., 127*, 35–49, 2001.

Connerney, J. E. P., M. H. Acuña, P. J. Wasilewski, N. F. Ness, H. Rème, C. Mazelle, D. Vignes, R. P. Lin, D. L. Mitchell, and P. A. Cloutier, Magnetic lineations in the ancient crust of Mars, *Science, 284*, 794–798, 1999.

Cooper, P. A., and B. Taylor, Polarity reversal in the Solomon Islands arc, *Nature, 314*, 428–430, 1985.

Dahlen, F. A., Critical taper model of fold-and-thrust belts and accretionary wedges, *Annu. Rev. Earth Planet. Sci., 18*, 55–99, 1990.

Danyushevsky, L. V., The effect of small amounts of H_2O on crystallization of mid-ocean ridge and backarc basin magmas, *J. Volcanol. Geotherm. Res., 110*, 265–280, 2001.

Danyushevsky, L. V., T. J. Falloon, A. V. Sobolev, A. J. Crawford, M. Carroll, and R. C. Price, The H_2O content of basalt glasses from southwest Pacific back-arc basins, *Earth Planet. Sci. Lett., 117*, 347–362, 1993.

d'Ars, J. B., C. Jaupart, and R. S. J. Sparks, Distribution of volcanoes in active margins, *J. Geophys. Res., 100*(B10), 20,421–20,432, 1995.

Davies, G. F., On the emergence of plate tectonics, *Geology, 20*, 963–966, 1992.

Davies, G. F., Penetration of plates and plumes through the mantle transition zone, *Earth Planet. Sci. Lett., 133*, 507–516, 1995.

Davies, G. F., *Dynamic Earth*, Cambridge University Press, New York, 1999.

Davies, G. F., and M. A. Richards, Mantle convection, *J. Geol., 100*, 151–206, 1992.

Davies, J. H., The role of hydraulic fractures and intermediate-depth earthquakes in generating subduction-zone magmatism, *Nature, 398*, 142–145, 1999.

Davies, J. H., and D. J. Stevenson, Physical models of source region of subduction zone volcanics, *J. Geophys. Res., 97*(B2), 2037–2070, 1992.

DeBari, S. M., Evolution of magmas in continental and oceanic arcs: The role of the lower crust, *Can. Mineral., 35*, 501–519, 1997.

DeBari, S. M., B. Taylor, K. Spencer, and K. Fujioka, A trapped Philippine Sea plate origin for MORB from the inner slope of the Izu-Bonin trench, *Earth Planet. Sci. Lett., 174*, 183–197, 1999.

Defant, M. J., and M. S. Drummond, Derivation of some modern arc magmas by melting of young subducted lithosphere, *Nature, 347*, 662–665, 1990.

DePaolo, D. J., Trace element and isotopic effects of combined wallrock assimilation and fractional crystallization, *Earth Planet. Sci. Lett., 53*, 189–202, 1981.

Dickinson, W. R., Forearc basins, in *Tectonics of Sedimentary Basins*, edited by C. J. Busby and R. V. Ingersoll, pp. 221–261, Blackwell Sci., Malden, Mass., 1995.

Dickinson, W. R., and D. R. Seely, Structure and stratigraphy of forearc regions, *AAPG Bull., 63*, 2–31, 1979.

Ducea, M., Constraints on the bulk composition and root foundering rates of continental arcs: A California arc perspective, *J. Geophys. Res., 107*(B11), 2304, doi:10.1029/2001JB000643, 2002.

Ducea, M. N., and J. B. Saleeby, The age and origin of a thick mafic-ultramafic keel from beneath the Sierra Nevada batholith, *Contrib. Mineral. Petrol., 133*, 169–185, 1998.

Eiler, J. M., A. Crawford, T. Elliott, K. A. Farley, J. W. Valley, and E. M. Stolper, Oxygen isotope geochemistry of oceanic-arc lavas, *J. Petrol., 41*, 229–256, 2000.

Elliott, T., T. Plank, A. Zindler, W. White, and B. Bourdon, Element transport from slab to volcanic front at the Mariana arc, *J. Geophys. Res., 102*(B7), 14,991–15,019, 1997.

Ernst, W. G., Metamorphism, partial preservation, and exhumation of ultrahigh-pressure belts, *Isl. Arc, 8*, 125–153, 1999.

Ewart, A., The mineralogy and petrology of Tertiary-Recent orogenic volcanic rocks; With special reference to the andesitic-basaltic compositional range, in *Andesites: Orogenic Andesites and Related Rocks*, edited by R. S. Thorpe, pp. 25–95, John Wiley, New York, 1982.

Fabbri, O., and M. Fournier, Extension in the southern Ryukyu arc (Japan): Link with oblique subduction and back arc rifting, *Tectonics, 18*, 486–497, 1999.

Forsyth, D., and S. Uyeda, On the relative importance of the driving forces of plate motions, *Geophys. J. R. Astron. Soc., 43*, 163–200, 1975.

Fryer, P., K. L. Saboda, L. E. Johnson, M. E. Mackay, G. F. Moore, and P. Stoffers, Conical Seamount: SeaMARC II, ALVIN submersible, and seismic-reflection studies, *Proc. Ocean Drill. Program Sci. Results, 125*, 3–11, 1990.

Fryer, P., C. G. Wheat, and M. Mottle, Mariana blueschist mud volcanism: Implications for conditions within the subduction zone, *Geology, 27*, 103–106, 1999.

Fryer, P., J. P. Lockwood, N. Becker, S. Phipps, and C. S. Todd, Significance of serpentine mud volcanism in convergent margins, in *Ophiolites and Oceanic Crust*, edited by Y. Dilek et al., *Spec. Pap. Geol. Soc. Am., 349*, 35–51, 2000.

Fujiwara, T., T. Yamazaki, and M. Joshima, Bathymetry and magnetic anomalies in the Havre Trough and southern Lau Basin; From rifting to spreading in back-arc basins, *Earth Planet. Sci. Lett., 185*, 253–263, 2001.

Gaetani, G., and T. L. Grove, The influence of water on melting of mantle peridotite, *Contrib. Mineral. Petrol., 131*, 323–346, 1998.

Garfunkel, Z., C. A. Anderson, and G. Schubert, Mantle circulation and the lateral migration of subducted slabs, *J. Geophys. Res., 91*(B7), 7205–7223, 1986.

Gill, J. B., *Orogenic Andesites and Plate Tectonics*, Springer-Verlag, New York, 1981.

Grellet, C., and J. Dubois, The depth of trenches as a function of the subduction rate and age of the lithosphere, *Tectonophysics, 82*, 45–56, 1982.

Gribble, R. F., R. J. Stern, S. Newman, S. H. Bloomer, and T. O'Hearn, Chemical and isotopic composition of lavas from the northern Mariana Trough: Implications for magmagenesis in back-arc basins, *J. Petrol., 39*, 125–154, 1998.

Gubbels, T. L., B. L. Isacks, and E. Farrar, High-level surfaces,

plateau uplift, and foreland development, Bolivian central Andes, *Geology, 21*, 695–698, 1993.
Haberland, C., and A. Rietbock, Attenuation tomography in the western central Andes: A detailed insight into the structure of a magmatic arc, *J. Geophys. Res., 106*(B6), 11,151–11,167, 2001.
Hall, P. S., and C. Kincaid, Diapiric flow at subduction zones: A recipe for rapid transport, *Nature, 292*, 2472–2475, 2001.
Hamilton, W. B., Plate tectonics and island arcs, *Geol. Soc. Am. Bull., 100*, 1503–1527, 1988.
Hawkesworth, C. J., K. Gallagher, J. M. Hergt, and F. McDermott, Mantle and slab contributions in arc magmas, *Annu. Rev. Earth Planet. Sci., 21*, 175–204, 1993.
Hawkesworth, C. J., S. P. Turner, F. McDermott, D. W. Peate, and P. van Calstern, U-Th isotopes in arc magmas: Implications for element transfer from the subducted crust, *Science, 276*, 551–555, 1997.
Hawkins, J. W., Petrologic synthesis: Lau Basin transect (Leg 135), *Proc. Ocean Drill. Program Sci. Results, 135*, 427–470, 1994.
Hawkins, J. W., and J. T. Melchior, Petrology of Mariana Trough and Lau Basin basalts, *J. Geophys. Res., 90*(B13), 11,431–11,468, 1985.
Hawkins, J. W., S. H. Bloomer, C. A. Evans, and J. T. Melchior, Evolution of intra-oceanic arc-trench systems, *Tectonophysics, 102*, 175–205, 1984.
Hawkins, J. W., P. F. Lonsdale, J. D. Macdougall, and A. M. Volpe, Petrology of the axial ridge of the Mariana Trough backarc spreading center, *Earth Planet. Sci. Lett., 100*, 226–250, 1990.
Hay, W. W., J. L. Sloan II, and C. N. Wold, Mass/age distribution and composition of sediments on the ocean floor and the global rate of sediment subduction, *J. Geophys. Res., 93*(B12), 14,933–14,940, 1988.
Helffrich, G. R., and B. J. Wood, The Earth's mantle, *Nature, 412*, 501–507, 2001.
Herzberg, C. T., W. S. Fyfe, and M. J. Carr, Density constraints on the formation of the continental Moho and crust, *Contrib. Mineral. Petrol., 84*, 1–5, 1983.
Hilde, T. C., Sediment subduction versus accretion around the Pacific, *Tectonophysics, 99*, 381–397, 1983.
Hildreth, W., and S. Moorbath, Crustal contributions to arc magmatism on the Andes of central Chile, *Contrib. Mineral. Petrol., 98*, 455–489, 1988.
Hochstaedter, A. G., J. B. Gill, M. Kusakabe, S. Newman, M. Pringle, B. Taylor, and P. Fryer, Volcanism in the Sumisu Rift, I, Major element, volatile, and stable isotope geochemistry, *Earth Planet. Sci. Lett., 100*, 179–194, 1990.
Hofmann, A. W., Chemical differentiation of the Earth: The relationship between mantle, continental crust, and oceanic crust, *Earth Planet. Sci. Lett., 90*, 297–314, 1988.
Hofmann, A. W., Mantle geochemistry: The message from oceanic volcanism, *Nature, 385*, 219–229, 1997.
Holbrook, W. S., D. Lizarralde, S. McGeary, N. Bangs, and J. Deibold, Structure and composition of the Aleutian island arc and implications for continental crustal growth, *Geology, 27*, 31–34, 1999.
Hyndman, R. D., M. Yamano, and D. A. Oleskevich, The seismogenic zone of subduction thrust faults, *Isl. Arc, 6*(3), 244–260, 1997.
Ida, Y., Convection in the mantle wedge above the slab and tectonic processes in subduction zones, *J. Geophys. Res., 88*(B9), 7449–7456, 1983.
Irifune, T., Phase transformations in the Earth's mantle and subducting slabs: Implications for their compositions, seismic velocity and density structures and dynamics, *Isl. Arc, 2*, 55–71, 1993.
Ishii, T., P. T. Robinson, H. Maekawa, and R. Fiske, Petrological studies of peridotites from diapiric serpentinite seamounts in the Izu-Ogasawara-Mariana forearc, Leg 125, *Proc. Ocean Drill. Program Sci. Results, 125*, 445–485, 1992.
Ishikawa, T., and E. Nakamura, Origin of the slab component in arc lavas from across-arc variation of B and Pb isotopes, *Nature, 370*, 205–208, 1994.
Iwamori, H., Transportation of H_2O and melting in subduction zones, *Earth Planet. Sci. Lett., 160*, 65–80, 1998.
Jarrard, R. D., Relations among subduction parameters, *Rev. Geophys., 24*(2), 217–283, 1986.
Johnson, M. C., and T. Plank, Dehydration and melting experiments constrain the fate of subducted sediments, *Geochem. Geophys. Geosyst., 1*, 199GC000014, 1999.
Johnson, M. C., J. A. T. Anderson, and M. J. Rutherford, Pre-eruptive volatile contents of magmas, in *Volatiles in Magmas, Rev. Mineral.*, vol. 30, edited by M. R. Carroll and J. R. Holloway, pp. 281–330, Mineral. Soc. of Am., Washington D. C., 1994.
Jolly, W. T., E. G. Lidiak, A. P. Dickin, and T.-W. Wu, Secular geochemistry of central Puerto Rican island arc lavas: Constraints on Mesozoic tectonism in the eastern Greater Antilles, *J. Petrol., 42*, 2197–2214, 2001.
Jordan, T. E., Retroarc foreland and related basins, in *Tectonics of Sedimentary Basins*, edited by C. J. Busby and R. V. Ingersoll, pp. 331–362, Blackwell, Malden, Mass., 1995.
Jull, M., and P. B. Kelemen, On the conditions for lower crustal convective instability, *J. Geophys. Res., 106*(B4), 6423–6446, 2001.
Kárason, H., and van der Hilst, R. D., Constraints on mantle convection from seismic tomography, in *The History and Dynamics of Global Plate Motion, Geophys. Monogr. Ser.*, vol. 121, edited by M. A. Richards, R. Gordon, and R. D. van der Hilst, pp. 277–288, AGU, Washington, D. C., 2000.
Karson, J. A., Internal structure of oceanic lithosphere: A perspective from tectonic windows, in *Faulting and Magmatism at Mid-Ocean Ridges*, edited by W. R. Buck et al., Geophys. Monogr. Ser., vol. 106, pp. 177–218, AGU, Washington, D. C., 1998.
Kawate, S., and M. Arima, Petrogenesis of the Tanzawa plutonic complex, central Japan: Exposed felsic middle crust of the Izu-Bonin-Mariana arc, *Isl. Arc, 7*, 342–358, 1998.
Kay, R. W., Aleutian magnesian andesites; Melts from subducted Pacific Ocean crust, *J. Volcanol. Geotherm. Res., 4*, 117–132, 1978.
Kay, R. W., and S. M. Kay, Delamination and delamination magmatism, *Tectonophysics, 219*, 177–189, 1993.
Kay, S. M., and R. W. Kay, Role of crystal cumulates and the oceanic crust in the formation of the lower crust of the Aleutian Arc, *Geology, 13*, 461–464, 1985.
Kay, S. M., and R. W. Kay, Aleutian magmas in space and time, in *The Geology of North America*, vol. G-1, The Geology of Alaska, G. Pfalker and H. C. Berg, pp. 687–722, Geol. Soc. of Am., Boulder, Colo., 1994.
Kearey, P., and F. J. Vine, *Global Tectonics*, Blackwell Sci., Malden, Mass., 1990.
Kelemen, P. B., Genesis of high Mg# andesites and the continental crust, *Contrib. Mineral. Petrol., 120*, 1–19, 1995.
Kennett, J. P., *Marine Geology*, Prentice-Hall, Englewood Cliffs, N .J., 1982.
Kent, A. J. R., and T. R. Elliott, Melt inclusions from Marianas arc lavas: Implications for the composition and formation of island arc magmas, *Chem. Geol., 183*, 263–286, 2002.
Kerrick, D. M., and J. A. D. Connolly, Subduction of ophicarbonates and recycling of CO_2 and H_2O, *Geology, 26*, 375–378, 1998.
Kerrick, D. M., and J. A. D. Connolly, Metamorphic devolatilization of subducted marine sediments and the transport of volatiles into the Earth's mantle, *Nature, 411*, 293–296, 2001a.
Kerrick, D. M., and J. A. D. Connolly, Metamorphic devola-

tilization of subducted oceanic metabasalts: Implications for seismicity, arc magmatism, and volatile recycling, *Earth Planet. Sci. Lett., 189*, 19–29, 2001b.

Kincaid, C., and I. S. Sacks, Thermal and dynamical evolution of the upper mantle in subduction zones, *J. Geophys. Res., 102*(B6), 12,295–12,315, 1997.

Kirby, S. H., W. B. Durham, and L. A. Stern, Mantle phase changes and deep-earthquake faulting in subducting lithosphere, *Science, 252*, 216–225, 1991.

Kirby, S. H., S. Stein, E. A. Okal, and D. C. Rubie, Metastable mantle phase transformations and deep earthquakes in subducting oceanic lithosphere, *Rev. Geophys., 34*, 261–306, 1996.

Lallemand, S., *La Subduction Oceanique*, Gordon and Breach, Newark, N. J., 1999.

Lee, J., and R. J. Stern, Glass inclusions in Mariana arc phenocrysts; A new perspective on magmatic evolution in a typical intra-oceanic arc, *J. Geol., 106*, 19–33, 1998.

Le Pichon, X., P. Henry, and S. Lallemant, Accretion and erosion in subduction zones: The role of fluids, Annu. Rev. *Earth Planet. Sci., 21*, 307–331, 1993.

Maekawa, H., M. Shozuni, T. Ishii, P. Fryer, and J. A. Pearce, Blueschist metamorphism in an active subduction zone, *Nature, 364*, 520–523, 1993.

Maekawa, H., P. Fryer, and A. Ozaki, Incipient blueschist-facies metamorphism in the active subduction zone beneath the Mariana Forearc, in *Active Margins and Marginal Basins of the Western Pacific, Geophys. Monogr. Ser.*, vol. 88, edited by B. Taylor and J. Natland, pp. 281–289, AGU, Washington D. C., 1995.

Manning, C. E., Effect of sediment on aqueous silica transport in subduction zones, in *Subduction: Top to Bottom, Geophys. Monogr. Ser.*, vol. 96, edited by G. E. Bebout et al., pp. 277–284, AGU, Washington, D. C., 1996.

Marsh, B. D., Island arc development: Some observations, experiments, and speculations, *J. Geol., 87*, 867–713, 1979.

Martin, H., Adakitic magmas: Modern analogues of Archaean granitoids, *Lithos, 46*, 411–429, 1999.

Martinez, F., and B. Taylor, Mantle wedge control on back-arc crustal accretion, *Nature, 416*, 417–420, 2002.

Martinez, F., P. Fryer, N. A. Baker, and T. Yamazaki, Evolution of backarc rifting: Mariana Trough, 20°–24°N, *J. Geophys. Res., 100*(B3), 3807–3828, 1995.

Marty, B., and I. N. Tolstikhim, CO_2 fluxes from mid-ocean-ridges, arcs and plumes, *Chem. Geol., 145*, 233–248, 1998.

Mazzotti, S., P. Henry, X. LePichon, and T. Sagiya, Strain partitioning in the zone of transition from Nankai subduction to Izu-Bonin collision (central Japan): Implications for an extensional tear within the subducting slab, *Earth Planet. Sci. Lett., 172*, 1–10, 1999.

McCaffrey, R., Global variability in subduction thrust zone-forearc systems, *Pure Appl. Geophys., 142*, 173–224, 1994.

McLennan, S. M., Relationships between the trace element composition of sedimentary rocks and upper continental crust, *Geochem. Geophys. Geosyst., 2*, 2000GB0001009, 2001.

McLennan, S. M., and S. R. Taylor, Heat flow and the chemical composition of continental crust, *J. Geol., 104*, 369–377, 1996.

Mibe, K., T. Fuji ,and A. Yasuda, Control of the location of the volcanic front in island arcs by aqueous fluid connectivity in the mantle wedge, *Nature, 401*, 259–262, 1999.

Miller, D. J., and N. I. Christensen, Seismic signature and geochemistry of an island arc; A multidisciplinary study of the Kohistan accreted terrane, northern Pakistan, *J. Geophys. Res., 99*(B6), 11,623–11,642, 1994.

Molina, J. F., and S. Poli, Carbonate stability and fluid composition in subducted oceanic crust: An experimental study on H_2O-CO_2-bearing basalts, *Earth Planet. Sci. Lett., 176*, 295–310, 2000.

Molnar, P., D. Freedman, and J. S. F. Shih, Lengths of intermediate and deep seismic zones and temperatures in downgoing slabs of lithosphere, *Geophys. J. R. Astron. Soc., 56*, 41–54, 1979.

Moore, J. C., and P. Vrolijk, Fluids in accretionary prisms, *Rev. Geophys., 30*, 113–135, 1992.

Morris, J. D., and S. R. Hart, Isotopic and incompatible element constraints on the genesis of island arc volcanics from Cold Bay and Amak Island, Aleutians, and implications for mantle structure, *Geochim. Cosmochim. Acta, 47*, 2015–2030, 1983.

Morris, J. D., W. P. Leeman, and F. Tera, The subducted component in island arc lavas: Constraints from Be isotopes and B-Be systematics, *Nature, 344*, 31–36, 1990.

Mottl, M. J., Pore waters from serpentinite seamounts in the Mariana and Izu-Bonin forearcs, Leg 125: Evidence for volatiles from the subducting slab, *Proc. Ocean Drill. Program Sci. Results, 125*, 373–385, 1992.

Nakajima, K., and M. Arima, Melting experiments on hydrous low-K tholeiite: Implications for the genesis of tonalitic crust in the Izu-Bonin-Mariana arc, *Isl. Arc, 7*, 359–373, 1998.

Nakamura, M., and E. B. Watson, Experimental study of aqueous fluid infiltration into quartzite: Implications for the kinetics of fluid re-distribution and grain growth driven by interfacial energy reduction, *Geofluids, 1*, 73–89, 2001.

Navon, O., and E. Stolper, Geochemical consequences of melt percolation; The upper mantle as a chromatographic column, *J. Geol., 95*, 285–307, 1987.

Newman, S., E. Stolper, and R. J. Stern, H_2O and CO_2 in magmas from the Mariana arc and back arc systems, *Geochem. Geophys, Geosyst., 1*, 1999GC000027 [15,062 words], 2000.

Nichols, G. T., P. J. Wyllie, and C. R. Stern, Experimental melting of pelagic sediment, constraints relevant to subduction, in *Subduction: Top to Bottom, Geophys. Monogr. Ser.*, vol. 96, edited by G. E. Bebout et al., pp. 293–298, AGU, Washington D. C., 1996.

O'Brien, P. J., Subduction followed by collision: Alpine and Himalayan examples, *Phys. Earth Planet. Inter., 127*, 277–291, 2001.

Ohara, Y., R. J. Stern, T. Ishii, H. Yurimoto, and T. Yamazaki, Peridotites from the Mariana Trough backarc basin, *Contrib. Mineral. Petrol., 143*, 1–18, 2002.

Pacheco, J. F., and L. R. Sykes, Seismic moment catalog of large shallow earthquakes, 1900 to 1989, *Bull. Seismol. Soc. Am., 82*, 1306–1349, 1992.

Pacheco, J. F., L. R. Sykes, and C. H. Scholz, Nature of seismic coupling along simple plate boundaries of the subduction type, *J. Geophys. Res., 98*, 14,133–14,159, 1993.

Parkinson, I. J., and J. A. Pearce, Peridotites from the Izu-Bonin-Mariana forearc (ODP Leg 125); Evidence for mantle melting and melt-mantle interaction in a supra-subduction zone setting, *J. Petrol., 39*, 1577–1618, 1998.

Parsons, B., Causes and consequences of the relation between area and age of the sea floor, *J. Geophys. Res., 87*, 289–302, 1982.

Parsons, T., A. M. Trehu, J. H. Leutgert, K. Miller, F. Kilbride, R. E. Wells, M. A. Fisher, E. Flueh, U. S. ten Brink, and N. I. Christiansen, A new view into the Cascadia subduction zone and volcanic arc: Implications for earthquake hazards along the Washington margin, *Geology, 26*, 199–202, 1998.

Pawley, A. R., and J. R. Holloway, Water sources for subduction zone volcanism: New experimental constraints, *Science, 260*, 664–667, 1993.

Peacock, S. M., Thermal and petrologic structure of subduction zones, in *Subduction: Top to Bottom, Geophys. Monogr.*

Ser., vol. 96, edited by G. E. Bebout et al., pp. 119–133, AGU, Washington D. C., 1996.

Peacock, S. M., Are the lower planes of double seismic zones caused by serpentine dehydration in subduction oceanic mantle?, *Geology, 29*, 299–302, 2001.

Peacock, S. M., Thermal structure and metamorphic evolution of subducting slabs, in *Geophysical Monograph Series*, edited by J. Eiler and G. A. Abers, AGU, Washington, D. C., in press, 2002.

Peacock, S. M., and R. D. Hyndman, Hydrous minerals in the mantle wedge and the maximum depth of subduction thrust earthquakes, *Geophys. Res. Lett., 26*, 2517–2520, 1999.

Peacock, S. M., and K. Wang, Seismic consequences of warm versus cool subduction metamorphism: Examples from southwest and northeast Japan, *Science, 286*, 937–939, 1999.

Peacock, S. M., T. Rushmer, and A. B. Thompson, Partial melting of subducting oceanic crust, *Earth Planet. Sci. Lett., 121*, 227–244, 1994.

Pearce, J. A., and D. W. Peate, Tectonic implications of the composition of volcanic arc magmas, *Annu. Rev. Earth Planet. Sci., 23*, 251–285, 1995.

Pearce, J., S. J. Lippard, and S. Roberts, Characteristics and tectonic significance of supra-subduction zone ophiolites, in Marginal Basin Geology, edited by B. P. Kokelaar and M. F. Howells, *Geol. Soc. Spec. Publ., 16*, 77–94. 1984.

Pearce, J. A., S. R. Van Der Laan, R. J. Arculus, B. J. Murton, T. Ishii, J. A. Peate, and I. J. Parkinson, Boninite and harzburgite from Leg 125 (Bonin-Mariana forearc): A case study of magma genesis during the initial stages of subduction, *Proc. Ocean Drill. Program Sci. Results, 125*, 623–659, 1992.

Pearcy, L. G., S. M. DeBari, and N. H. Sleep, Mass balance calculations for two sections of island arc crust and implications for the formation of continents, *Earth Planet. Sci. Lett., 96*, 427–442, 1990.

Peate, D. W., J. A. Pearce, C. J. Hawkesworth, H. Colley, C. M. H. Edwards, and K. Hirose, Geochemical variations in Vanuatu Arc lavas: The role of subducted material and a variable mantle wedge composition, *J. Petrol., 38*, 1331–1358, 1997.

Perfit, M. R., D. A. Gust, A. E. Bence, R. J. Arculus, and S. R. Taylor, Chemical characteristics of island-arc basalts; Implications for mantle sources, *Chem. Geol., 30*, 227–256, 1980.

Phillips, R. J., and V. L. Hansen, Geological evolution of Venus: Rises, plains, plumes, and plateaus, *Science, 279*, 1492–1497, 1998.

Plank, T., and C. H. Langmuir, An evaluation of the global variations in the major element chemistry of arc basalts, Earth Planet. Sci. Lett., 90, 349–370, 1988.

Plank, T., and C. H. Langmuir, Tracing trace elements from sediment input to volcanic output at subduction zones, *Nature, 362*, 739–742, 1993.

Plank, T., and C. Langmuir, The chemical composition of subducting sediment and its consequence for the crust and mantle, *Chem. Geol., 145*, 325–394, 1998.

Rea, D. K., and L. J. Ruff, Composition and mass flux of sediment entering the world's subduction zones: Implications for global sediment budgets, great earthquakes, and volcanism, *Earth Planet. Sci. Lett., 140*, 1–12, 1996.

Reymer, A., and G. Schubert, Phanerozoic addition rates to the continental crust and crustal growth, *Tectonics, 3*, 63–77, 1984.

Rieder, R., T. Economou, H. Wänke, A. Turkevich, J. Crisp, J. Brückner, G. Dreibus, and H. Y. McSween Jr., The chemical composition of Martian soil and rocks returned by the mobile alpha proton X-ray spectrometer: Preliminary results from the X-ray mode, *Science, 278*, 1771–1774, 1997.

Robinson, J. A. C., and B. J. Wood, The depth of the spinel to garnet transition at the peridotite solidus, *Earth Planet. Sci. Lett., 164*, 277–284, 1998.

Roggensack, K., S. N. Williams, S. J. Schaefer, and J. R. A. Parnell, Volatiles from the 1994 eruption of Rabaul: Understanding large caldera systems, *Science, 273*, 490–493, 1996.

Roggensack, K., R. L. Hervig, S. B. McKnight, and S. N. Williams, Explosive basaltic volcanism from Cerro Negro Volcano: Influence of volatiles on eruptive style, *Science, 277*, 1639–1642, 1997.

Rudnick, R. L., and D. M. Fountain, Nature and composition of the continental crust: A lower crustal perspective, *Rev. Geophys., 33*, 267–309, 1995.

Ruff, L. J., and H. Kanamori, Seismicity and the subduction process, *Phys. Earth Planet. Inter., 23*, 240–252, 1980.

Ruff, L. J., and B. W. Tichelaar, What controls the seismogenic plate interface in subduction zones?, *Subduction: Top to Bottom, Geophys. Monogr. Ser.*, vol. 96, edited by G. E. Bebout et al., pp. 105–111, AGU, Washington D. C., 1996.

Sano, Y., and S. N. Williams, Fluxes of mantle and subducted carbon along convergent plate boundaries, *Geophys. Res. Lett., 23*, 2749–2752, 1996.

Scambelluri, M., and P. Philippot, Deep fluids in subduction zones, *Lithos, 55*, 213–227, 2001.

Schmidt, M. W., and S. Poli, Experimentally based water budgets for dehydrating slabs and consequences for arc magma generation, *Earth Planet. Sci. Lett., 163*, 361–379, 1998.

Shervais, J. W., Birth, death, and resurrection: The life cycle of suprasubduction zone ophiolites, *Geochem. Geophys. Geosyst., 2*, 2000GC000080 [20,925 words], 2001.

Sisson, T. W., and S. Bronto, Evidence for pressure-release melting beneath magmatic arcs from basalt at Galunggung, Indonesia, *Nature, 391*, 883–886, 1998.

Sisson, T. W., and G. D. Layne, H_2O in basalt and basaltic andesite glass inclusions from four subduction-related volcanoes, *Earth Planet. Sci. Lett., 117*, 619–835, 1993.

Smith, G. P., D. A. Wiens, K. M. Fischer, L. M. Dorman, S. C. Webb, and J. A. Hildebrand, A complex pattern of mantle flow in the Lau Basin, *Science, 292*, 713–716, 2001.

Smith, H. J., A. J. Spivack, H. Staudigel, and S. R. Hart, The boron isotopic composition of altered oceanic crust, *Chem. Geol., 126*, 119–135, 1995.

Smithies, R. H., The Archaean tonalite-trondhjemite-granodiorite (TTG) series is not an analogue of Cenozoic adakite, *Earth Planet. Sci. Lett., 182*, 115–125, 2000.

Sobolev, A. V., and M. Chaussidon, H_2O concentrations in primary melts from supra-subduction zones and mid-ocean ridges: Implications for H_2O storage and recycling in the mantle, *Earth Planet. Sci. Lett., 137*, 45–55, 1996.

Solomon, S. C., and D. R. Toomey, The structure of mid-ocean ridges, *Annu. Rev. Earth Planet. Sci., 20*, 329–364, 1992.

Staudigel, H., T. Plank, B. White, and H.-U. Schmincke, Geochemical fluxes during seafloor alteration of the basaltic upper oceanic crust: DSDP sites 417 and 418, in *Subduction: Top to Bottom, Geophys. Monogr. Ser.*, vol. 96, edited by G. E. Bebout et al., pp. 19–38, AGU, Washington D. C., 1996.

Stein, S. A., and D. C. Rubie, Deep earthquakes in real slabs, *Science, 286*, 909–910. 1999.

Stein, S., and C. A. Stein, Thermo-mechanical evolution of oceanic lithosphere: Implications for the subduction process and deep earthquakes, in *Subduction: Top to Bottom, Geophys. Monogr. Ser.*, vol. 96, edited by G. E. Bebout et al., pp. 1–17, AGU, Washington, D. C., 1996.

Stern, R. J., A subduction primer for instructors of introductory geology courses and authors of introductory geology textbooks, *J. Geosci. Educ., 46*, 221–228, 1998.

Stern, R. J., and S. H. Bloomer, Subduction zone infancy:

Examples from the Eocene Izu-Bonin-Mariana and Jurassic California, *Geol. Soc. Am. Bull., 104*, 1621–1636, 1992.

Stern, R. J., and N. C. Smoot, A bathymetric overview of the Mariana forearc, *Isl. Arc, 7*, 525–540, 1998.

Stern, R. J., S. H. Bloomer, F. Martinez, T. Yamazaki, and T. M. Harrison, The composition of back-arc basin lower crust and upper mantle in the Mariana Trough: A first report, *Isl. Arc, 5*, 354–372, 1996.

Stern, R. J., M. J. Fouch, and S. Klemperer, An overview of the Izu-Bonin-Mariana, in *Geophysical Monograph Series*, edited by J. M. Eiler and G. A. Abers, AGU, Washington, D. C., in press, 2002.

Stolper, E., and S. Newman, The role of water in the petrogenesis of Mariana Trough magmas, *Earth Planet. Sci. Lett., 121*, 293–325, 1994.

Sun, C. H., and R. J. Stern, Genesis of Mariana shoshonites: Contribution of the subduction component, *J. Geophys. Res., 106*(B1), 589–608, 2001.

Suyehiro, K., et al., Continental crust, crustal underplating, and low-Q upper mantle beneath an oceanic island arc, *Science, 272*, 390–392, 1996.

Takahashi, N., K. Suyehiro, and M. Shinohara, Implications from the seismic crustal structure of the northern Izu-Bonin arc, *Isl. Arc, 7*, 383–394, 1998.

Tamura, Y., Y. Tatsumi, D. Zhao, Y. Kidoa, and H. Shukunoa, Hot fingers in the mantle wedge: New insights into magma genesis in subduction zones, *Earth Planet. Sci. Lett., 197*, 105–116, 2002.

Tatsumi, Y., and S. Eggins, *Subduction Zone Magmatism*, Blackwell, Malden, Mass., 1995.

Taylor, B., A. Klaus, G. R. Brown, G. F. Moore, Y. Okamura, and F. Murakami, Structural development of Sumisu Rift, Izu-Bonin arc, *J. Geophys. Res., 96*, 113–129, 1991.

Taylor, S. R., and S. M. Mclennan, *The Continental Crust: Its Composition and Evolution*, Blackwell Sci., Malden, Mass., 1985.

Tichelaar, B. W., and L. J. Ruff, Depth of seismic coupling along subduction zones, *J. Geophys. Res., 98*(B2), 2017–2037, 1993.

Tilling, R. I., Hazards and climatic impact of subduction-zone volcanism: A global and historical perspective, in *Subduction: Top to Bottom, Geophys. Monogr. Ser.*, vol. 96, edited by G. E. Bebout et al., pp. 331–335, AGU, Washington D. C., 1996.

Turner, I. M., C. Pierce, and M. C. Sinha, Seismic imaging of the axial region of the Valu Fa Ridge, Lau Basin—The accretionary processes of an intermediate back-arc spreading ridge, *Geophys. J. Int., 138*, 495–519, 1999.

Turner, S., B. Bourdon, C. Hawkesworth, and P. Evans, ^{226}Ra-^{230}Th evidence for multiple dehydration events, rapid melt ascent and the time scales of differentiation beneath the Tonga-Kermadec island arc, *Earth Planet. Sci. Lett., 179*, 518–593, 2000.

Ulmer, P., Partial melting in the mantle wedge—The role of H_2O in the genesis of mantle-derived 'arc-related' magmas, *Phys. Earth Planet. Inter., 127*, 215–232, 2001.

Ulmer, P., and V. Trommsdorf, Serpentine stability to mantle depths and subduction-related magmatism, *Science, 268*, 858–861, 1995.

Underwood, M. B., and G. F. Moore, Trenches and trench-slope basins, in *Tectonics of Sedimentary Basins*, edited by C. J. Busby and R. V. Ingersoll, pp. 179–219, Blackwell, Malden, Mass., 1995.

Uyeda, S., and H. Kanamori, Back-arc opening and the mode of subduction, *J. Geophys. Res., 84*, 1049–1061, 1979.

van Keken, P. E., B. Kiefer, and S. M. Peacock, High-resolution models of subduction zones: Implications for mineral dehydration reactions and the transport of water into the deep mantle, *Geochem. Geophys. Geosyst., 3*(10), 1056, doi: 10.1029/2001GC000256, 2002.

Veizer, J., and S. L. Jansen, Basement and sedimentary recycling, 2, Time dimension to global tectonics, *J. Geol., 93*, 625–643, 1985.

Vogt, P. R., Volcano spacing, fractures, and thickness of the lithosphere, *Earth Planet. Sci. Lett., 21*, 235–252, 1974.

von Huene, R., and D. W. Scholl, Observations at convergent margins concerning sediment subduction, subduction erosion, and the growth of continental crust, *Rev. Geophys., 29*, 279–316, 1991.

von Huene, R., and D. W. Scholl, The return of sialic material to the mantle indicated by terrigeneous material subducted at convergent margins, *Tectonophysics, 219*, 163–175, 1993.

Wallmann, K., The geological water cycle and the evolution of marine d18O values, *Geochim. Cosmochim. Acta, 65*, 2469–2485, 2001.

Watson, E. B., J. M. Brennan, and D. R. Baker, Distribution of fluids in the continental mantle, in *Continental Mantle*, edited by M. A. Menzies, pp. 111–125,Clarendon, Oxford, U.K., 1990.

White, D. A., D. H. Roeder, T. H. Nelson, and J. C. Crowell, Subduction, *Geol. Soc. Am., 81*, 3431–3432, 1970.

Wiens, D. A., Seismological constraints on the mechanism of deep earthquakes: Temperature dependence of deep earthquake source properties, *Phys. Earth Planet. Inter., 127*, 145–163, 2001.

Wiens, D. A., and G. P. Smith, Seismological constraints on structure and flow patterns within the mantle wedge, in *Geophysical Monograph Series*, edited by J. M. Eiler and G. A. Abers, AGU, Washington, in press, D. C., 2001.

Woodhead, J., S. Eggins, and J. Gamble, High field strength and transition element systematics in island arc and back-arc basin basalts; Evidence for multi-phase melt extraction and a depleted mantle wedge, *Earth Planet. Sci. Lett., 114*, 491–504, 1993.

Wörner, G., L. L. Escobar, S. Moorbath, S. Horn, J. Entenmann, R. S. Harmon, and J. D. Davidson, Variaciones geoquimicas, locales y regionales, en el arco volcanico Andino del Norte de Chile (17°30′S–22°00′S), *Rev. Geol. Chile, 19*(1), 37–56, 1992.

Yeats, R. S., K. Sieh, and C. R. Allen, *The Geology of Earthquakes*, Oxford Univ. Press, New York, 1997.

Yuan, X., et al., Subduction and collision processes in the central Andes constrained by converted seismic phases, *Nature, 408*, 958–961, 2000.

Zhao, D., New advances of seismic tomography and its applications to subduction zones and earthquake fault zones, *Isl. Arc, 10*, 68–84, 2001.

Zhao, D., A. Hasegawa, and H. Kanamori, Deep structure of Japan subduction zone as derived from local, regional, and teleseismic events, *J. Geophys. Res., 99*(B11), 22,313–22,329, 1994.

Zhao, D., Y. Xu, D. Wiens, L. M. Dorman, J. Hildebrand, and S. C. Webb, Depth extent of the Lau back-arc spreading center and its relation to subduction processes, *Science, 278*(5336), 254–257, 1997.

R. J. Stern, Geosciences Department, University of Texas at Dallas, Box 830688, Richardson, TX 75083-0688, USA. rjstern@utdallas.edu

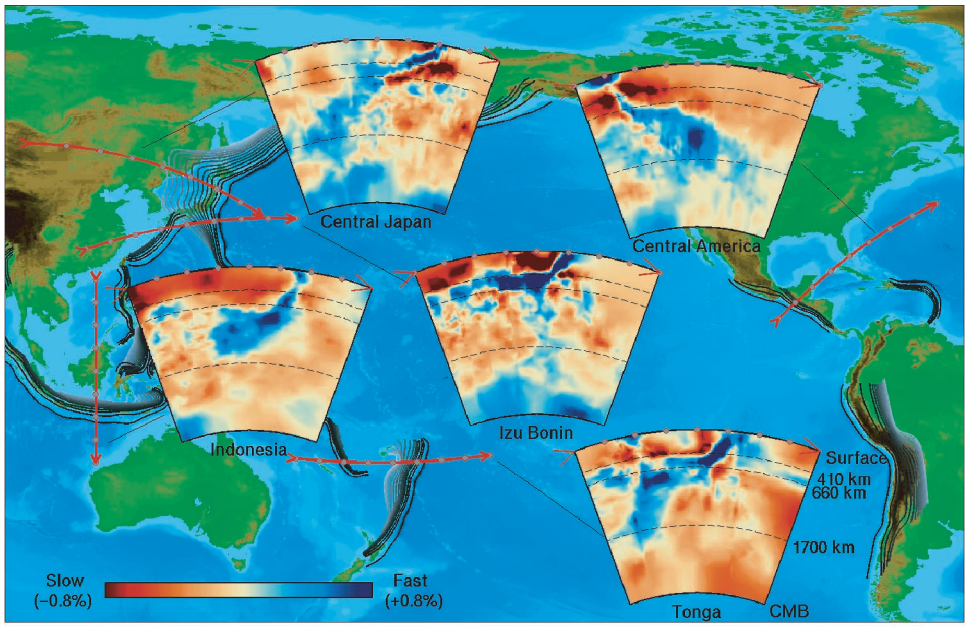

Figure 2. Structure of subducted slabs as inferred from mantle tomography (from *Kárason and van der Hilst* [2000]). Red lines show the surface projection of each section. The base of each section is the core-mantle boundary (CMB); dashed lines show the location of mantle discontinuities at 410, 660, and 1700 km. Red and blue colors in each section denote regions where the *P* wave velocities are relatively slow and fast, respectively, compared to average mantle at the same depth. Fast regions are most easily interpreted as relatively cool areas corresponding to the subducted slab and its viscous mantle blanket. This allows the cool, subducted slab to be traced well below the deepest earthquake. Note that some slabs penetrate the 660 km discontinuity and descend into the lower mantle (e.g., Central America, central Japan, and Indonesia), while other slabs seem to stagnate in the upper mantle (such as Izu-Bonin). The subducted slab beneath Tonga seems to stagnate at the 660 km discontinuity for a while, then cascade into the lower mantle.

Figure 6. (opposite) Geophysical images of subduction zones. (a) *P* wave tomographic image of NE Japan (modified after *Zhao et al.* [1994]). There is no vertical exaggeration. (b) *P* wave tomographic image of Tonga subduction zone (modified after *Zhao et al.* [1997]). There is no vertical exaggeration. For both Figures 6a and 6b, red and blue colors denote regions where the *P* wave velocities are relatively slow and fast, respectively, compared to average mantle at the same depth. (c) *P* wave velocity structure across the Cascadia Subduction Zone (modified after *Parsons et al.* [1998]). Yellow dots show earthquakes during 1970–1996 between 45° and 47° latitude, $>M1$ at depths >25 km and $>M4$ at shallower depths. Note vertical exaggeration is 2x. Note that the subduction zones in Figure 6a and 6b subduct old, cold lithosphere, which is relatively easy to identify tomographically, whereas the subduction zone in Figure 6c subducts young lithosphere, which differs less in velocity relative to the surrounding mantle and is more difficult to image tomographically.

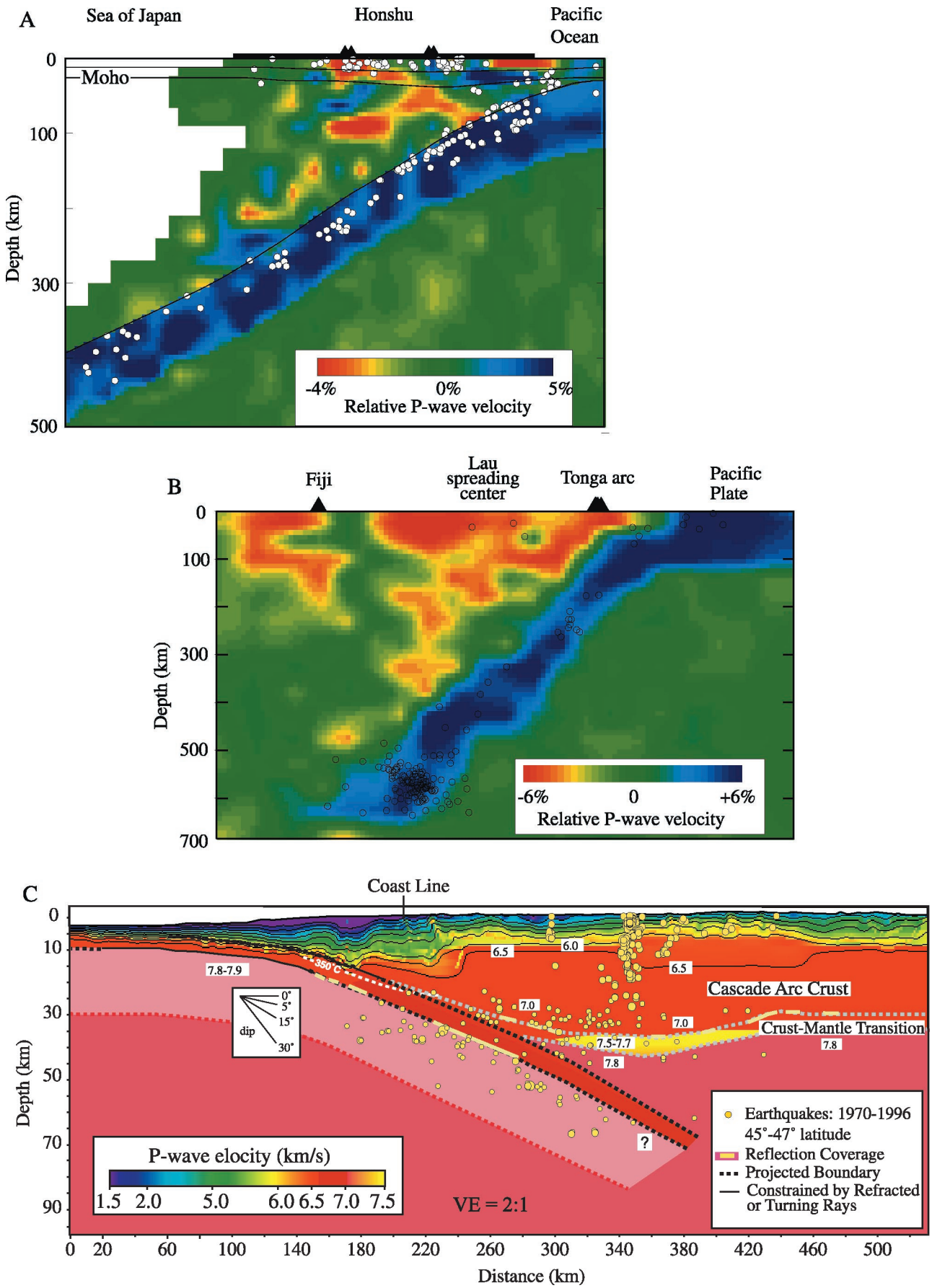
A
Sea of Japan
Honshu
Pacific Ocean
Moho
Depth (km)
0
100
300
500
-4%
0%
5%
Relative P-wave velocity
B
Fiji
Lau spreading center
Tonga arc
Pacific Plate
Depth (km)
0
100
300
500
700
-6%
0
+6%
Relative P-wave velocity
C
Coast Line
Depth (km)
0
10
30
50
70
90
7.8-7.9
350°C
dip
0°
5°
15°
30°
6.5
6.0
6.5
Cascade Arc Crust
7.0
7.0
Crust-Mantle Transition
7.5-7.7
7.8
7.8
?
P-wave elocity (km/s)
1.5 2.0 5.0 6.0 6.5 7.0 7.5
VE = 2:1
Earthquakes: 1970-1996
45°-47° latitude
Reflection Coverage
Projected Boundary
Constrained by Refracted or Turning Rays
0 20 60 100 140 180 220 260 300 340 380 420 460 500
Distance (km)

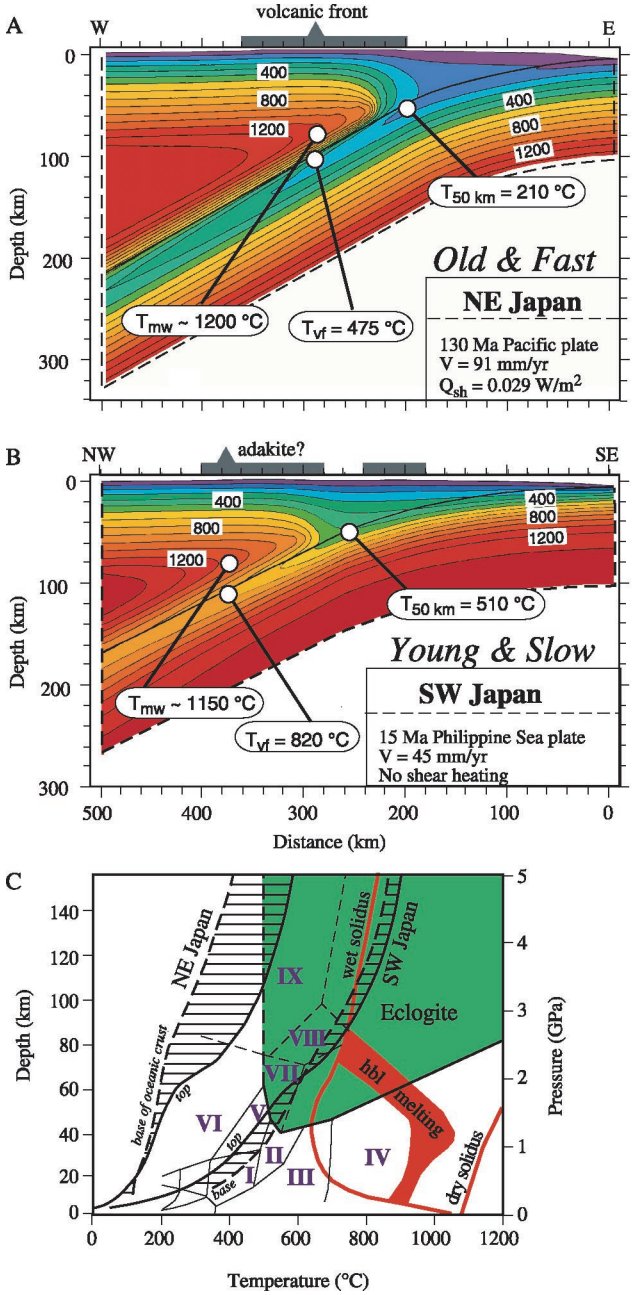

Figure 7. Thermal models of end-member (young and hot versus old and cold) subduction zones. (a) NE Japan arc, a good example of a cold subduction zone. (b) SW Japan arc, a good example of a hot subduction zone. Note the great difference in the temperature of the slab interface at 50 km depth (T_{50} km) and beneath the volcanic front (T_{vf}) but the small difference in the maximum temperature of the mantle wedge beneath the volcanic front (T_{mw}). (c) Pressue-temperature diagram showing metamorphic facies and melting relations for basaltic oceanic crust, along with trajectories for crust subducted beneath NE and SW Japan Roman numerals identify fields for metamorphic facies: I, greenschist; II, epidote amphibolite; III, amphibolite; IV, granulite; V, epidote blueschist; VI, lawsonite blueschist (green field shows location of the eclogite field, with the dark dashed line separating this from blueschist); VII, chloritoid-amphibolite-zoisite eclogite; VIII, zoisite-chloritoid eclogite; and IX, lawsonite-chloritoid eclogite. Note that oceanic crust subducted beneath SW Japan enters the eclogite field at ~40 km depth and, if hydrous, begins to melt at ~90 km, whereas oceanic crust subducted beneath NE Japan barely enters the eclogite field at 120 km depth. Figures 6a–6c are modified after *Peacock and Wang* [1999] and *Peacock* [2002].

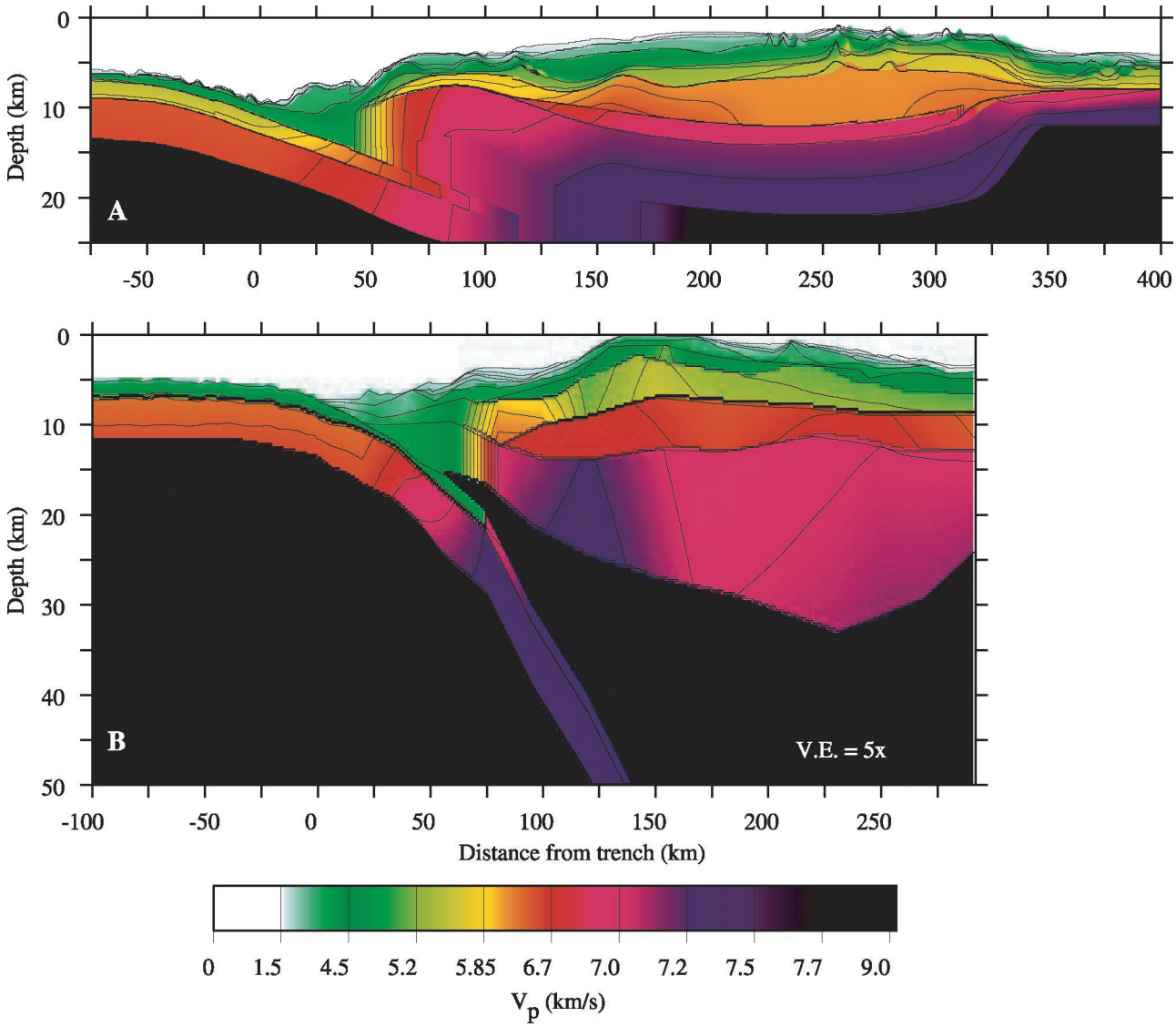

Figure 15. Crustal structure of typical arcs, based on *P* wave velocities. Note vertical exaggeration is ~5x. (a) Izu arc, 33°N (modified after *Suyehiro et al.* [1996]). (b) Eastern Aleutian arc (modified after *Holbrook et al.* [1999]). Note differences in thickness and velocity structure. We do not have comparable tomographic images of Andean-type arc crust.